Chemical Probes for Bioimaging

Kai Johnsson

Department of Chemical Biology
Max Planck Institute for Medical Research, Heidelberg

Institute of Chemical Sciences and Engineering
EPFL, Lausanne

Edoc Course “Chemical probes for imaging in biology”

The course focusses on the visualization and manipulation of biological activities in live cells. Topics discussed in the class will be (i) the design of new fluorescent probes for live-cell imaging, including superresolution microscopy; (ii) methods for the direct and specific localization of chemical probes in living cells; (iii) the design of semisynthetic protein sensors for basic research and diagnostics; (iv) methods for labelling of DNA; (v) approaches for manipulating biology processes with chemical probes. The class will be comprised of five lectures of 2 hours each around these topics. At the end of the course, each participant will write a short report of how her or his PhD project and could benefit from the approaches discussed in this course of this class.

Synthetic probes for the second messenger Ca^{2+}

- Second messengers carry signals inside cells; in the easiest case through changes in their concentrations. Examples are cAMP, NO, cGMP, lipid-derived messengers and Ca^{2+}. Visualizing their concentrations in live cells with spatio-temporal resolution is critical for mechanistic studies.

- Ca^{2+} is involved in many process such as synaptic transmission, fertilization, secretion, muscle contraction and cytokinesis.

- A Ca^{2+} gradient exists across the plasma membrane, with resting concentrations in the cytosol around 100 nM. ATP-driven pumps that pump Ca^{2+} outside the cell or in the endoplasmic reticulum (ER) maintain the gradient. A wide array of different stimuli open Ca^{2+} channels in the plasma membrane or the ER and allow so-called Ca^{2+} sparks or Ca^{2+} transients to enter the cytoplasm. Peak Ca^{2+} cytoplasmic concentrations are in the micromolar range and signals lasts milliseconds to minutes.

- Signals work locally as there are efficient Ca^{2+} sequestering mechanisms and abundant Ca^{2+} binding proteins (estimated to be around 300 μM).

- Binding of Ca^{2+} to proteins can change their structures and activities. Examples are Ca^{2+}–activated ion channels and Ca^{2+}-bound calmodulin, which controls kinases and adenylyl cyclases.

Measuring Calcium in live cells

Calcium is a key second messenger in many signal transductions and its concentration varies significantly over time; we thus need indicators to track these concentration changes. Fura-2 and Indo-1 are two fluorescent dyes that change their spectroscopic properties upon binding to calcium. They were developed by Roger Tsien and published in 1985; this paper is now cited more than 20’000 times!

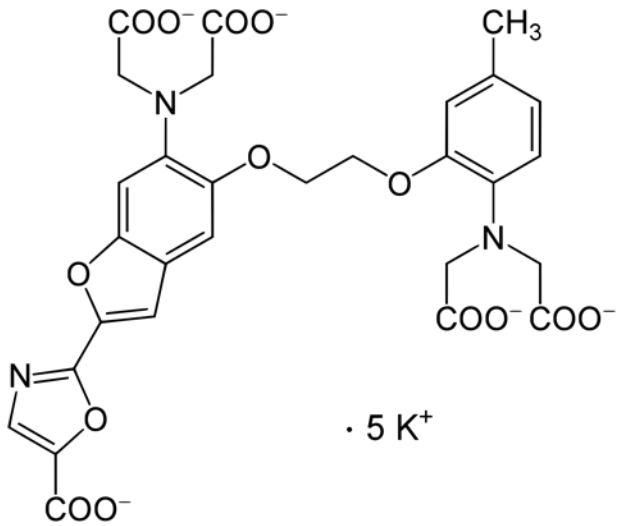

Fura-2

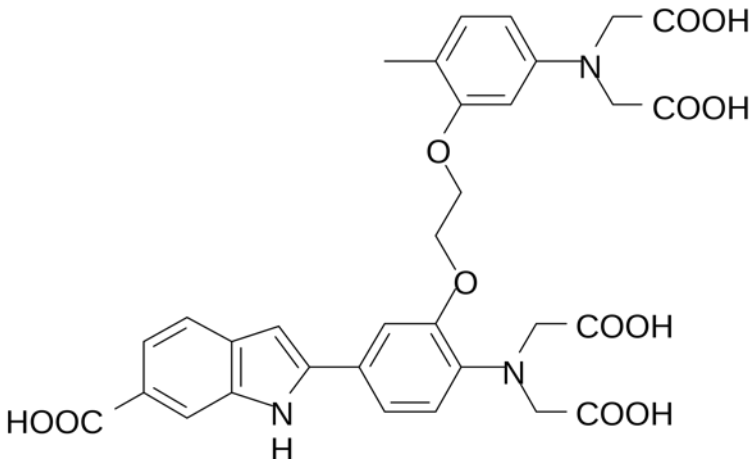

Indo-1

*R.Y. Tsien et al., JBC **260**, 3440 (1985); http://www.ncbi.nlm.nih.gov/pubmed/3838314*

Fura-2 and Indo-1

TABLE I

Properties of new fluorescent indicators of Ca^{2+}

Absorption maxima refer to the dominant peaks at longest wavelength, measured at 22 ± 2 °C in 100 mM KCl. The first number is the wavelength in nanometers, followed in parentheses by 10^{-3} × the corresponding extinction coefficient, M^{-1} cm^{-1}. The data for stil-2 are for the *cis-trans* mixture as saponified; both the wavelengths and extinction coefficients would increase for pure *trans*. Extinction coefficients for fura-1 and fura-3 may be underestimated since less effort was expended on their purification than on stil-1, indo-1, and fura-2. Emission maxima list the peak wavelengths in nanometers of the uncorrected and corrected (in parentheses) emission spectra. The differences between uncorrected and corrected values are greatest for stil-1 and fura-1 because they were measured on the Perkin-Elmer MPF44, whose emission characteristics are more biased than the Spex Fluorolog, on which the others were determined. Emission maxima and quantum efficiencies were measured in 100 mM KCl, 22 ± 2 °C.

Dye	Apparent K_d for Ca^{2+}	Absorption maxima		Emission maxima		Fluorescence quantum efficiency	
		Free anion	Ca complex	Free anion	Ca complex	Free anion	Ca complex
	nM						
stil-1	132[a], 200[b]	362 (27)	329 (34)	537 (585)	529 (ND[c])	0.14	ND
stil-2	224[d]	352 (12)	326 (12)	564 (590)	560 (587)	0.11	0.15
indo-1	250[b]	349 (34)	331 (34)	485 (482)	410 (398)	0.38	0.56
fura-1	107[b]	350 (21)	334 (27)	534 (585)	522 (548)	0.14	0.20
fura-2	135[a], 224[b]	362 (27)	335 (33)	512 (518)	505 (510)	0.23	0.49
fura-3	140[b]	370 (14)	343 (25)	564 (588)	551 (599)	0.13	0.21

Measuring Calcium with Indo-1 and Fura-2

Indo-1 is excited at around 350 nm and the ratio of the emission at two different wavelengths (400 nm and 475 nm) is measured. Fura-2 is excited at two different wavelengths (340 and 380 nm) and the emission intensities at 510 nm is measured as a function of excitation wavelength (i.e. a ratiometric measurement). The ratio in both cases permits the determination of the calcium concentration.

Emission spectra of Indo-1 as function of $[Ca^{2+}]$:

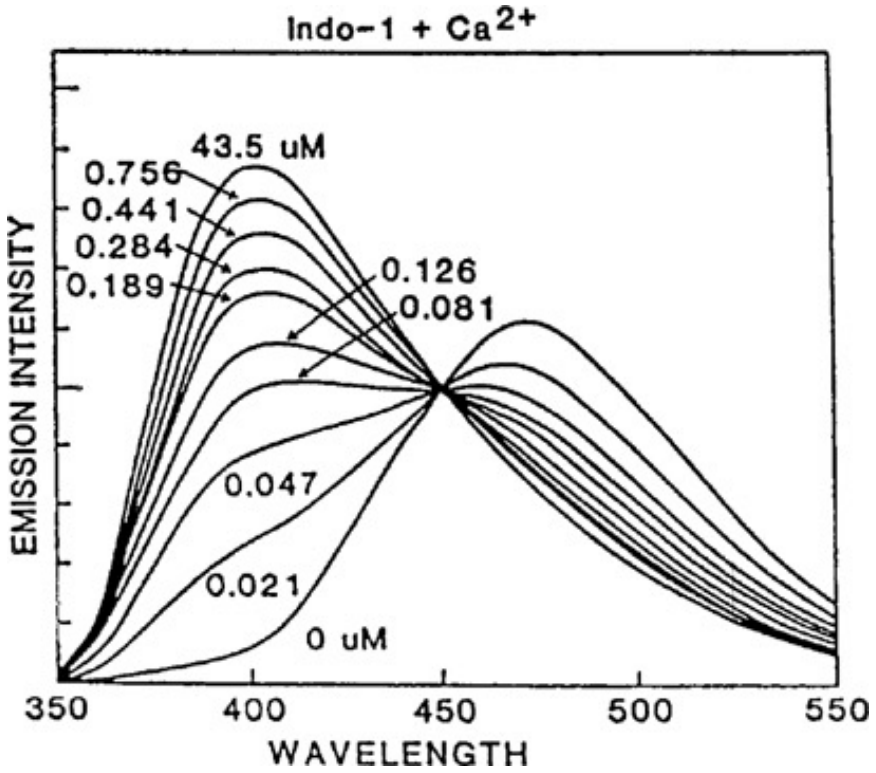

Excitation spectra of Fura-2 as function of $[Ca^{2+}]$:

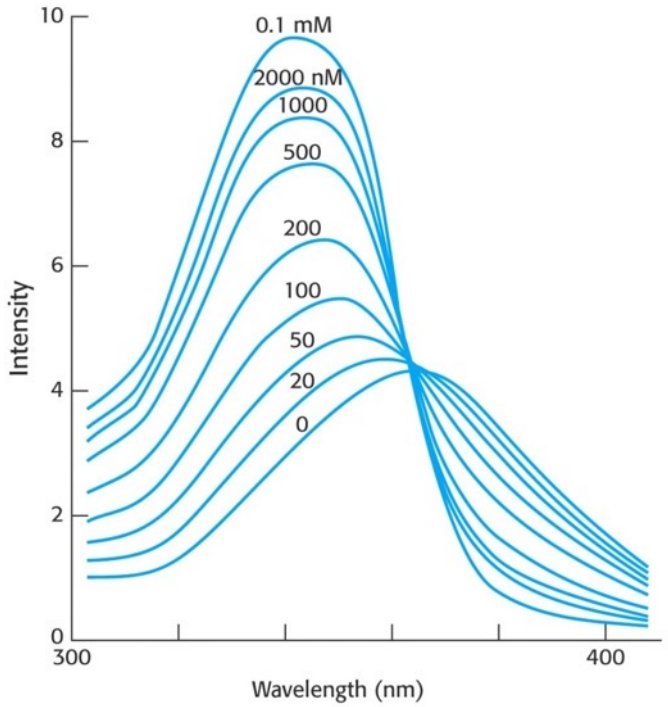

Measuring Calcium with Indo-1 and Fura-2

Ca^{2+} spreading across a cell visualized by Fura-2:

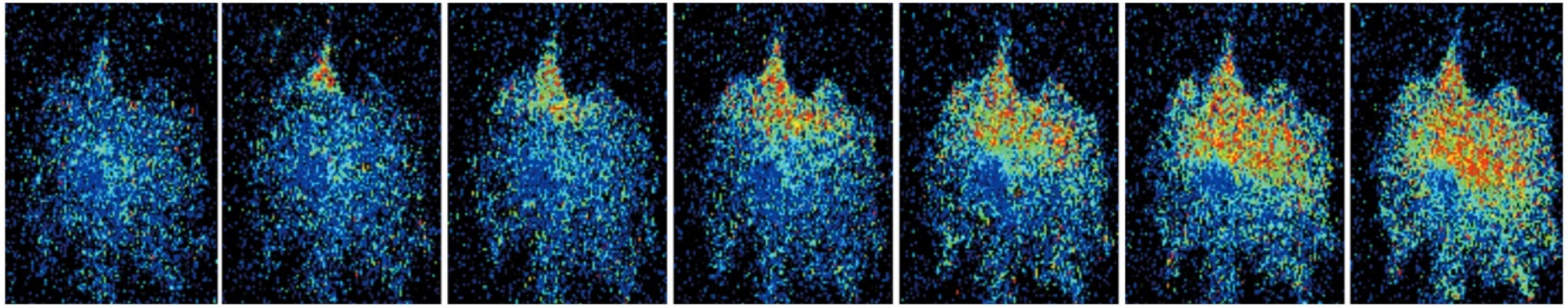

Ca^{2+} oscillations triggered by addition of norepinephrine (arrow) and visualized by Fura-2:

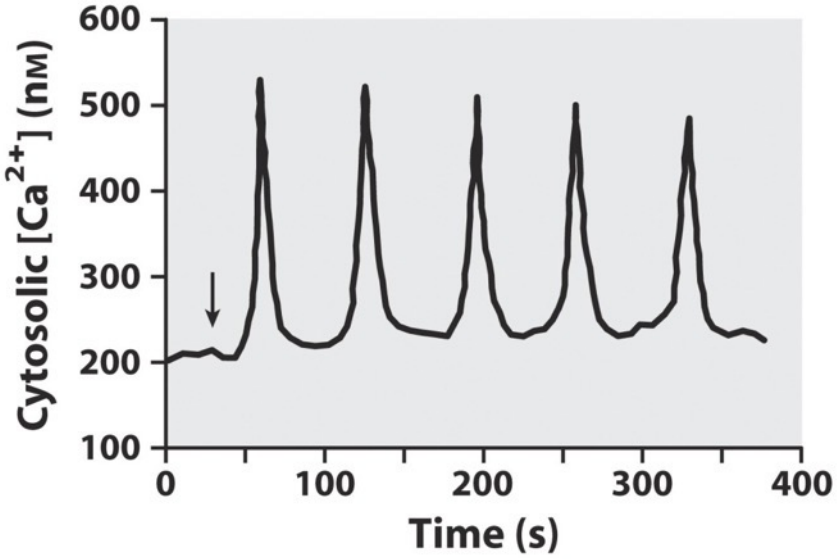

Some questions to Fura-2 and Indo-1

- What are the advantages of a ratiometric probe over an intensity-based probe?
- Why are the fluorescent properties of Indo-1 and Fura-2 so sensitive to Ca^{2+} concentrations?
- Do you think both probes are membrane permeable? How could they be introduced into cells?
- How could you change the response to higher calcium concentrations?
- What are the limitations of these two indicators?

Autofluorescent proteins

Jellyfish *Aequorea victoria*

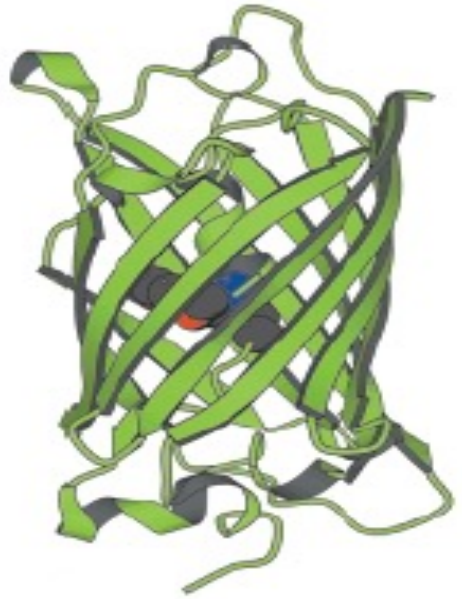

Structure of green fluorescent protein (GFP) from *Aequorea victoria*

Short history of the discovery of GFP

1962: GFP is discovered as a companion to aequorin, a chemiluminescent protein, in Aequorea jellyfish by Shimomura

1979: The structure of the chromphore is identified through hydroylsis of GFP by Shimomura

1992: The gene of GFP is cloned by Prasher

1994: Chalfie and Inouye & Tsuji report the use of GFP as a reporter protein that can be expressed in other organisms

1994: Roger Tsien reports first development of improved versions of GFP

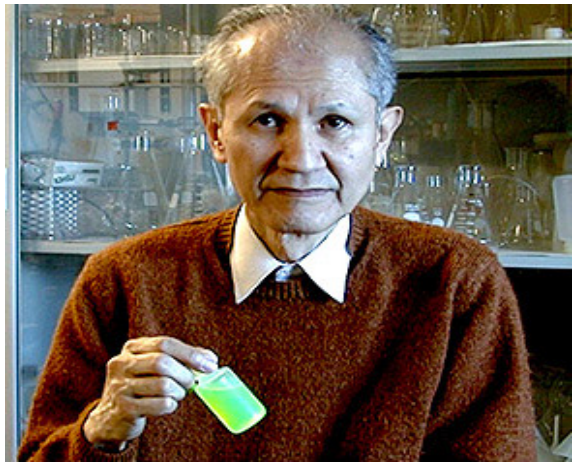

Osamu Shimomura
(Nobel Prize 2008)

Roger Tsien, UC San Diego
(Nobel Prize 2008)

Martin Chalfie, Columbia U.
(Nobel Prize 2008)

GREEN FLUORESCENT PROTEIN AS A MARKER FOR GENE-EXPRESSION

By:CHALFIE, M (CHALFIE, M); TU, Y (TU, Y); EUSKIRCHEN, G (EUSKIRCHEN, G); WARD, WW (WARD, WW); PRASHER, DC (PRASHER, DC)

SCIENCE, **Volume:** 263, **Issue:** 5148, **Pages:** 802-805

Abstract

A complementary DNA for the Aequorea victoria green fluorescent protein (GFP) produces a fluorescent product when expressed in prokaryotic (Escherichia coli) or eukaryotic (Caenorhabditis elegans) cells. Because exogenous substrates and cofactors are not required for this fluorescence, GFP expression can be used to monitor gene expression and protein localization in living organisms.

GFP

Bioluminescence of aequorin

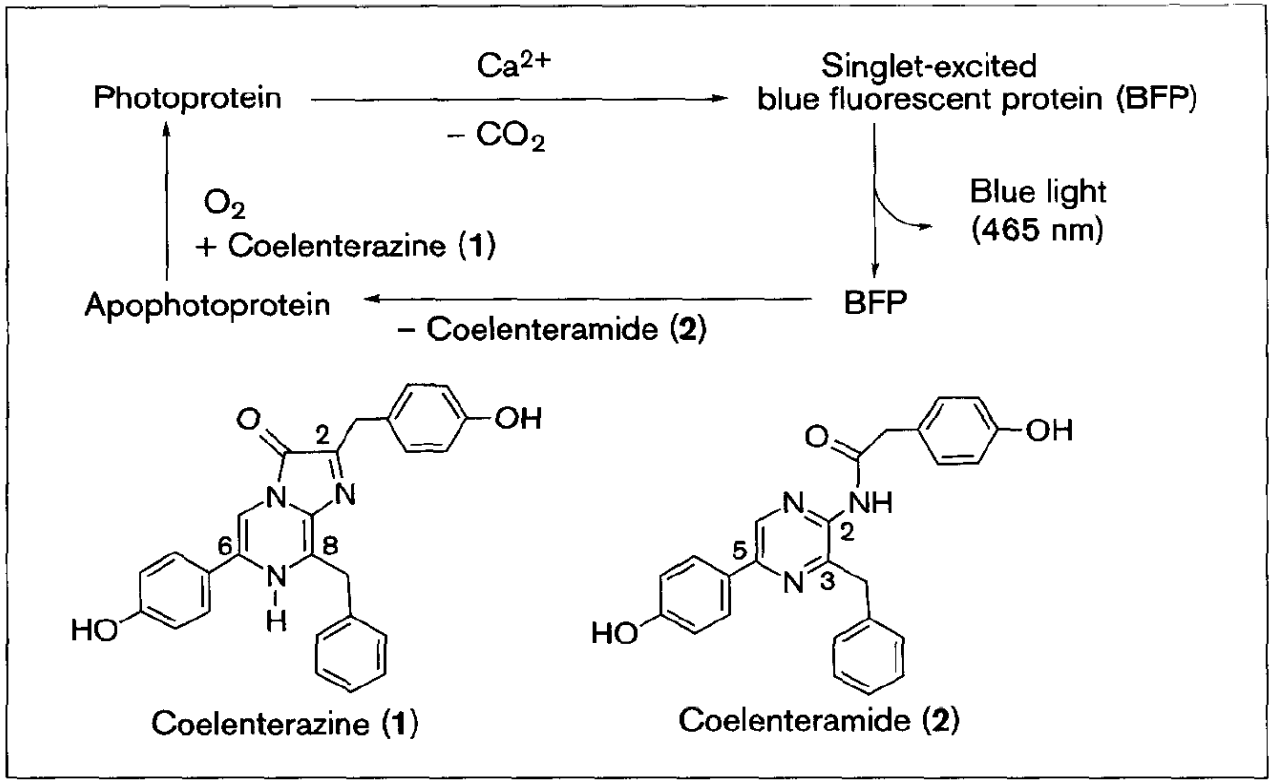

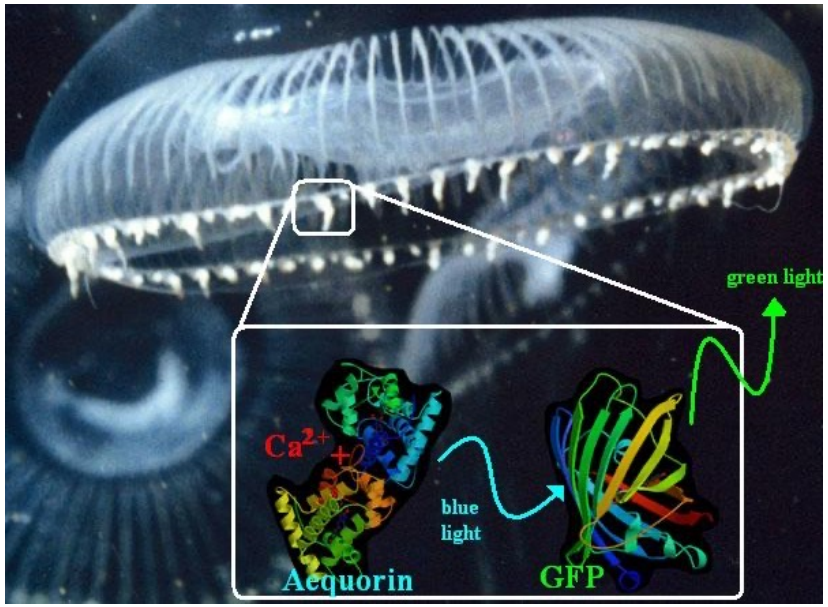

GFP converts the blue emission of aequorin into the green glow of the jellyfish

Structure of the chromophore of GFP

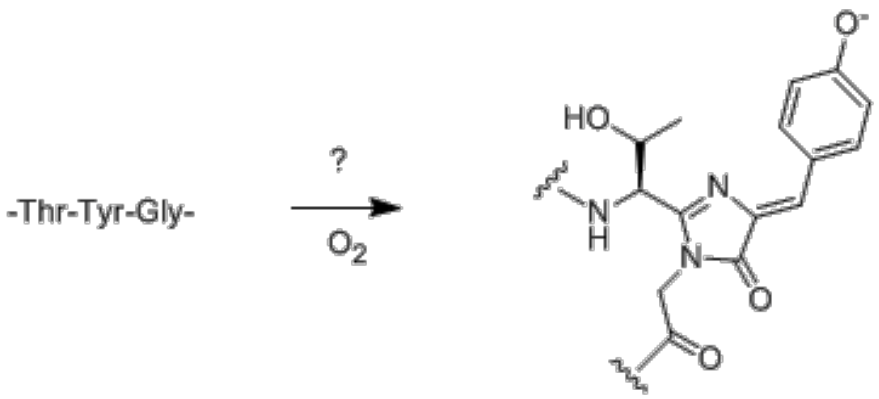

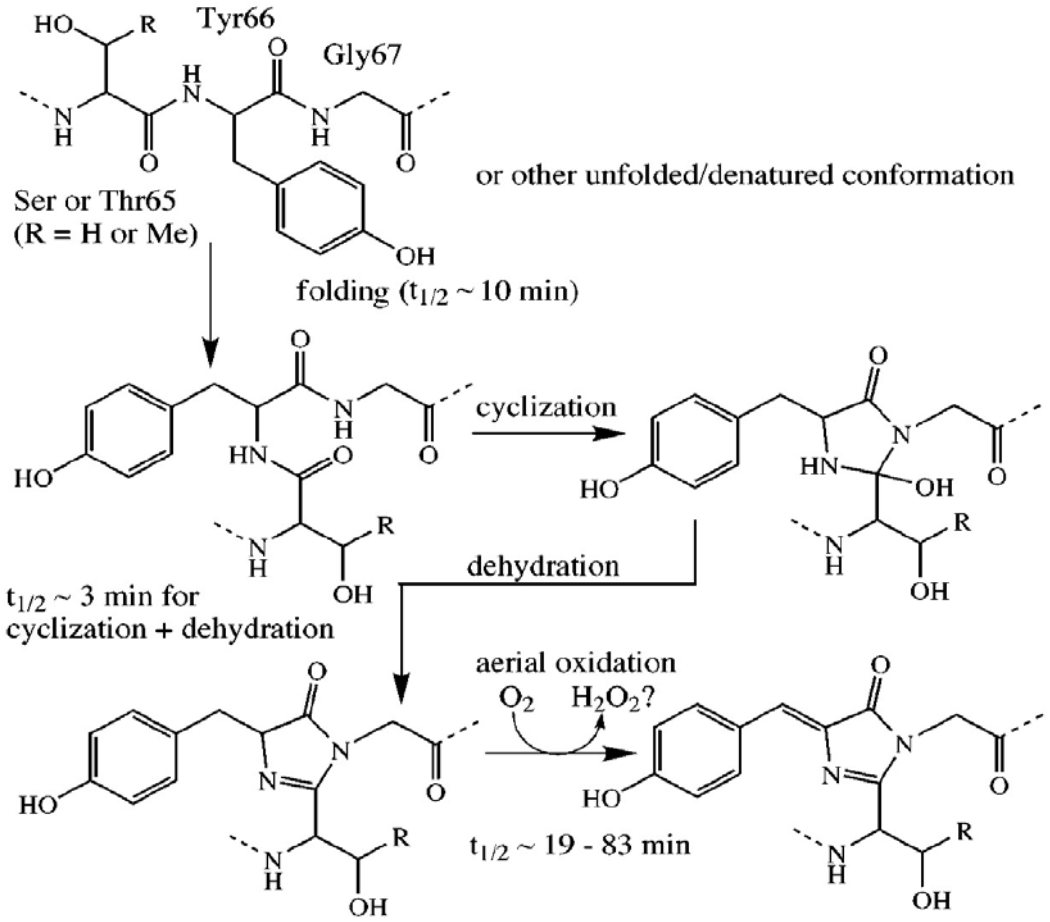

Red fluorescent protein from sea anemone *Anemonia majano*

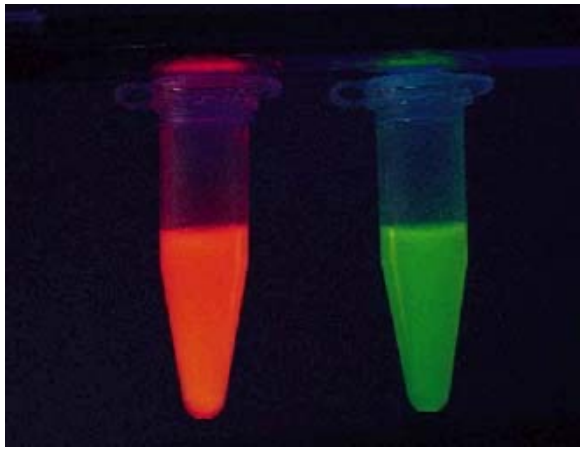

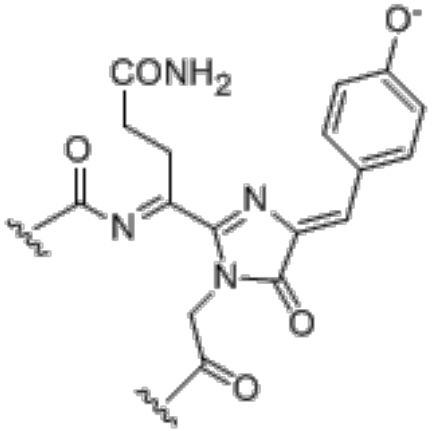

Structure of the chromophore

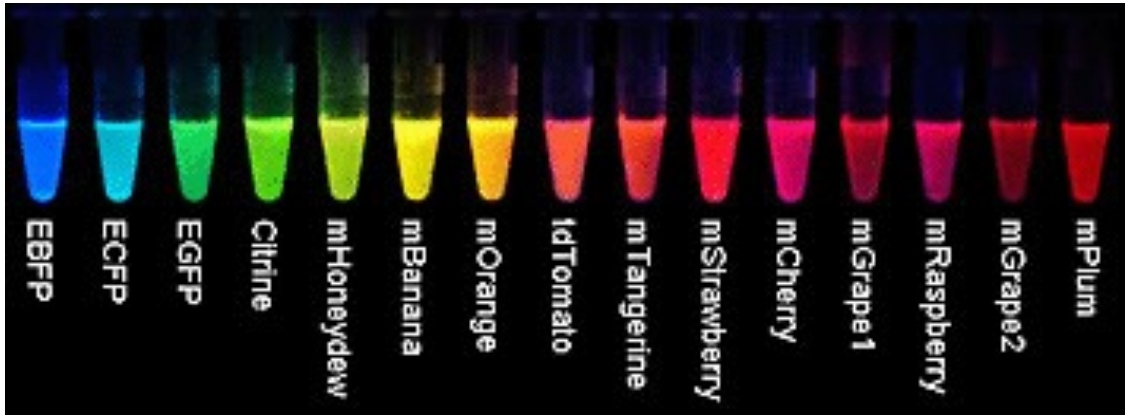

Engineered FPs span the range from blue to red……(R. Y. Tsien)

Use of autofluorescent proteins in cells and organisms

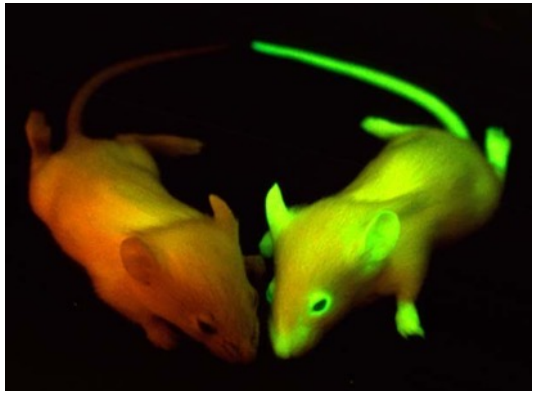

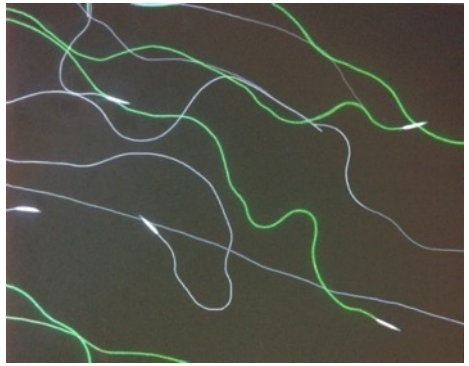

Sperm from fruit fly

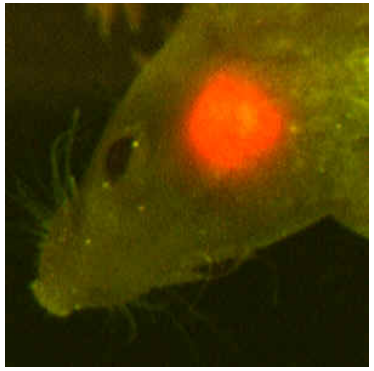

Tumor in mouse brain expressing RFP

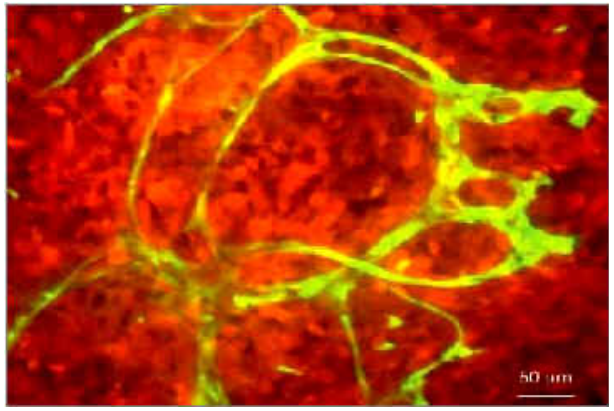

Mouse blood vessels expressing GFP in tumor expressing RFP

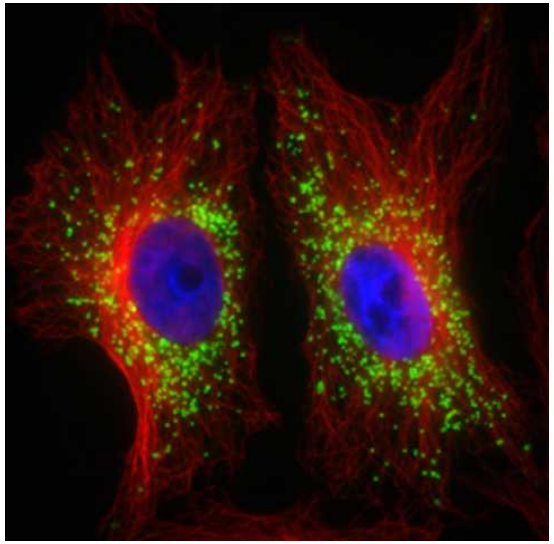

Two different autofluorescent proteins in one cell

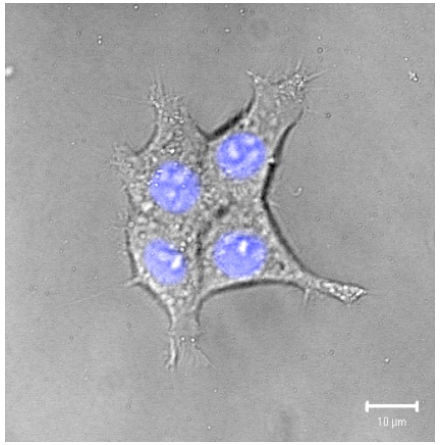

Nuclear localized protein expressed in cell culture as fusion with GFP

Förster resonance energy transfer (FRET)

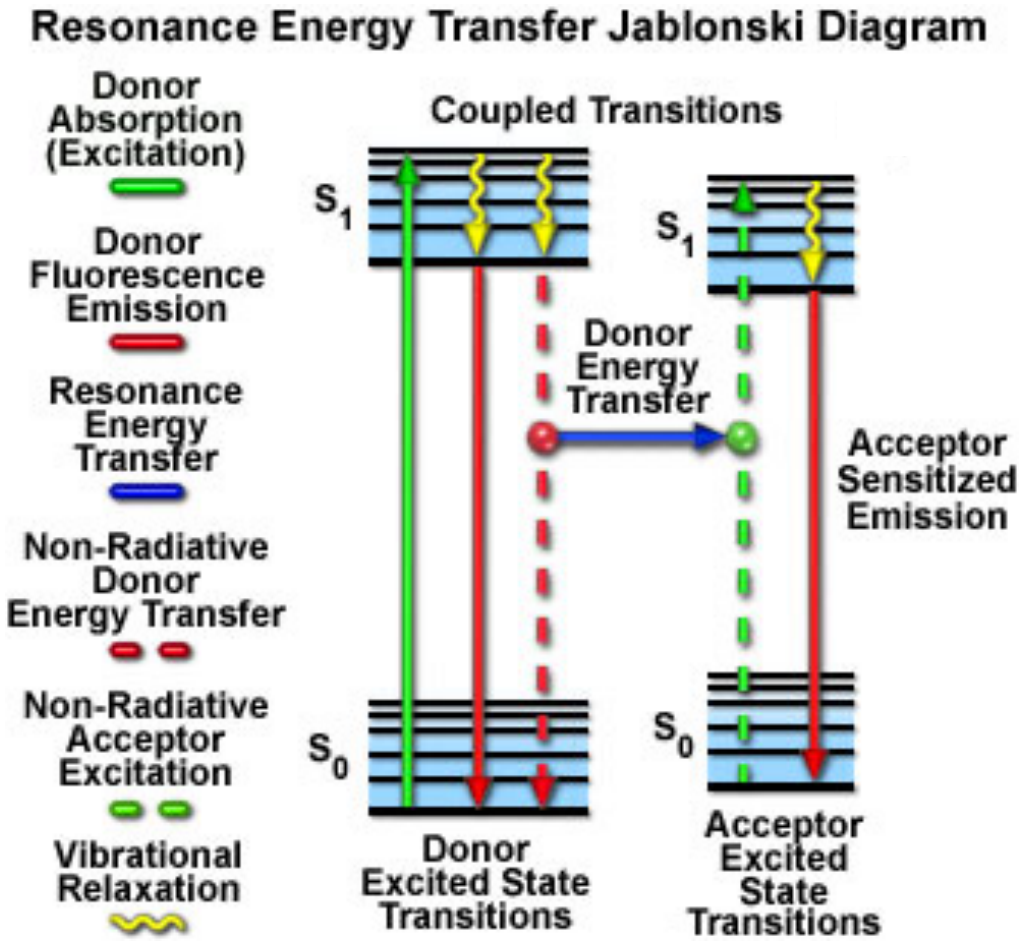

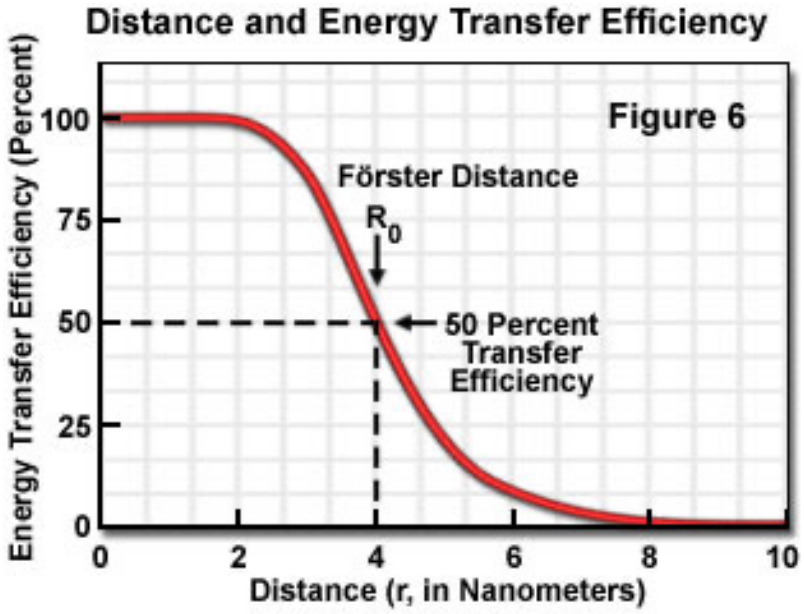

$$KT = (1/tD) \bullet [R_0/r]^6$$

FRET between autofluorescent fusion proteins

- use of GFP mutants with different excitation and emission spectra allows use of FRET to detect protein-protein interactions

Emission spectra of autofluorescent proteins

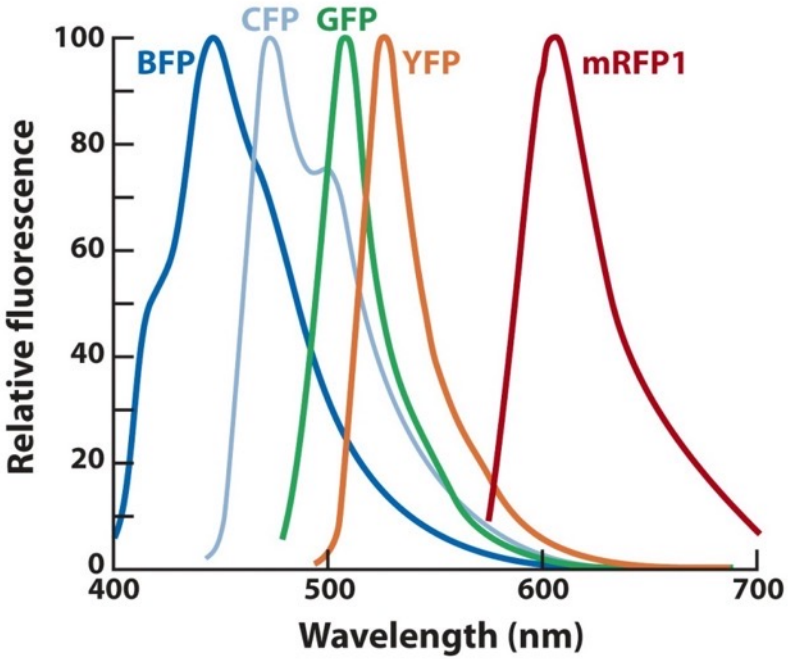

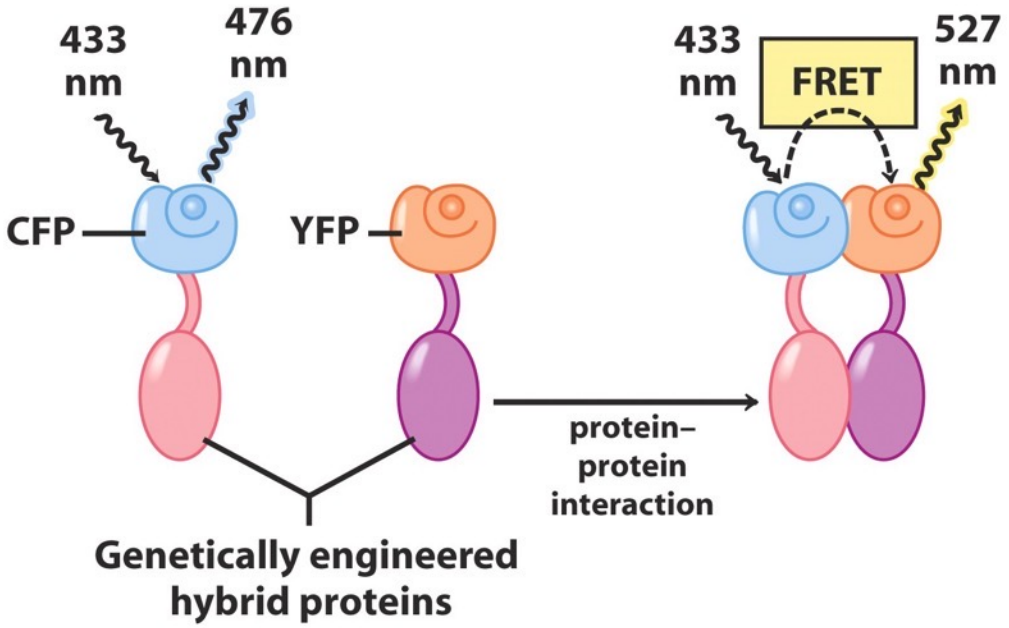

Calcium sensors based on autofluorescent proteins

Calmodulin (CaM) is a Ca^{2+}-binding protein that undergoes a a significant conformational change upon binding Ca^{2+} and associates with a variety of proteins to modulate their activity

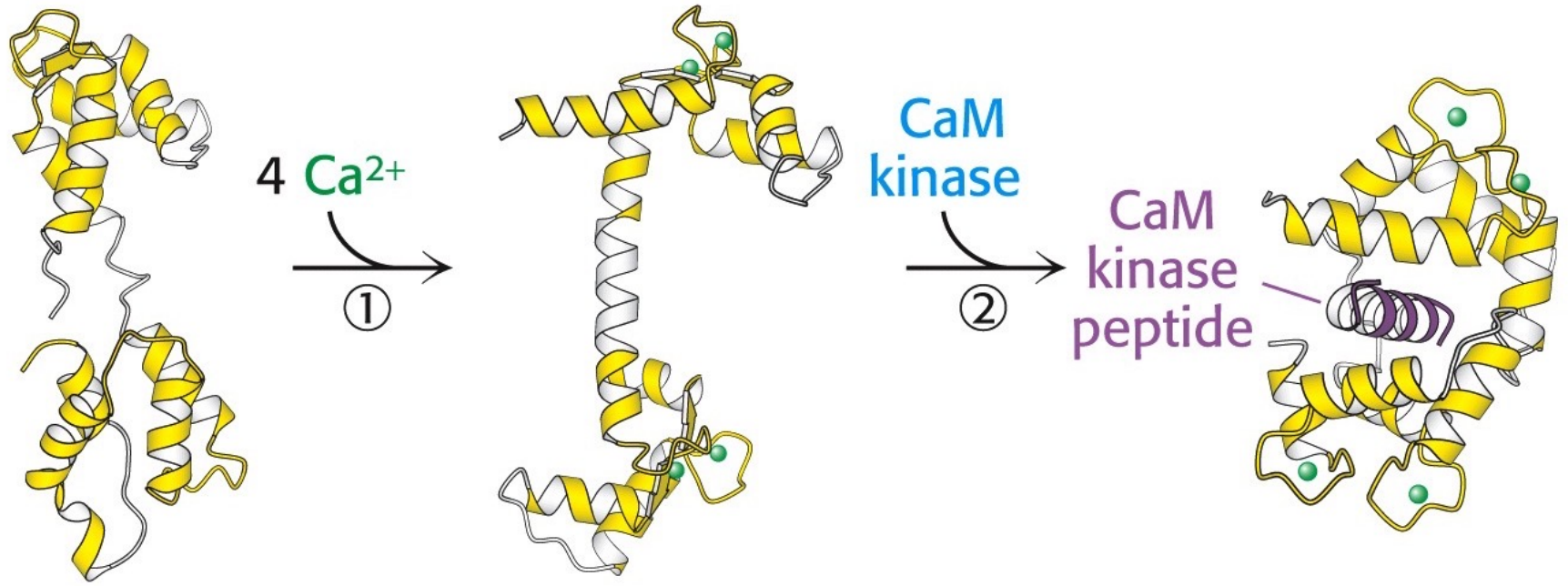

Calmodulin (apo)

Calcium sensors based on autofluorescent proteins

• Expression of a fusion protein that is comprised of CFP-CaM-M13-YFP, where M13 is a CaM-binding peptide, allows construction of genetically encoded Ca^{2+} sensor.

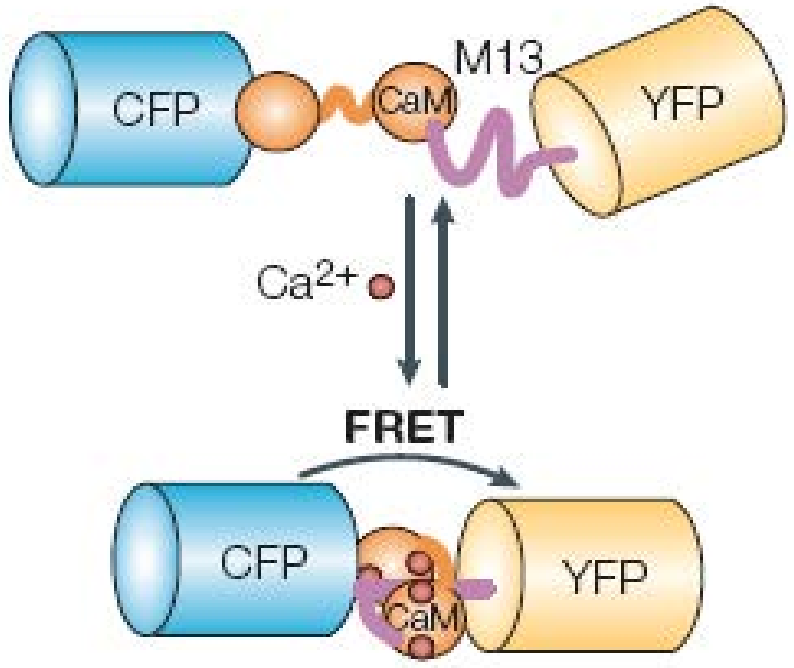

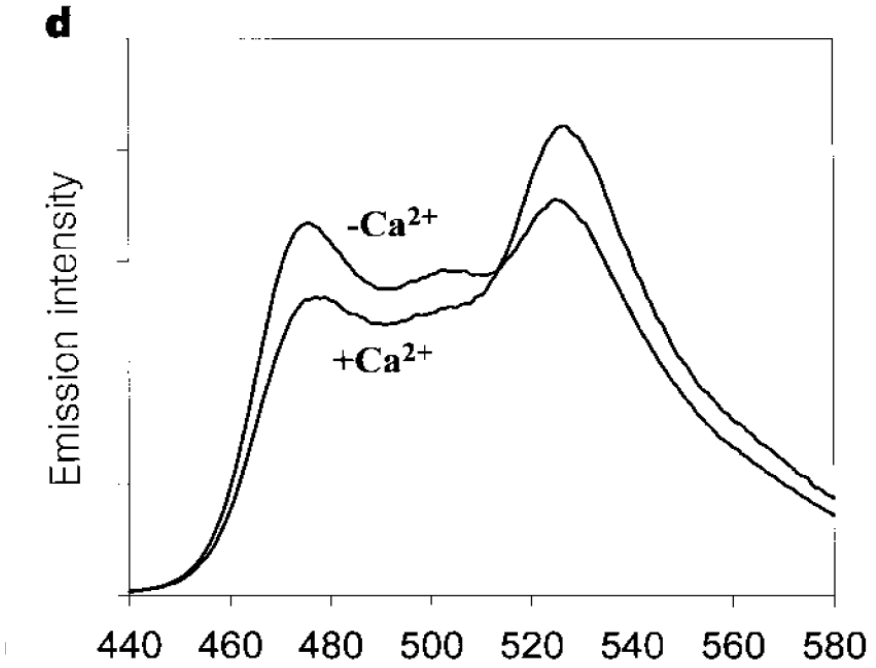

Nature **388**, 882 (1997); improved versions: *PNAS* **101**, 10554 (2004)

Specific labeling of proteins in vivo and in vitro

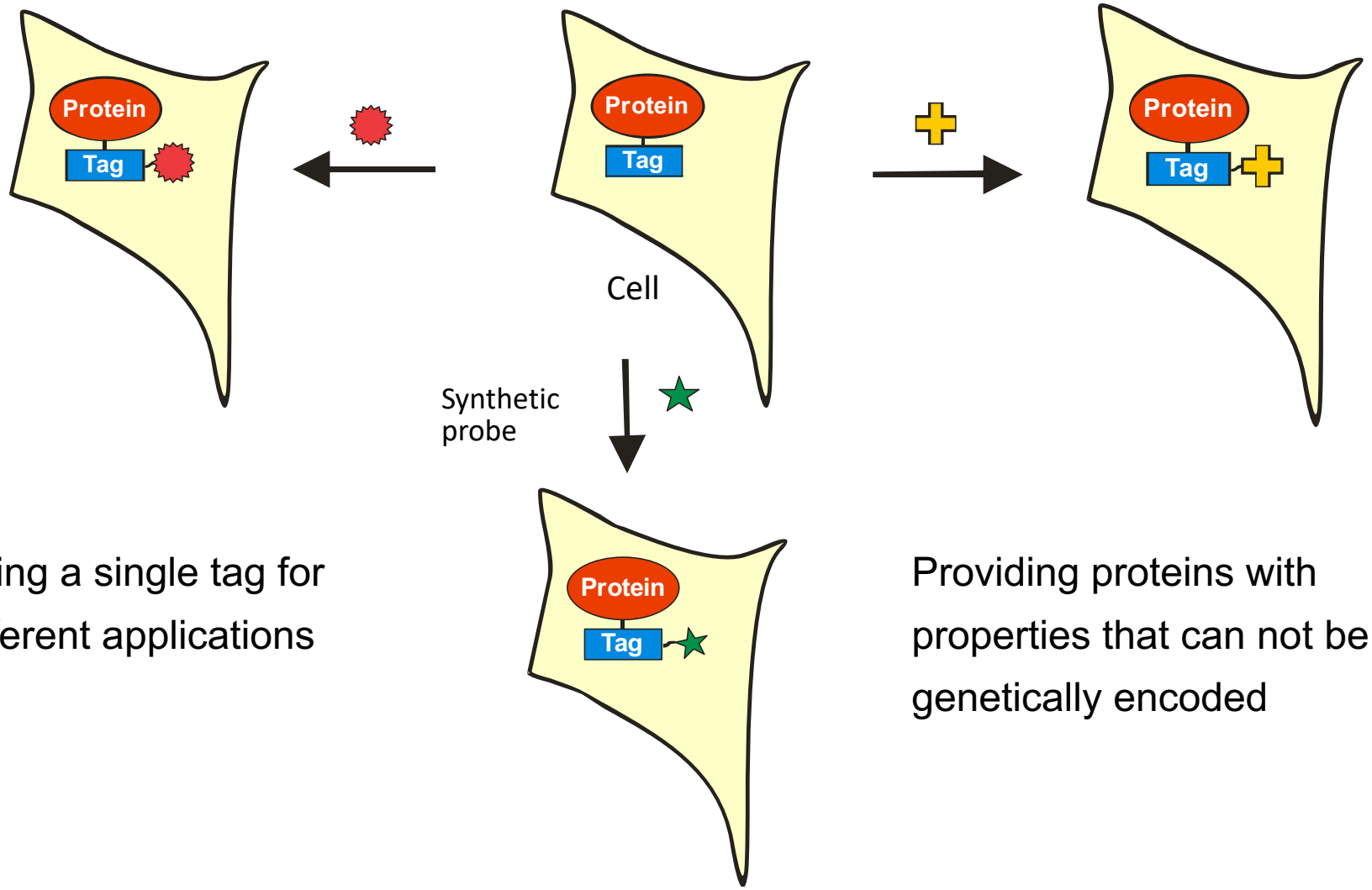

Using a single tag for different applications

Providing proteins with properties that can not be genetically encoded

Factors important for protein labeling in live cells

Specificity of the reaction

Speed of the reaction

Size of the tag

Availability of variety of different substrates

Cell permeability, toxicity, etc… of substrates

Tag-based protein labeling

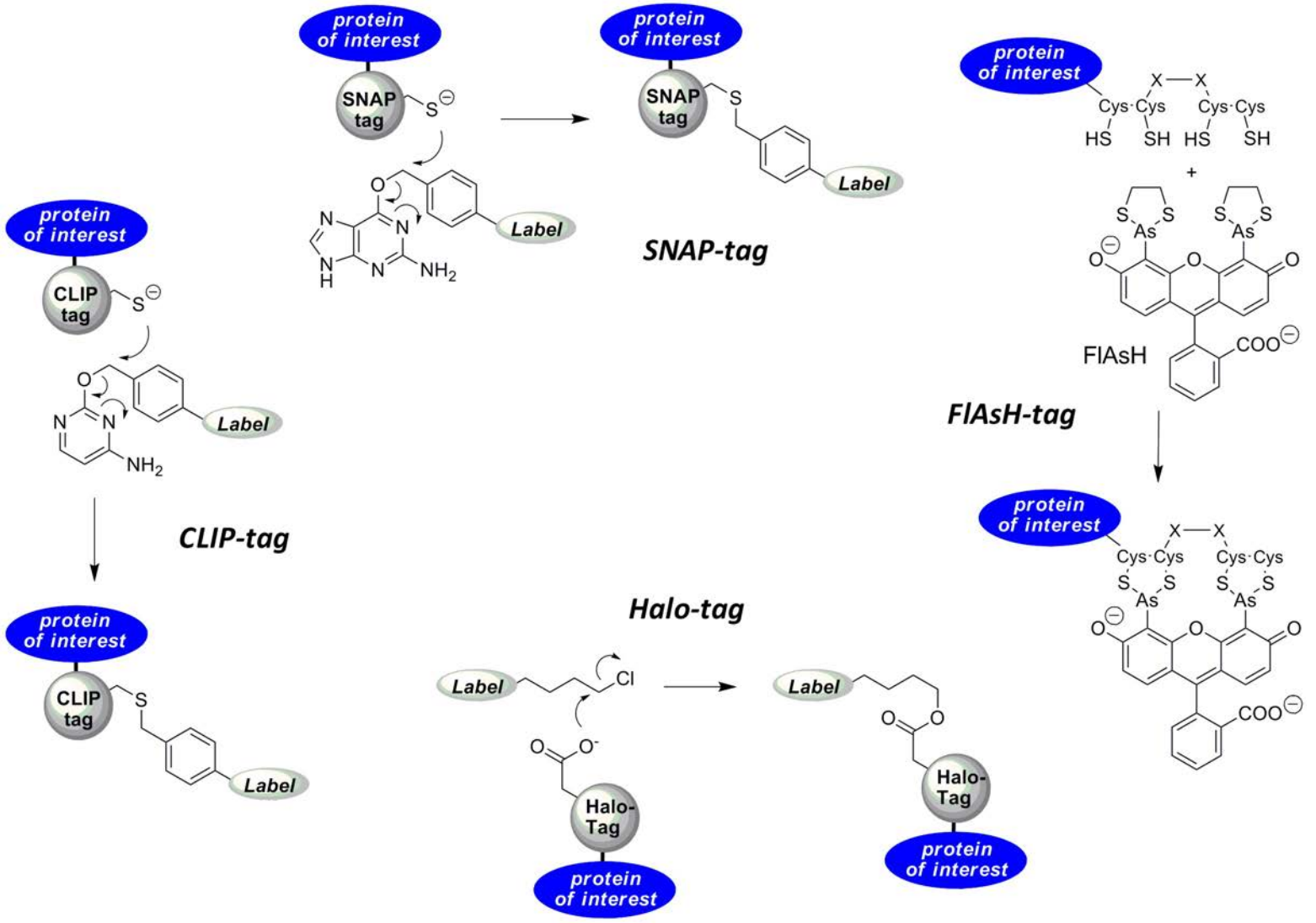

Protein labeling using the tetracysteine tag and biarsenical compounds (AKA FlAsH)

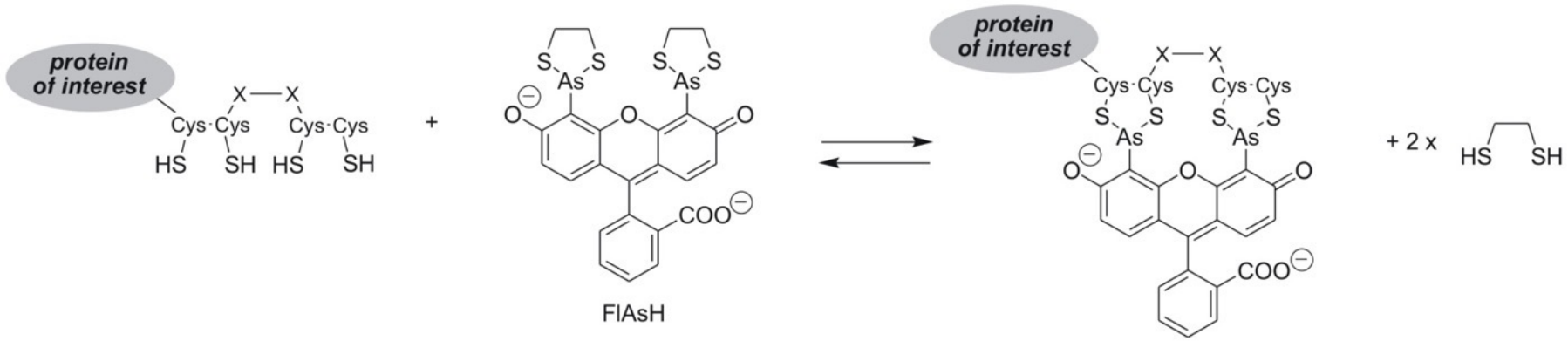

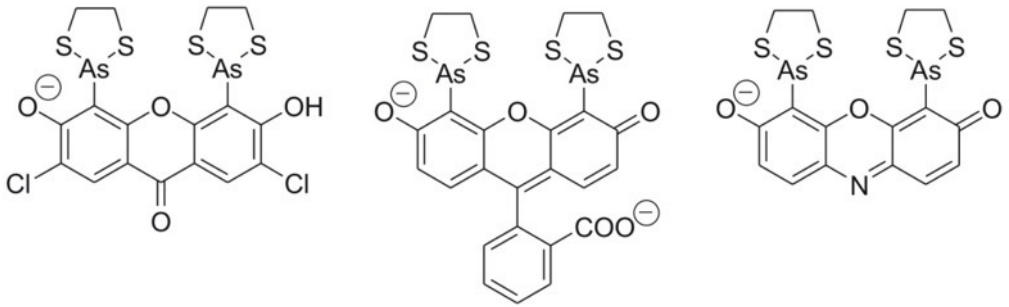

	CHoXAsH	FlAsH	ReAsH
Excitation/ Emission	380 nm/ 430 nm	508 nm/ 528 nm	593 nm/ 608 nm

Martin et al. Nature Biotech. **23**, 1308 (2005)

Binding of tetracysteine tag to biarsenical compounds increases fluorescence

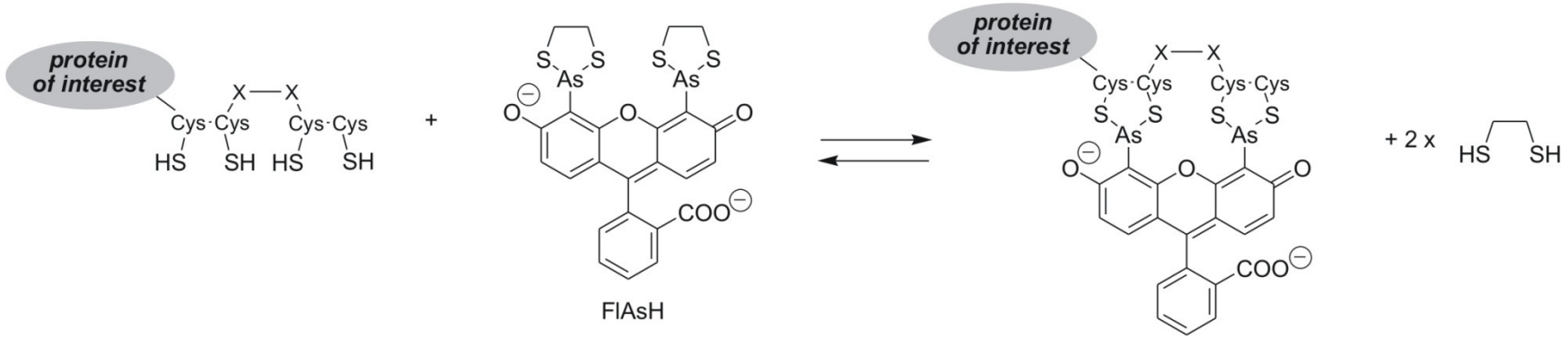

Fig. 2. Fluorescence of FLASH is induced by binding to a tetracysteine motif. (**A**) Fluorescence excitation (Exc) and emission (Em) spectra of 250 nM FLASH bound either to a model tetracysteine-containing peptide (*20*) in phosphate-buffered saline at pH 7.4 (solid lines) or to EDT at the same gain settings (dashed line, emission spectrum only). (**B**) Kinetics of binding of 1 μM FLASH to 10 μM peptide in the presence of 10 μM EDT and subsequent reversal by a higher concentration (5 mM) of EDT. The apparent fluorescence of FLASH-EDT_2 ranged from 0.05% (A) to 0.5% (B) of that of the FLASH-peptide complex and might merely reflect trace impurities such as free fluorescein.

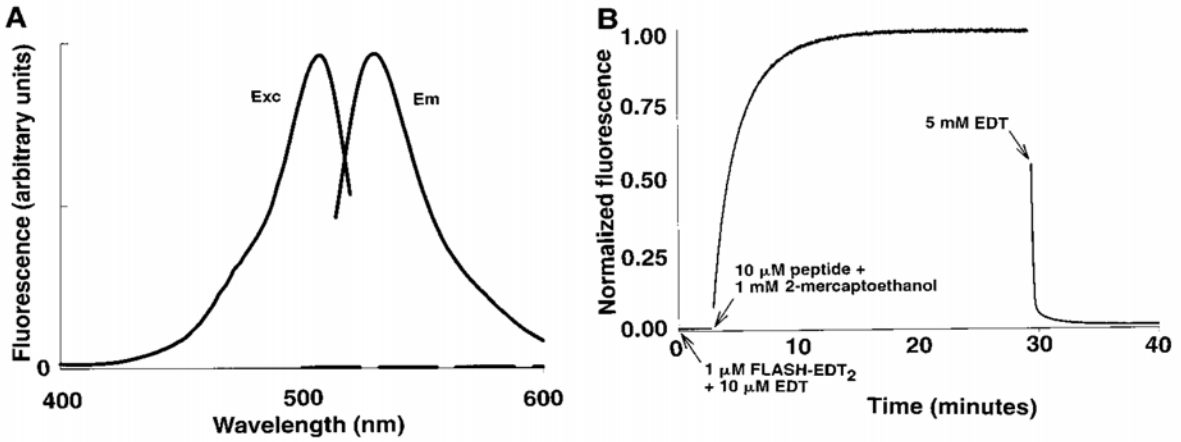

Multicolor labeling using the tetracysteine tag and biarsenical compounds

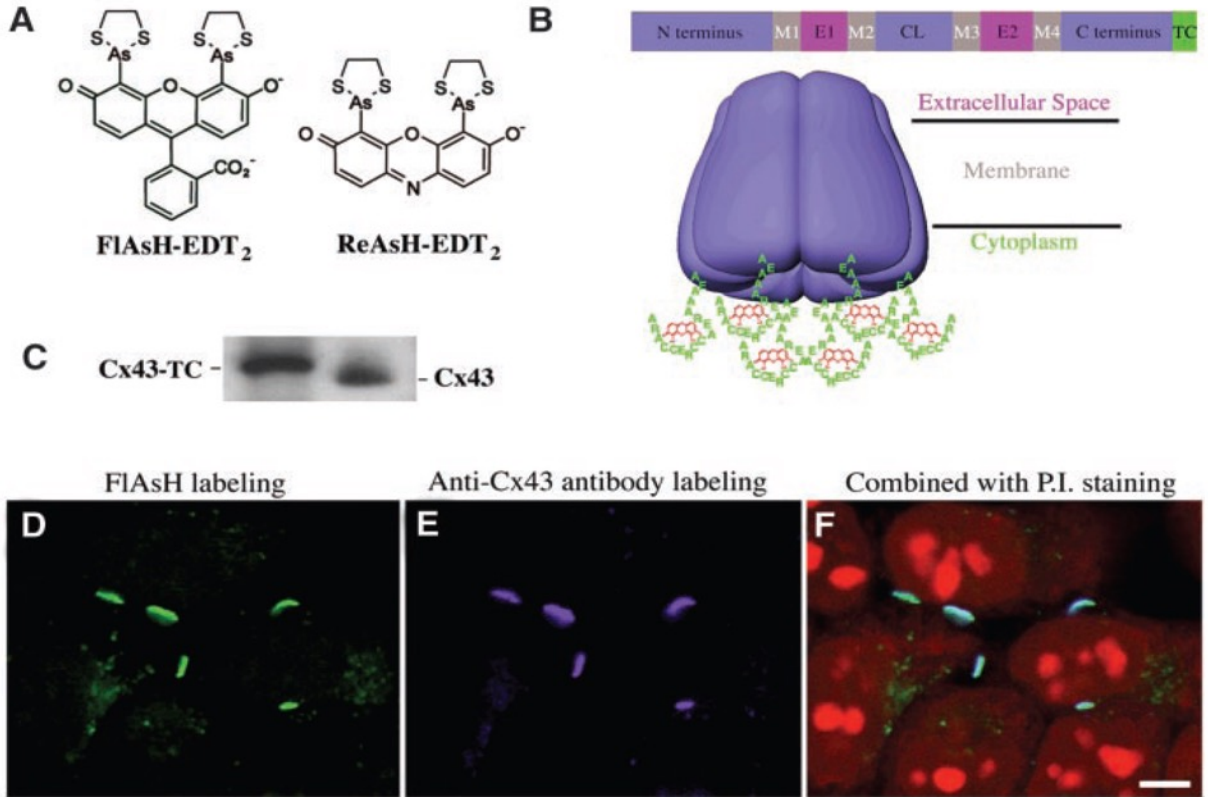

Fig. 1. Cx43-TC is expressed in HeLa cells and contributes to the formation of gap junction plaques. (**A**) Chemical structure of FlAsH-EDT$_2$ and ReAsH-EDT$_2$ ligands. (**B**) Schematic of the Cx43-TC construct. M1-4, transmembrane domains; E1-2, extracellular loop regions; CL, cytoplasmic loop; TC, tetracysteine domain; and a connexon hexamer with 6 ReAsH molecules bound to the tetracysteine domains. (**C**) Whole cell lysates from HeLa cells expressing Cx43-TC or wild-type Cx43 were Western blotted with a monoclonal antibody specific to Cx43. (**D** through **F**) pCI-neo-Cx43-TC was transfected in HeLa cells. Expression was checked 20 to 24 hours after transfection by double labeling with FlAsH-EDT$_2$ (D) and a Cx43-specific monoclonal antibody (E). Both labels recognized the same fusion protein, Cx43-TC as shown in (F). The cells were counterstained with propidium iodide (red) to highlight the cell bodies and nuclei. Bar, 5 μm.

ciencemag.org SCIENCE VOL 296 19 APRIL 2002

Multicolor labeling using the tetracysteine tag and biarsenical compounds

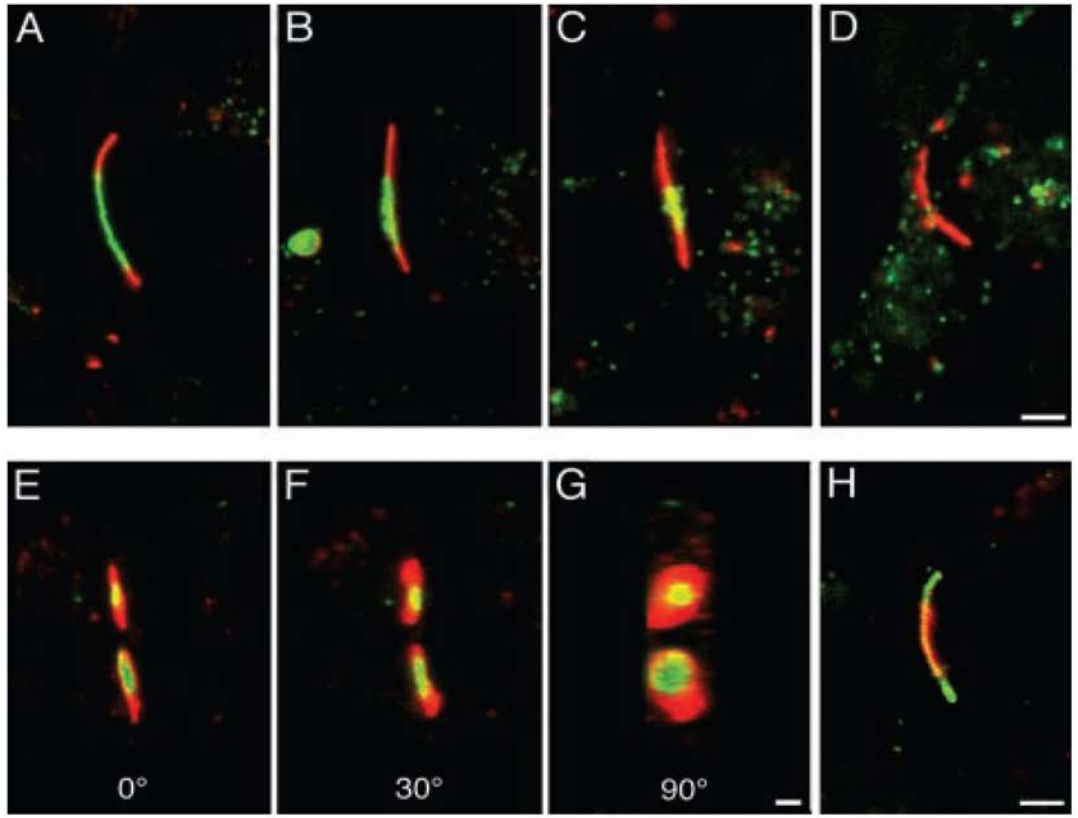

Fig. 2. FlAsH and ReAsH label two temporally separated pools of Cx43-TC and allow recording of junctional plaque renewal over time. HeLa cells stably expressing Cx43-TC were stained with FlAsH-EDT_2, incubated for 4 (**A** and **B**) or 8 (**C** and **D**) hours in complete medium at 37°C, stained with ReAsH-EDT_2, and imaged using a BioRad MRC-1024 confocal microscope. Panels (A) through (D) show Cx43-TC junctional plaques at different stages of refurbishing, as indicated by the different ratios of FlAsH (green) and ReAsH (red) stains. Panels (**E**) through (**G**) show a 3D volume projection of two Cx43-TC containing plaques rotated through various angles, from 0° to 90° showing that the newer protein (red) is added as a ring around the periphery of existing junctions (green). Reversing the order of staining with FlAsH-EDT_2 and ReAsH-EDT_2 results in the reversal of the staining pattern (**H**), showing that the color pattern reflects the age of the connexin rather than any intrinsic bias of ReAsH-EDT_2 for connexins at the periphery or FlAsH-EDT_2 for connexins at the center of a plaque. Bars, 1 μm.

SNAP-tag

DNA repair by O^6-alkylguanine-DNA alkyltransferases (AGT)

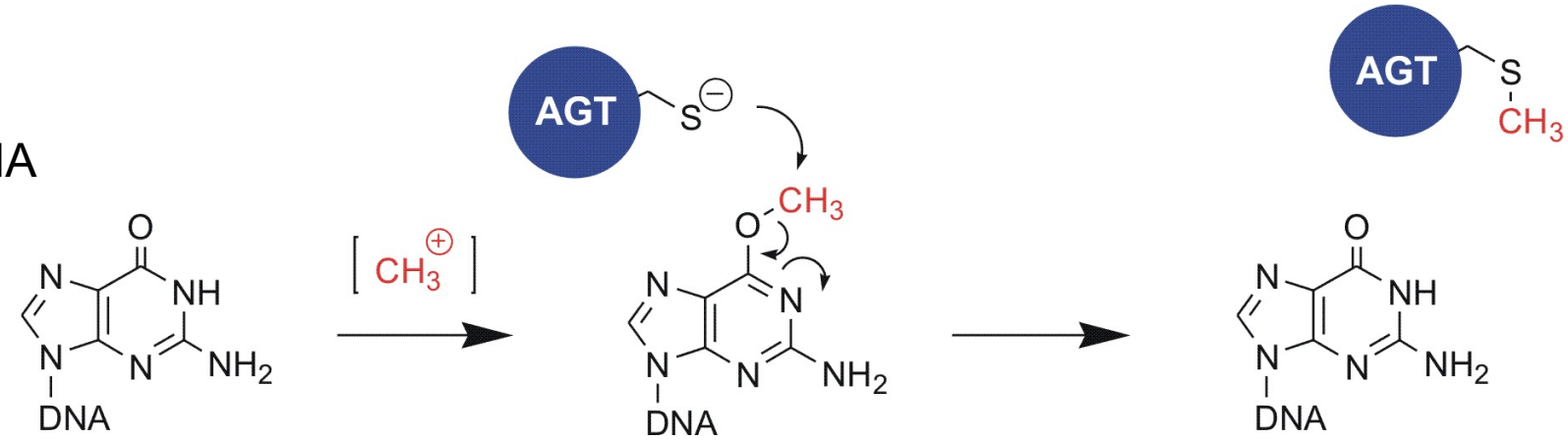

Inactivation of human AGT by benzylguanine

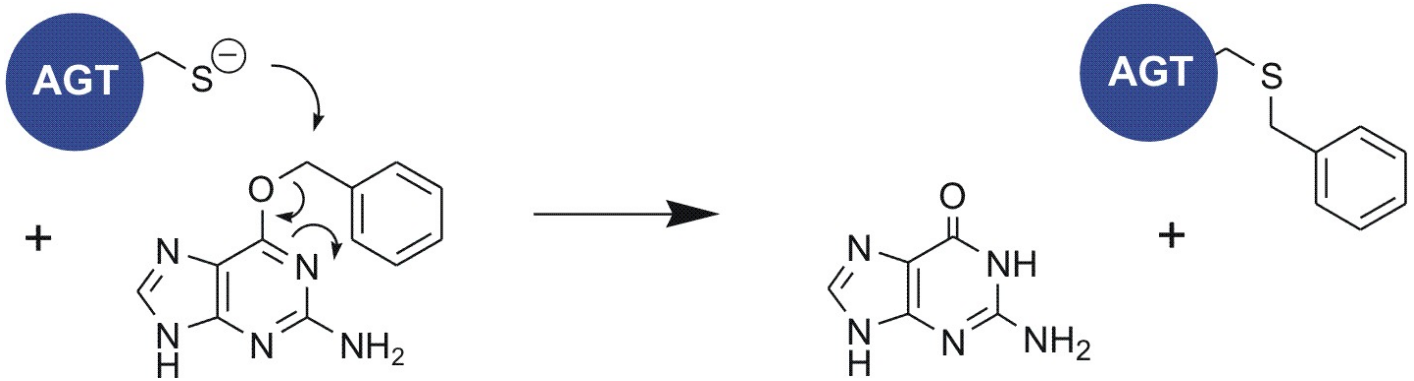

Labeling of SNAP-tag by benzylguanine derivatives

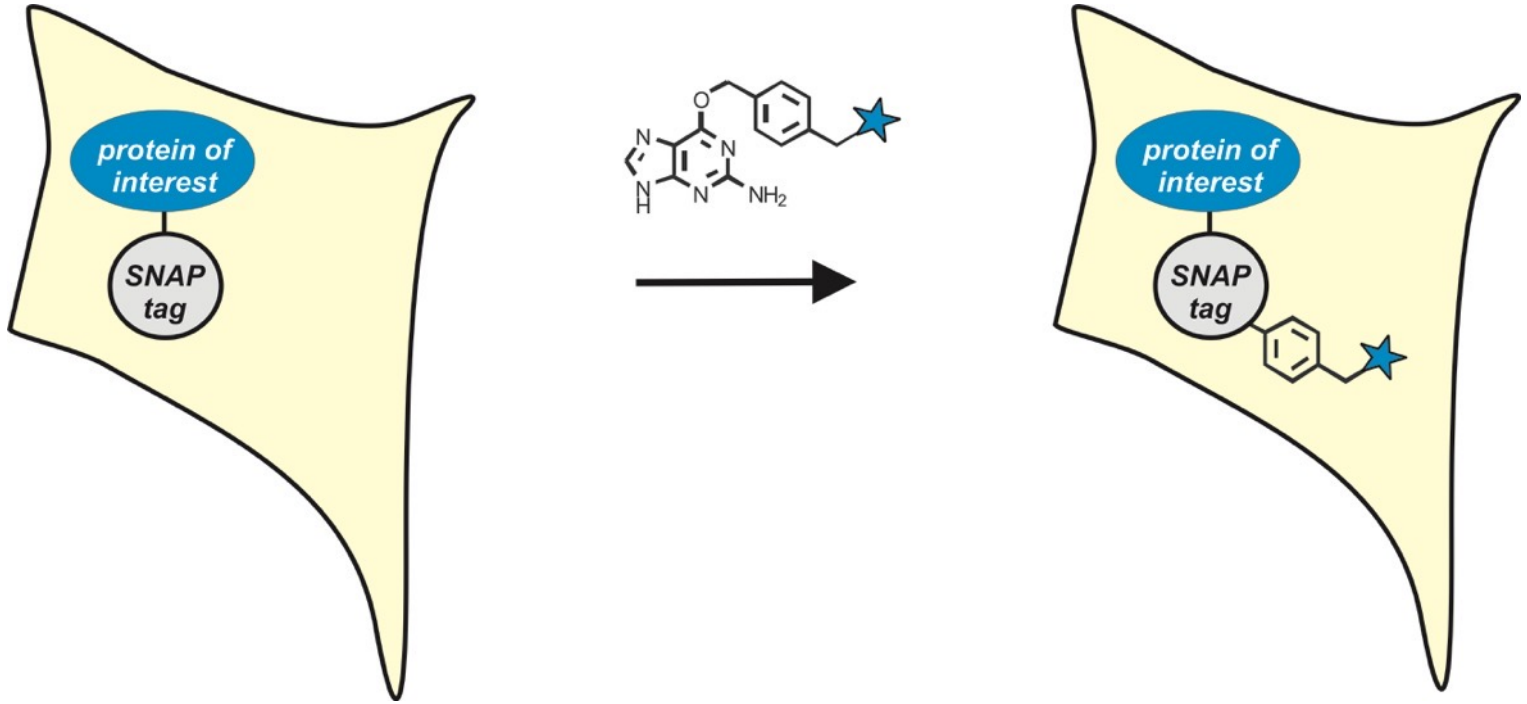

High reaction rate (up to 10^5 sec^{-1} M^{-1}) and low specificity towards label

Fluorescence labeling of SNAP-tag fusion proteins

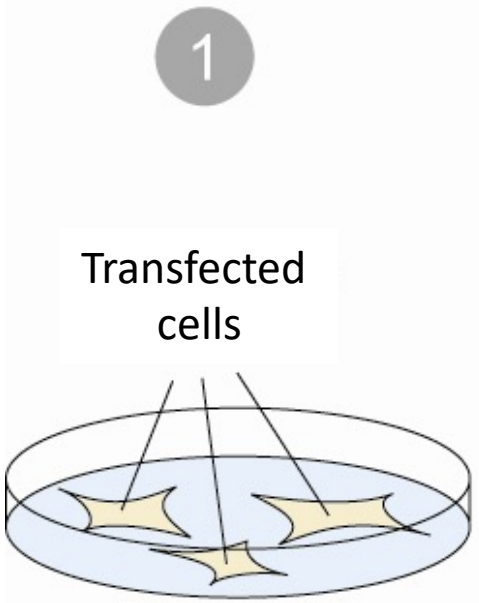

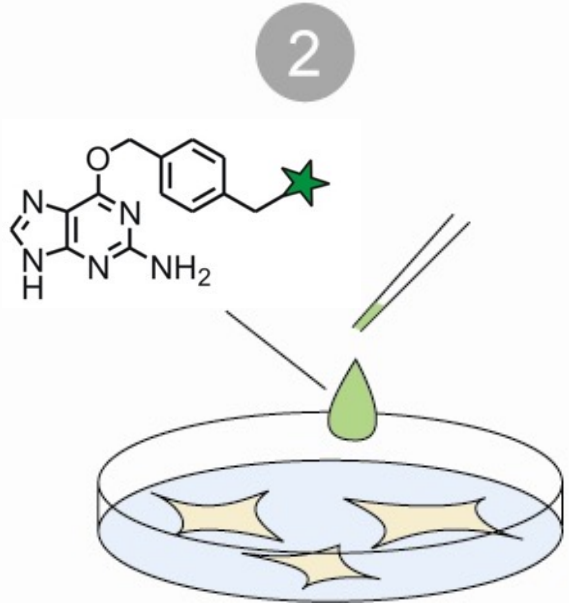

Incubation for >10 min
followed by washing

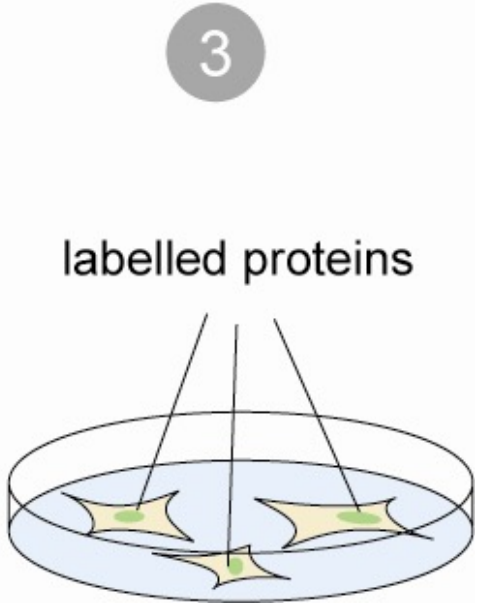

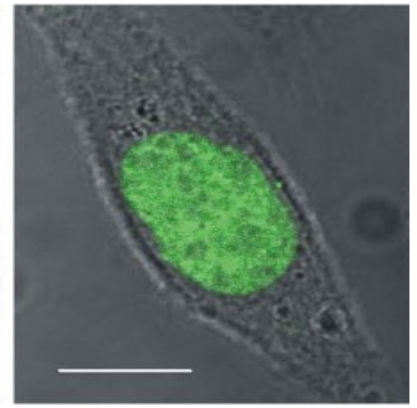

Probes for labeling of SNAP-tag fusion proteins

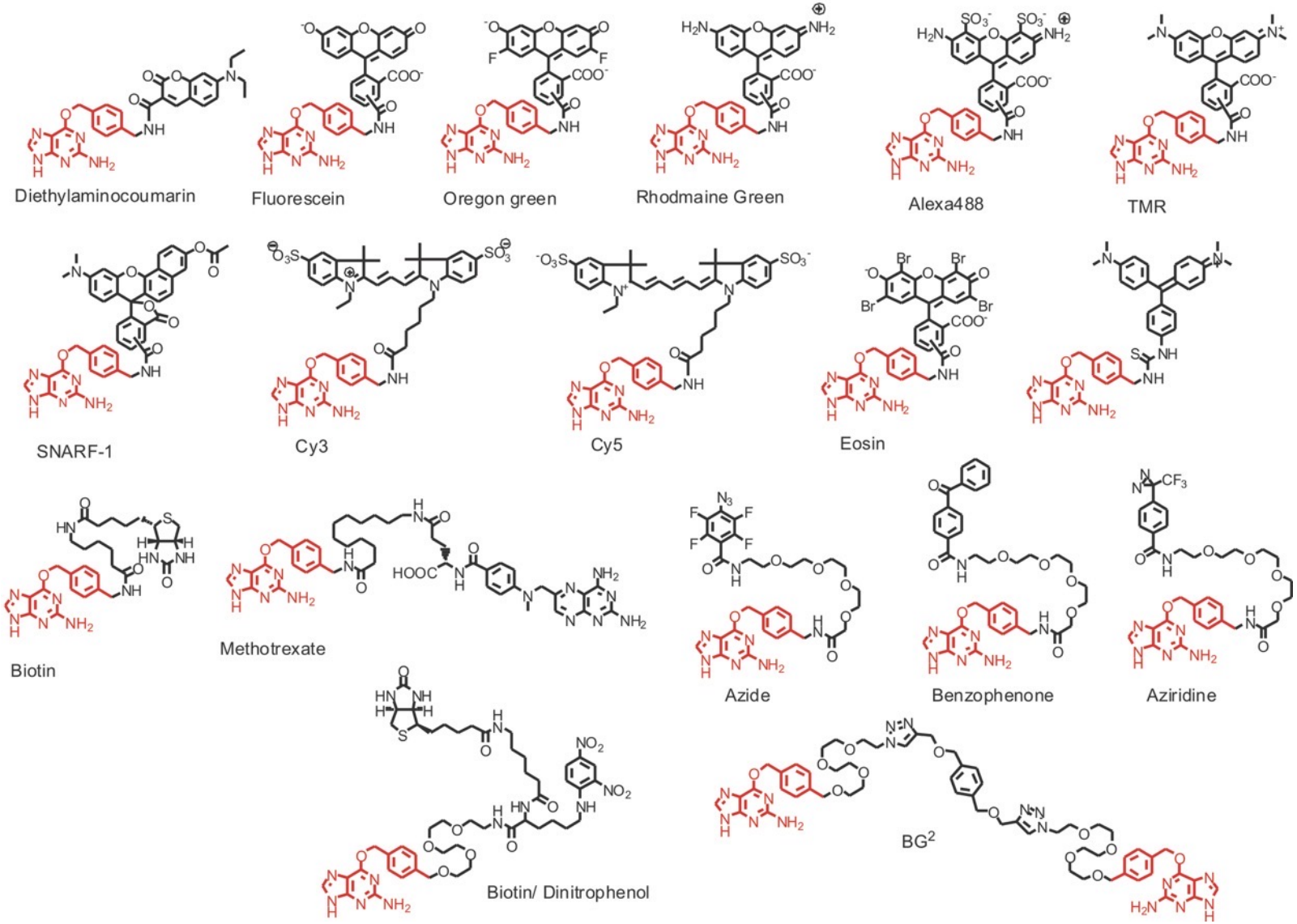

Properties of currently used SNAP-tag mutants

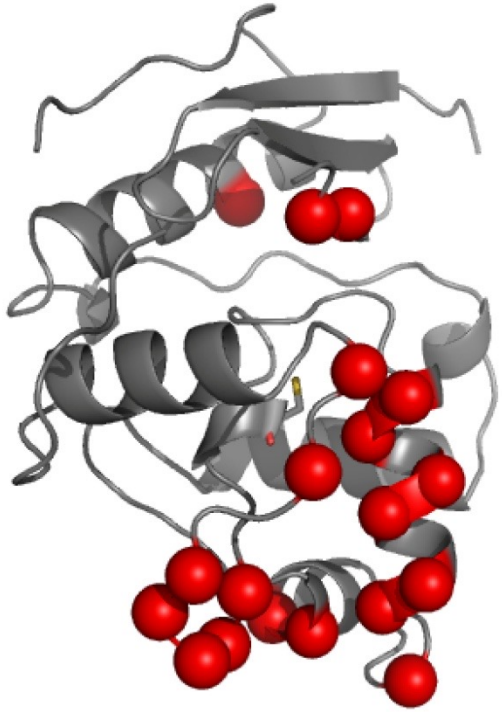

182 amino acids

monomeric

no significant affinity for DNA

up to 100x more active than wild-type

resistant to inhibitor of wild-type

fusion to N or C terminus possible

Structure of SNAP-tag C145A with bound benzylguanine

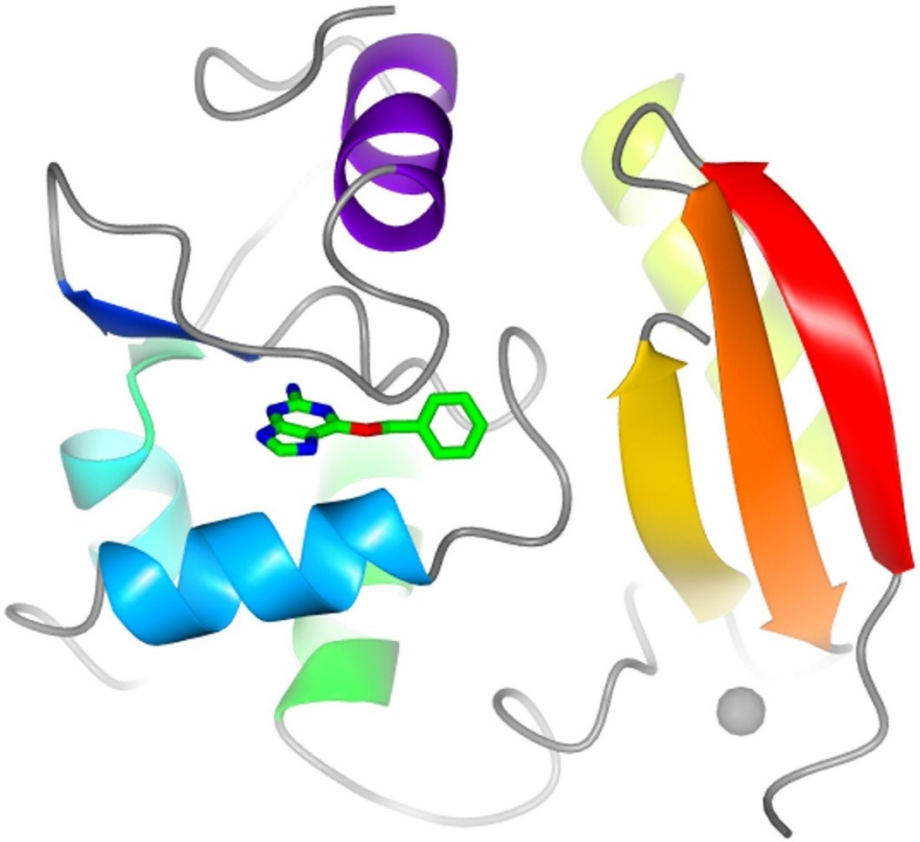

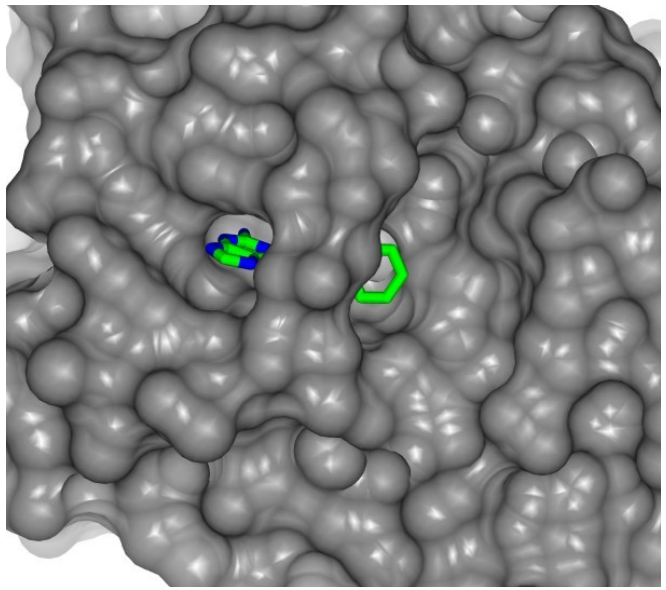

B. Mollwitz et al., Biochemistry 2013
pdbs available: 3KZY, 3KZZ, 3LOO at www.pdb.org

wtAGT undergoes a conformational change upon labeling, SNAP-tag not

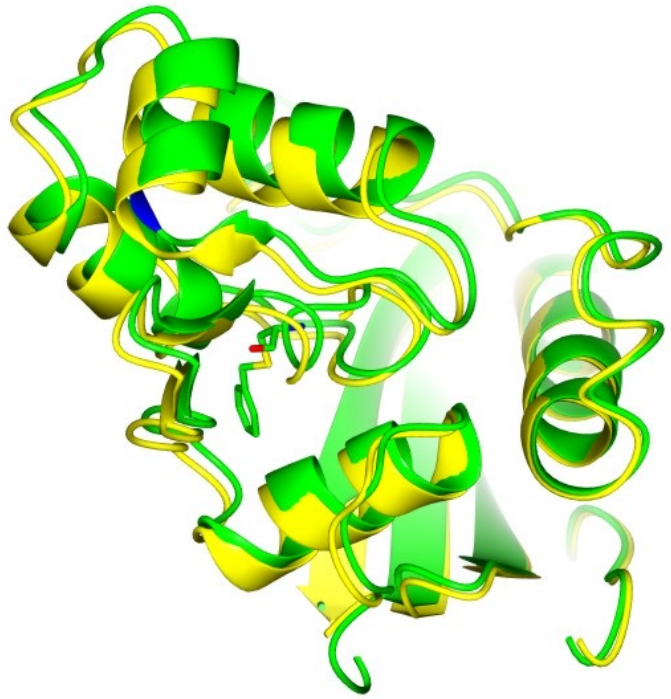

green: wtAGT
yellow: benzylated wtAGT
Daniels et al. EMBO J. 2000; **19**:1719-30

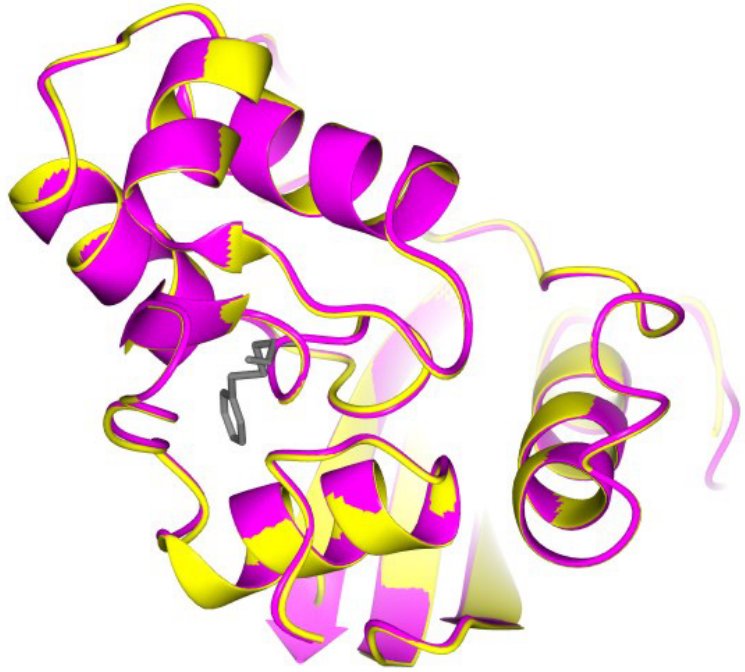

magenta: SNAP-tag
yellow: benzylated SNAP-tag

B. Mollwitz et al., Biochemistry 2013
pdbs available: 3KZY, 3KZZ, 3LOO at www.pdb.org

Labeling of SNAP-tag fusion proteins in living cells

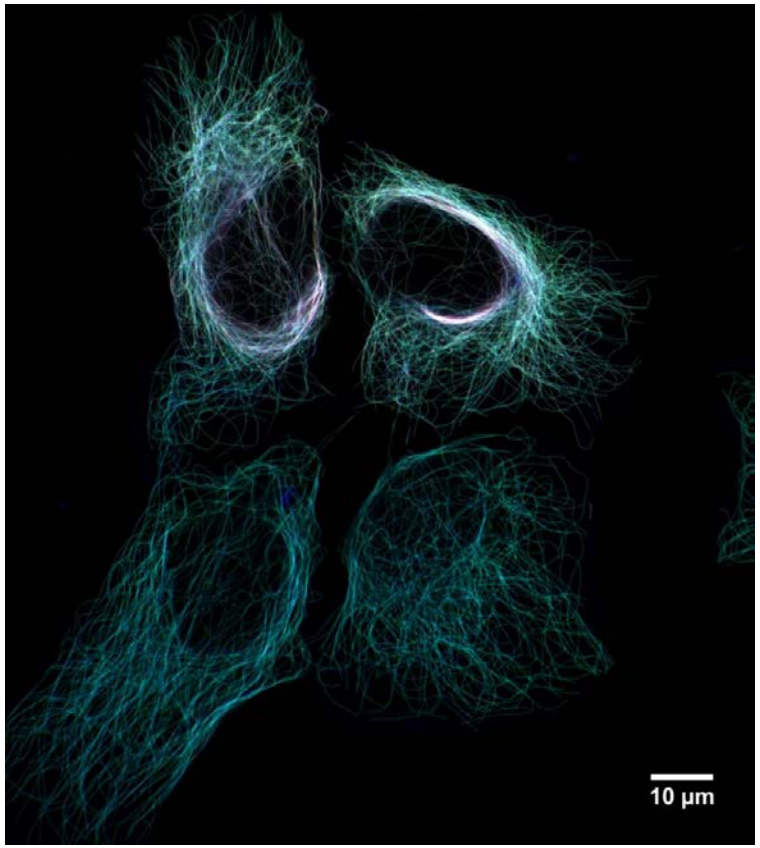

Labeling of CEP-41 with TMR in U2OS cells

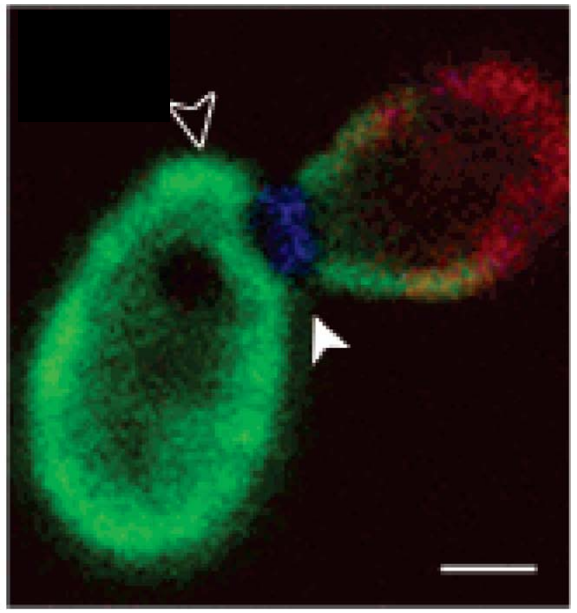

Sequential labeling of yeast Sag1p with Cy3, Cy5 and Fluorescein

Imaging of SNAP-tagged proteins in mice and zebra fish embryos

4 nmol BG-782
24h

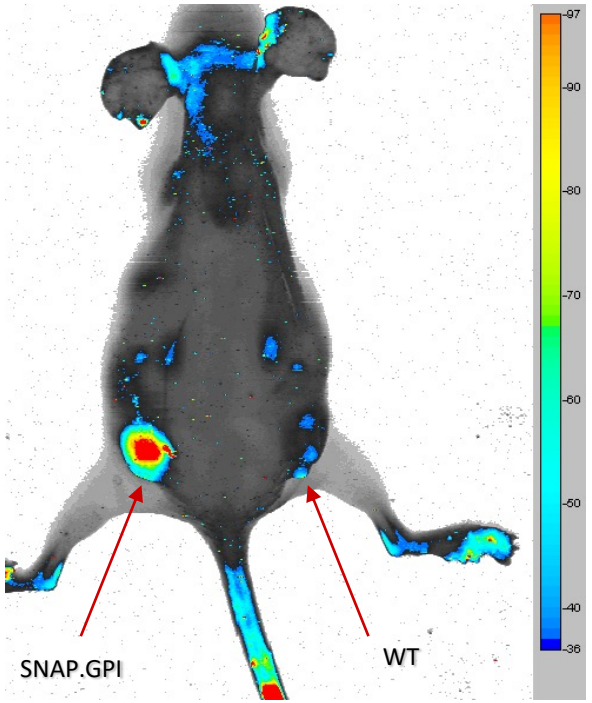

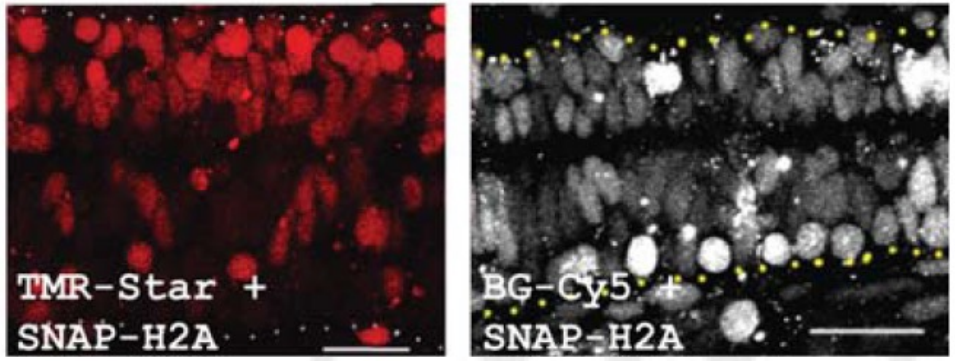

Projection of 5 planes in the spinal cord; 36-hpf embryos; anterior to the left; scale bars = 20 μm. *Developmental Dynamics*; in press

Cell-surface protein-protein interaction analysis with time-resolved FRET and snap-tag technologies: application to GPCR oligomerization

Damien Maurel[1–5], Laëtitia Comps-Agrar[1,2,5], Carsten Brock[1,2], Marie-Laure Rives[1,2], Emmanuel Bourrier[3], Mohammed Akli Ayoub[1,2], Hervé Bazin[3], Norbert Tinel[3], Thierry Durroux[1,2], Laurent Prézeau[1,2], Eric Trinquet[3] & Jean-Philippe Pin[1,2]

Nature Methods, **5**, 561 (2008)

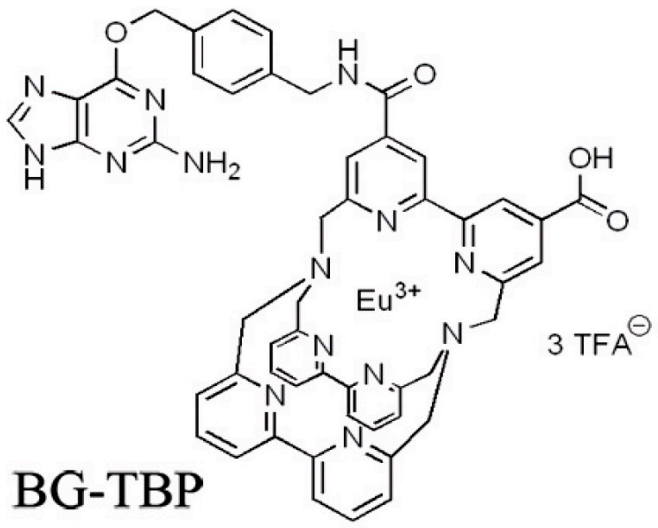

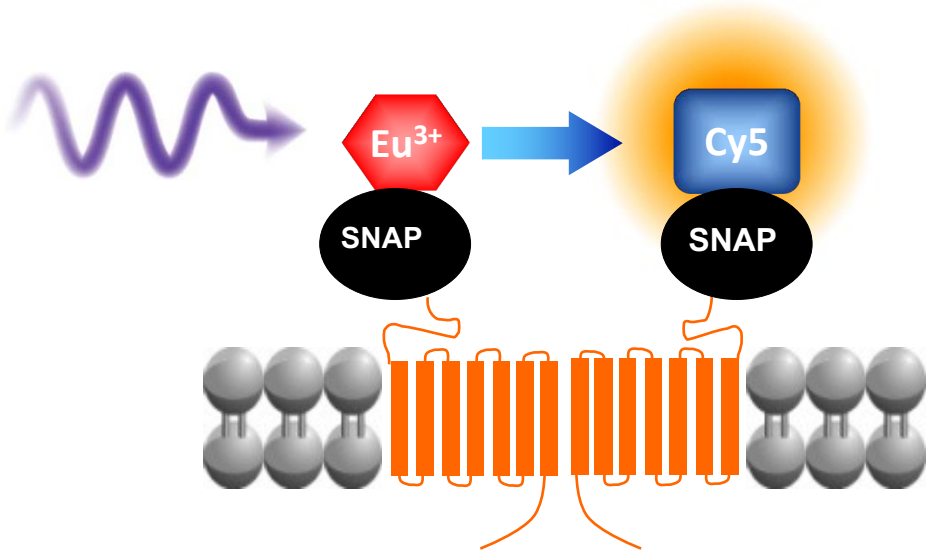

A fluorogenic probe for plasma membrane proteins based on Nile Red

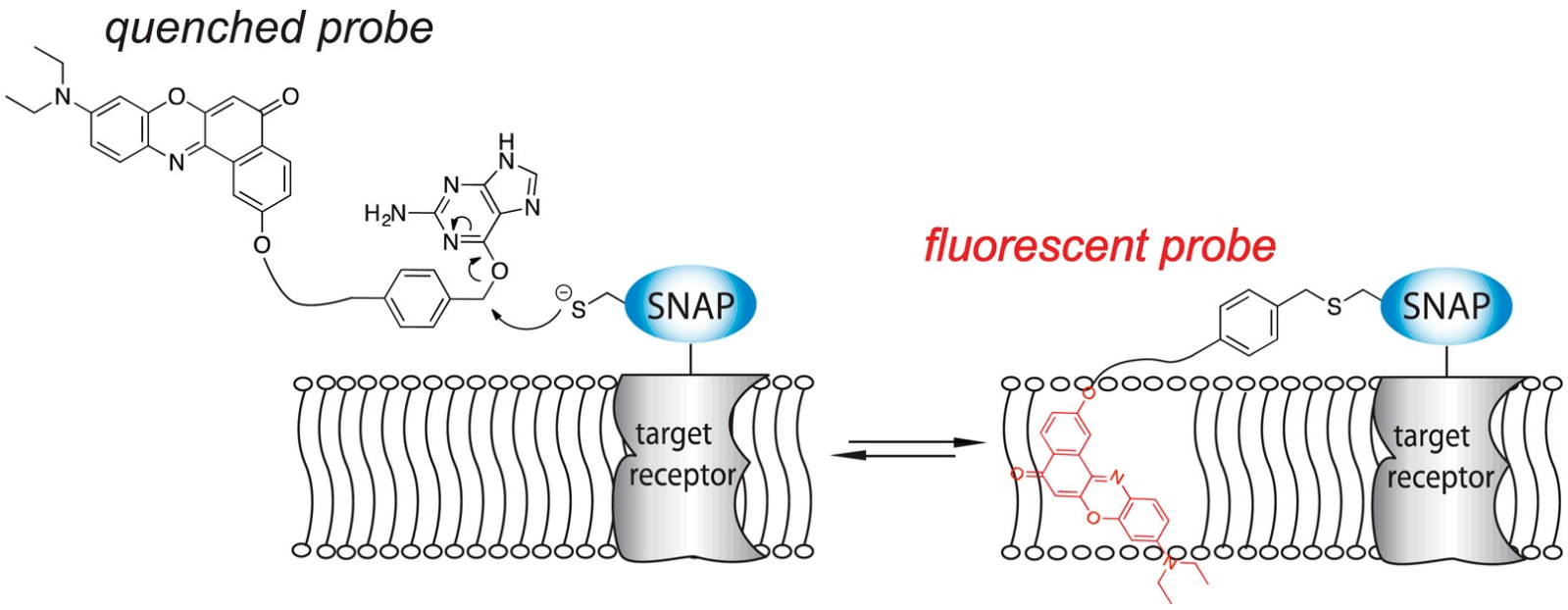

ACS Chemical Biology 2014

Localizable BODIPY-based calcium sensors

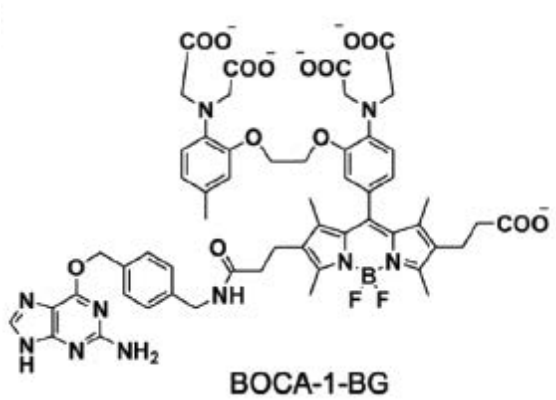

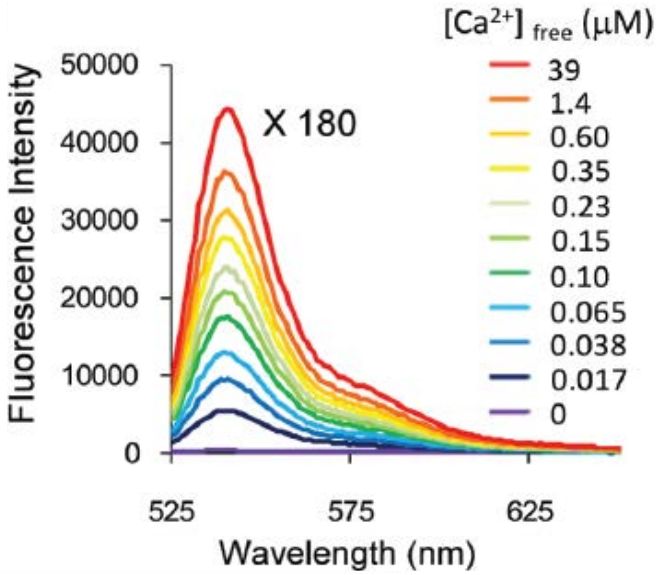

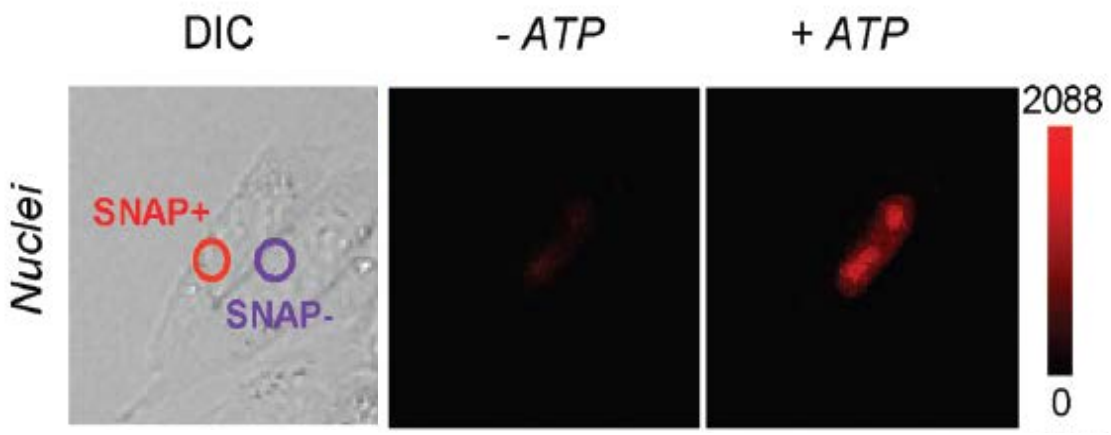

Analytical Chemistry, **82**, 6472-9 (2010)

Simultaneous labeling of two different fusion proteins

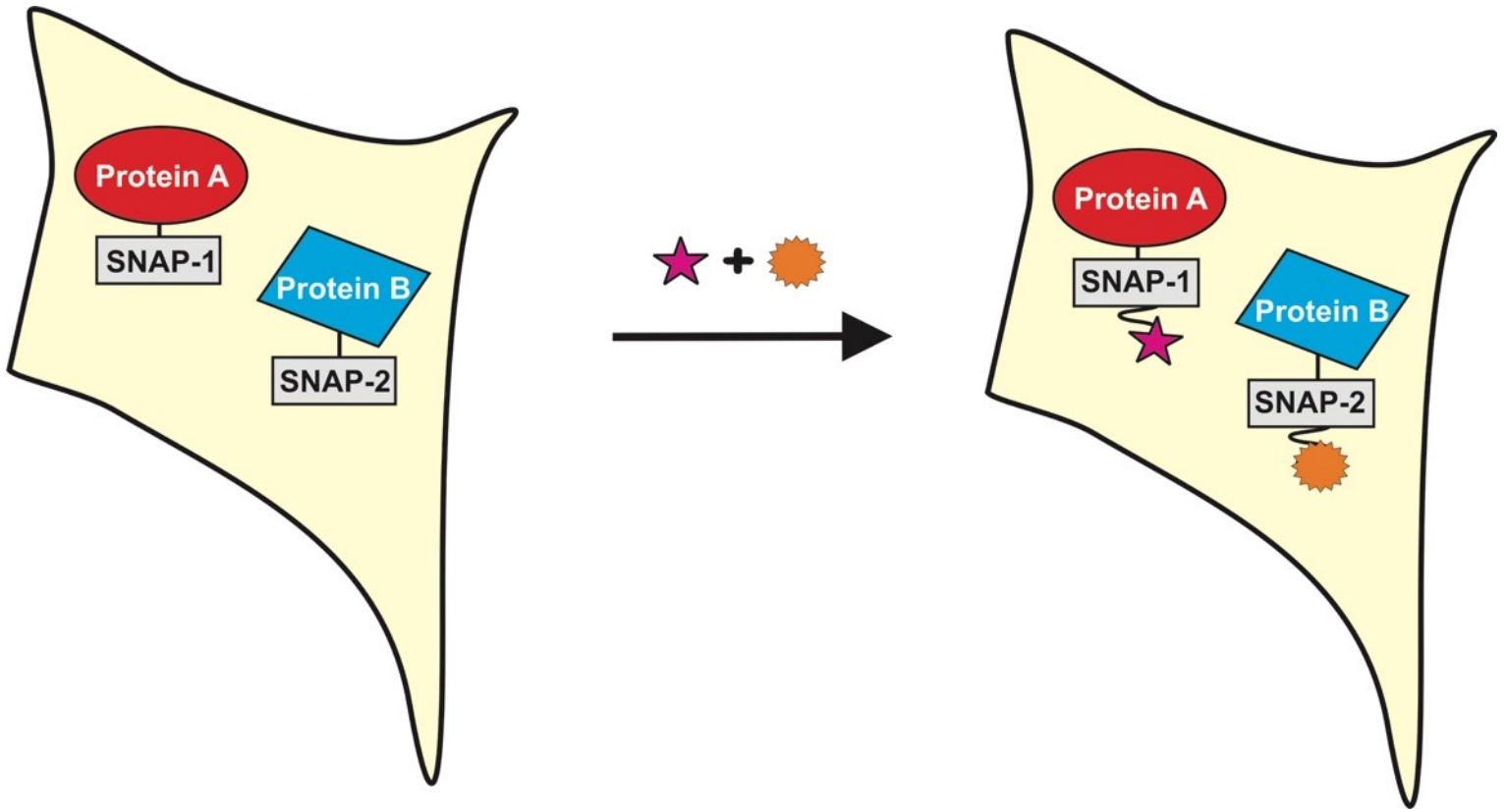

How could you develop an “orthogonal” SNAP-tag mutant?

See also A. Gautier et al. Chemistry&Biology **15**, 128-63 (2008)

Creating orthogonal SNAP-tag-substrate pairs

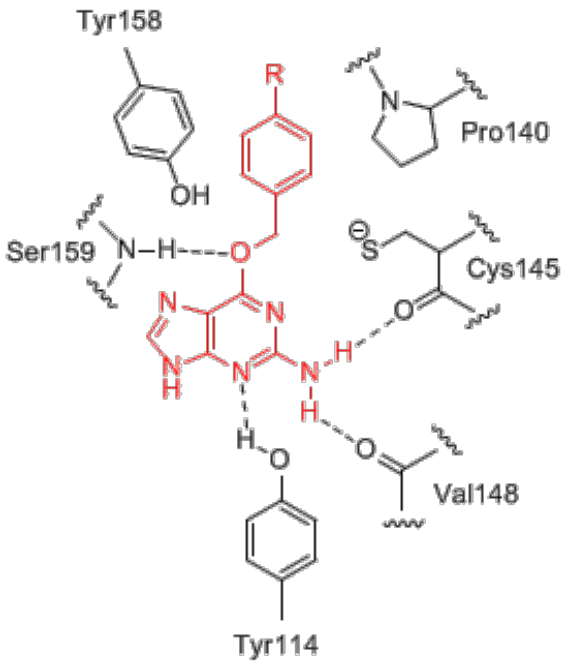

Benzylguanine (BG)

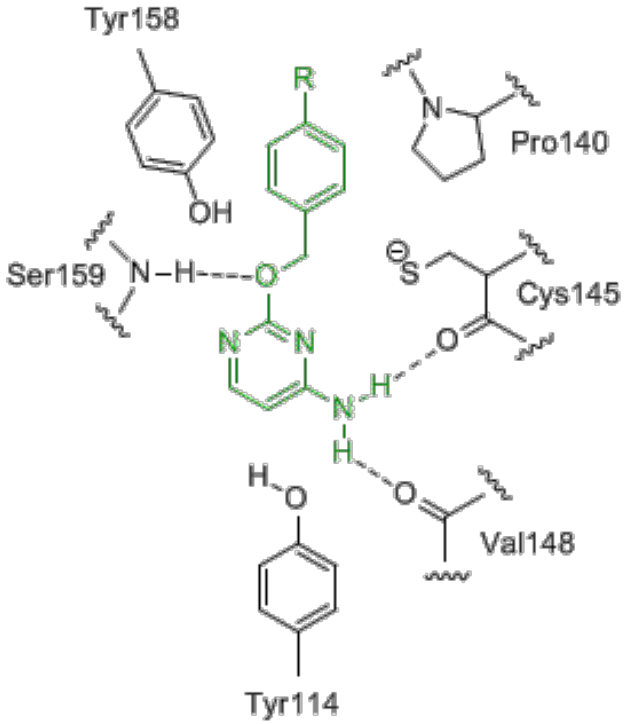

Benzylcytosine (BC)

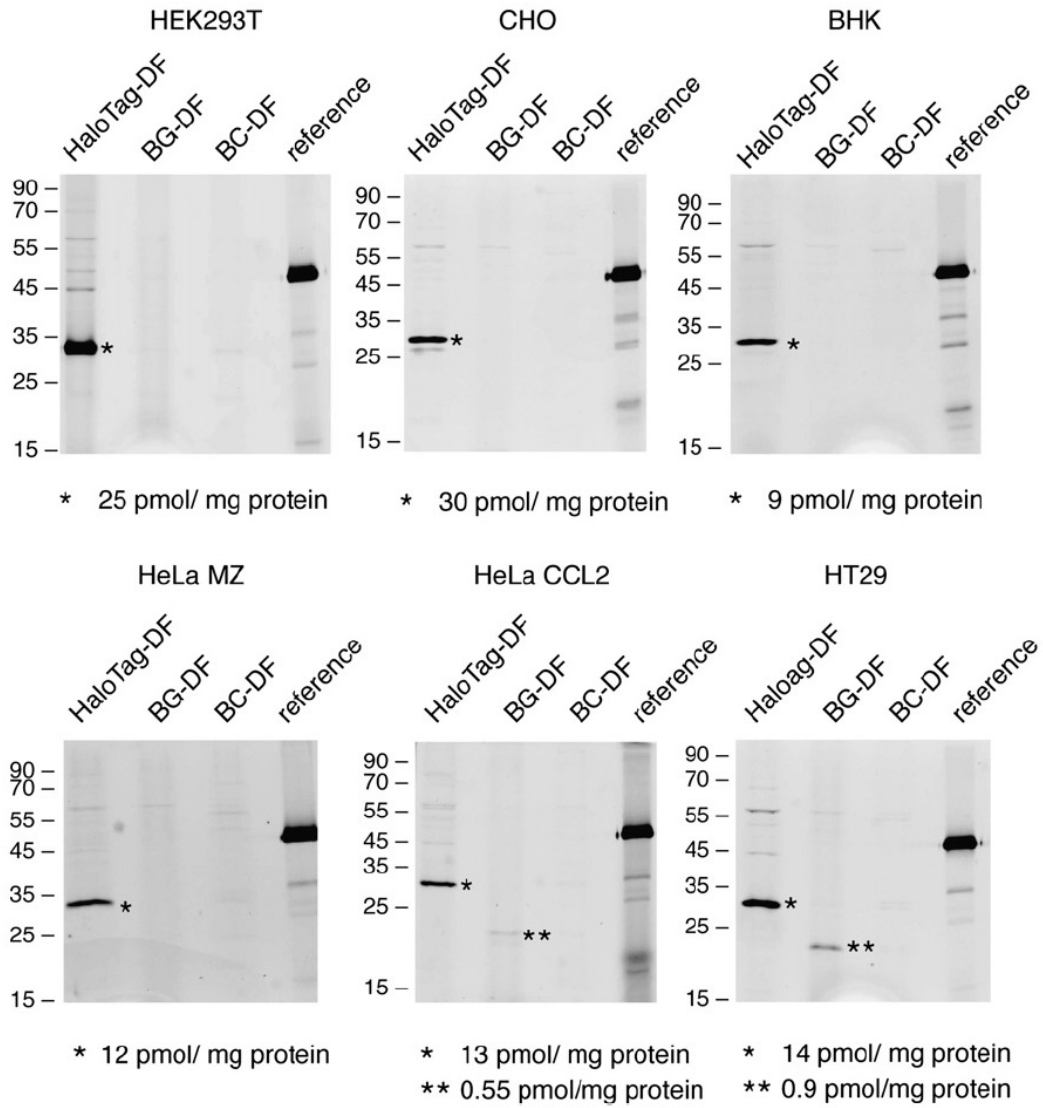

Figure 2. Reactivity of BC-DF, BG-DF, and HaloTag-DF with the Mammalian Proteome

Cells were incubated with 10 μM substrate for 1 hr at 37°C. After cell lysis, equal amounts of protein from crude extracts were analyzed by SDS-PAGE and in-gel fluorescence scanning. The 28 kDa endogenous protein labeled with fluorescein by HaloTag-DF (*) and the endogenous AGT labeled with BG-DF (**) were quantified (in pmol/mg of soluble extract) by comparison with the fluorescence intensity of a known amount of fluorescein-labeled GST-SNAP (reference).

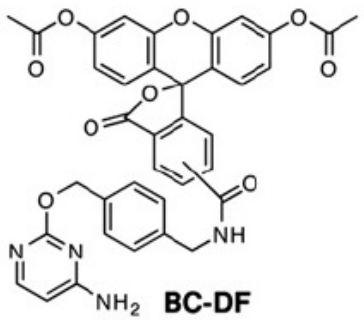

Phage display of proteins and peptides

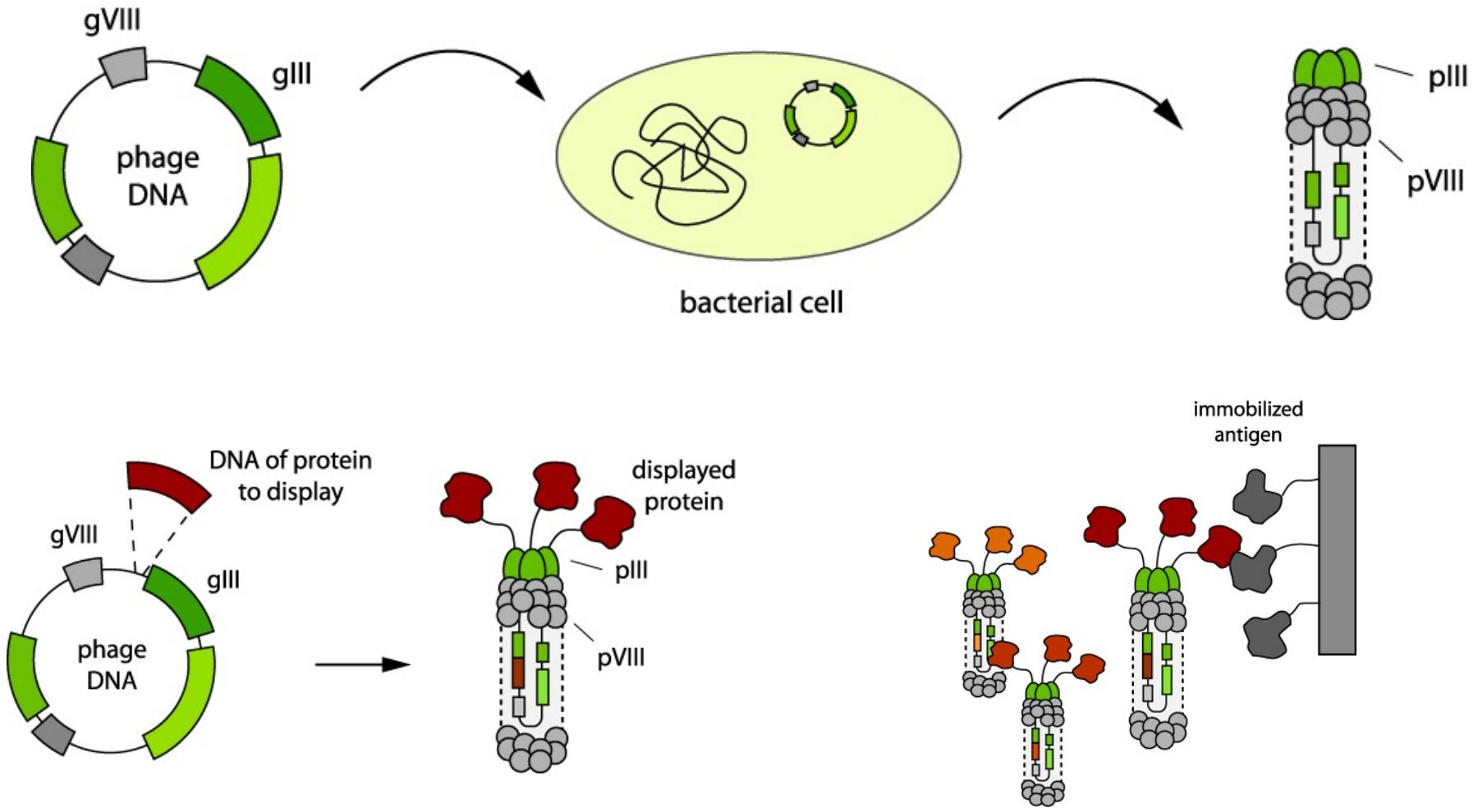

Images from C. Heinis

Table 1. Key AGT Mutants Described in This Work

Name	Description	Mutations/SNAP-tag	k_{BCFL} ($M^{-1}s^{-1}$)	k_{BGFL} ($M^{-1}s^{-1}$)	$[Urea]_{1/2}$ (M)
SNAP-tag	Previously described tag with 50-fold enhanced activity toward BG derivatives compared to wild-type AGT (Gronemeyer et al., 2006)	None	26 ± 5	2.8×10^4	6.3 ± 0.1
Mut1	Mutant selected by yeast display from a saturation mutagenesis library based on SNAP-tag	Y114E, K131N, S135D, G157P, E159F	90 ± 15	≤1	4.1 ± 0.2
CLIP-tag	Mutant selected by phage display from a random mutagenesis library based on Mut1	M60I, Y114E, A121V, K131N, S135D, L153S, G157P, E159L	1130 ± 150	≤10	5.1 ± 0.2

For each mutant, mutations relative to parental SNAP-tag, the second-order rate constants of the labeling reactions with BG-FL and BC-FL (k_{BGFL} and k_{BCFL}), and the urea concentrations necessary for 50% inactivation of protein ($[urea]_{1/2}$) are listed. Data represent mean ± SD.

Dual labeling with CLIP-tag and SNAP-tag

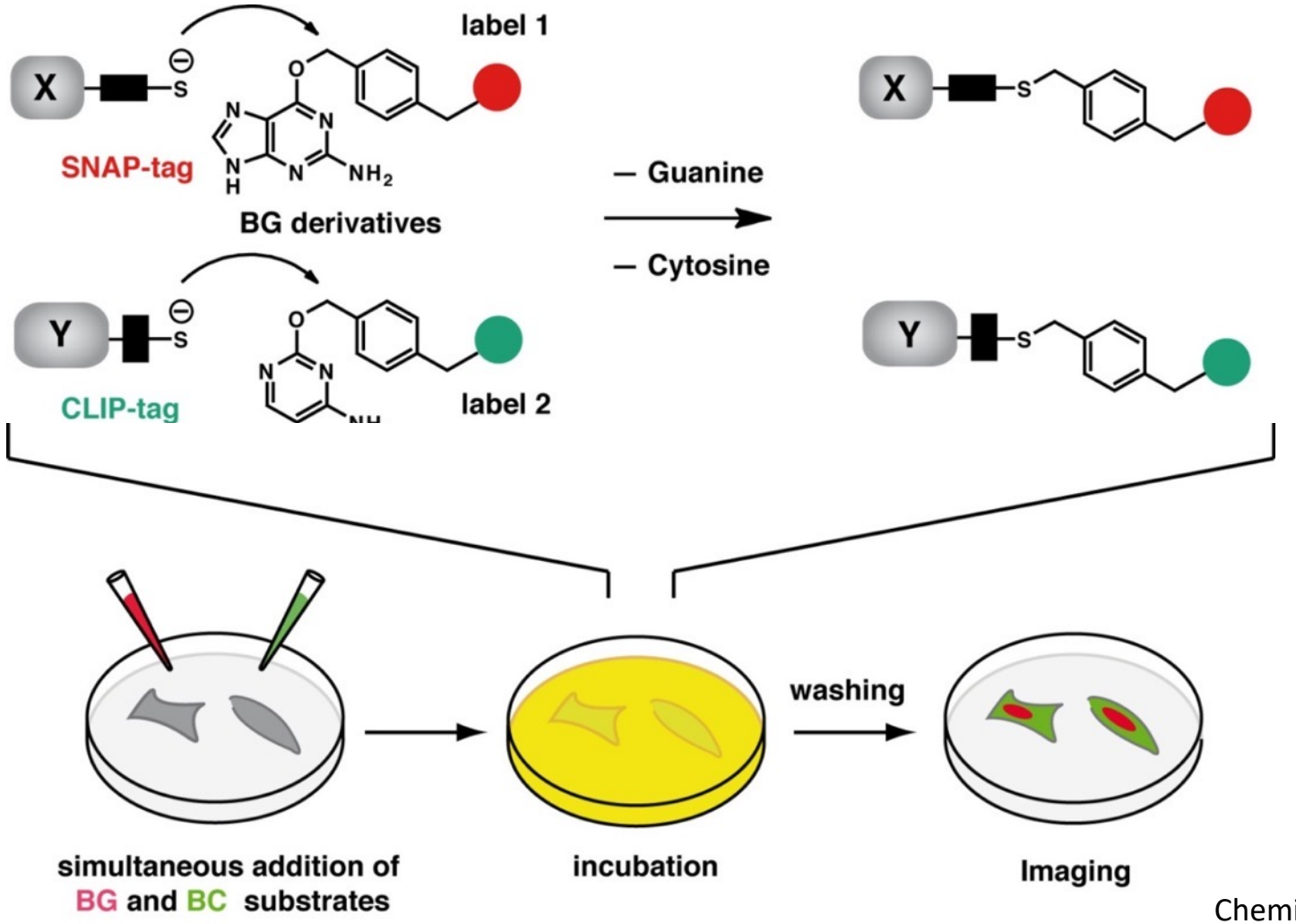

Chemistry & Biology **15**, 128-136 (2008)

Pulse-chase labeling

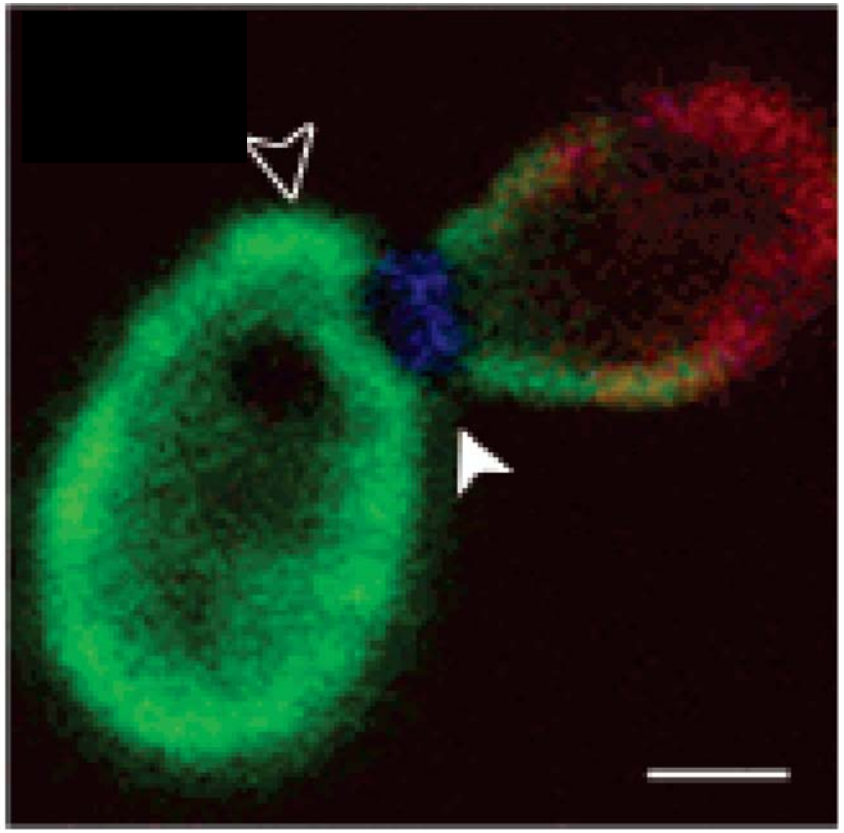

Localization of cell wall growth in Saccharomyces cerevisiae

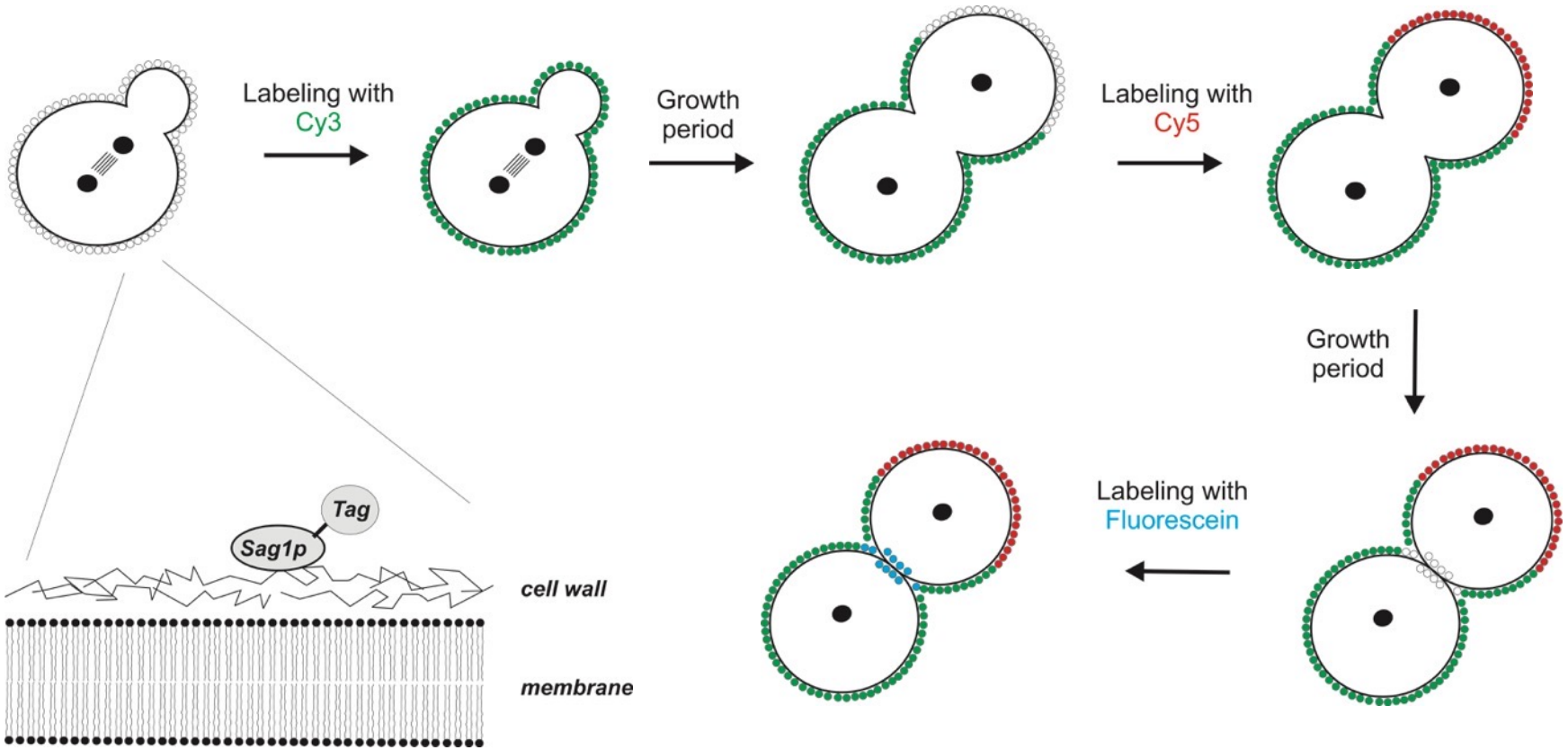

Localization of cell wall growth in Saccharomyces cerevisiae

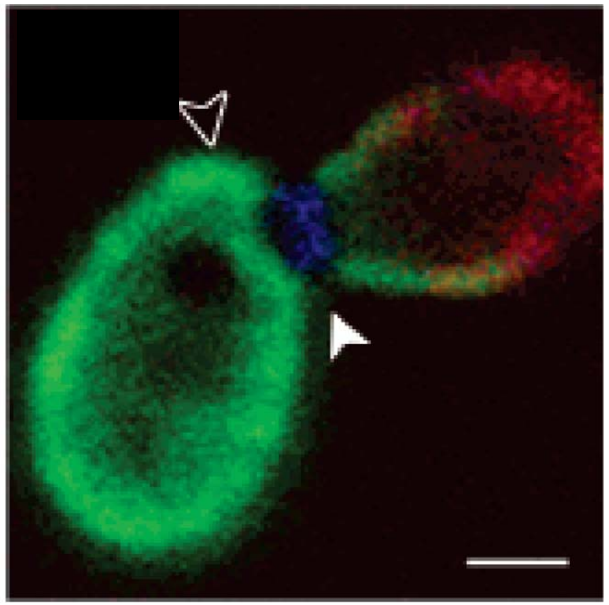

Sequential labeling of Sag1p with Cy3, Cy5 and Fluorescein

Tag-based protein labeling

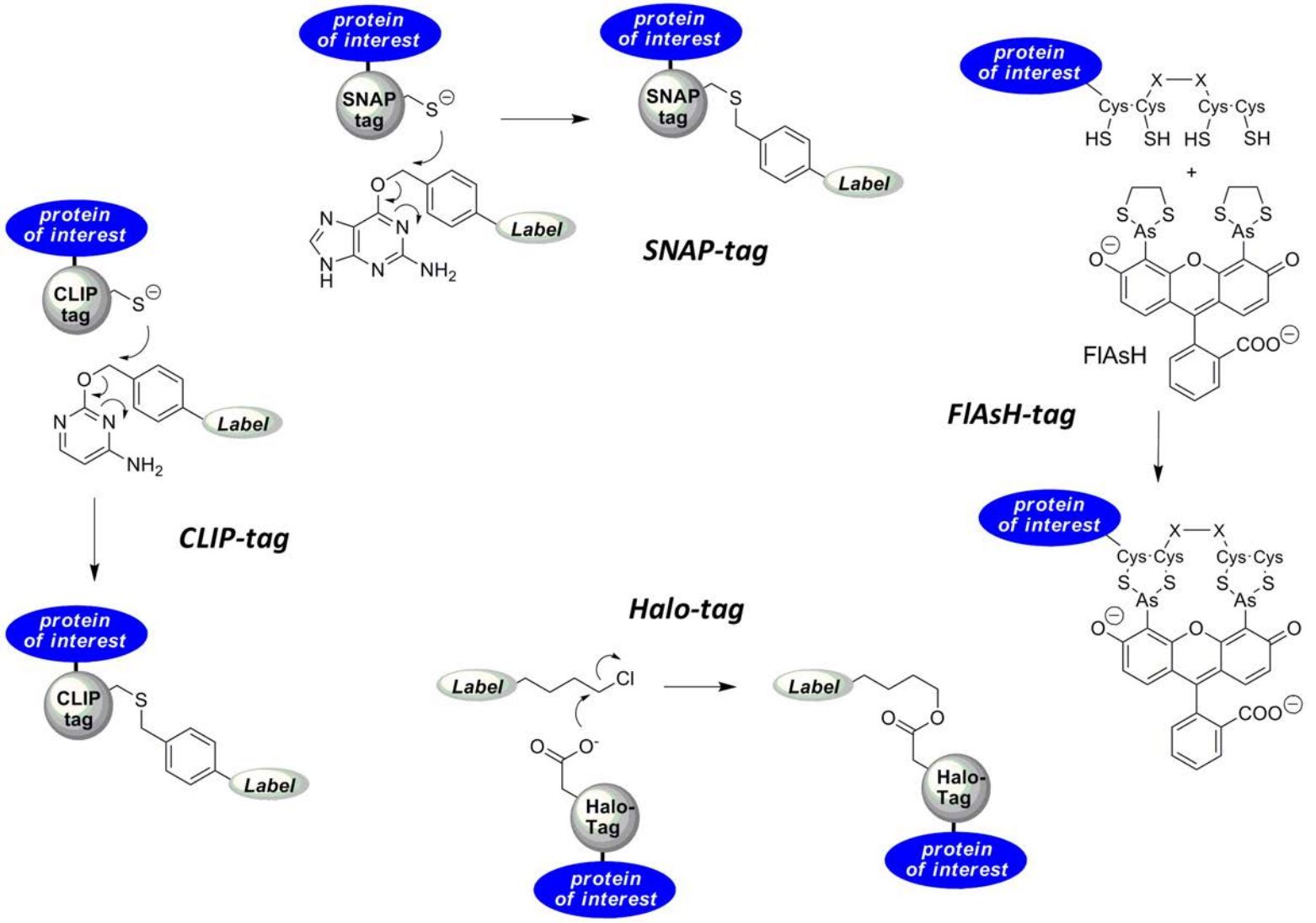

HaloTag7 reacts extremely fast with rhodamines

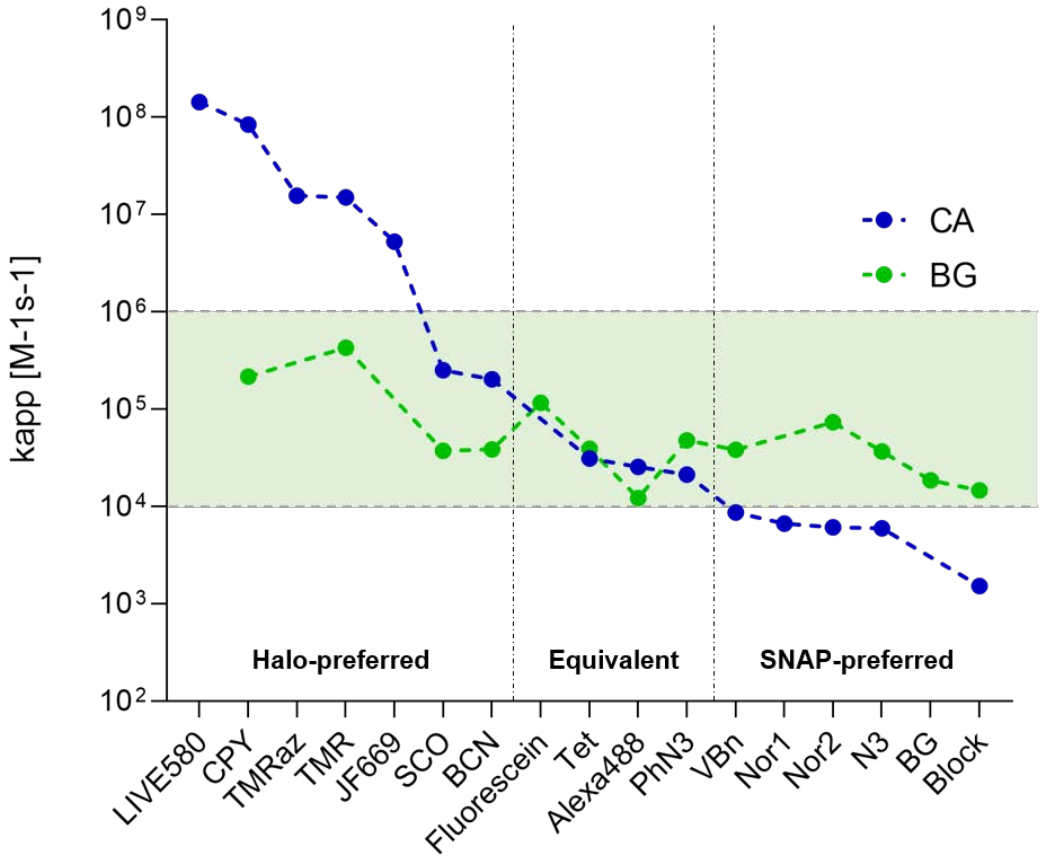

SLP substrate moiety

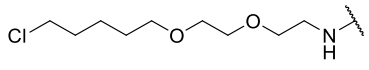

CA-

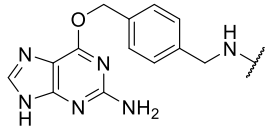

BG-

Fluorophore substrates

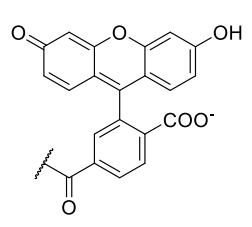

Fluorescein

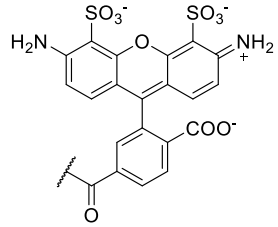

Alexa488

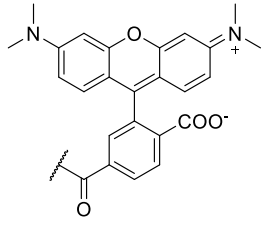

TMR

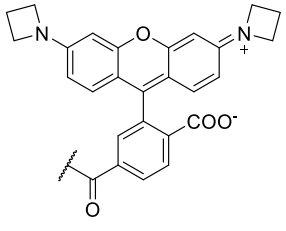

TMRaz

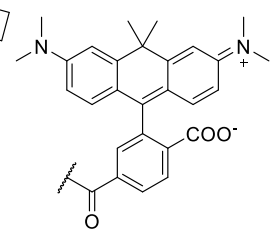

CPY

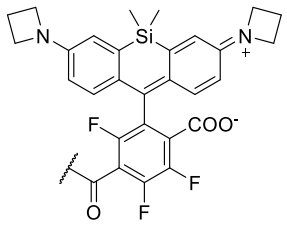

JF669

Non-fluorescent substrates

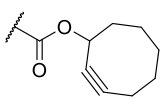

SCO

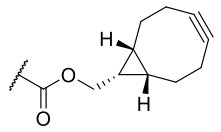

BCN

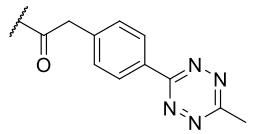

Tet

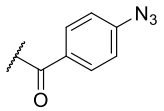

PhN_3

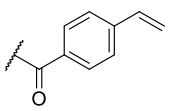

Vbn

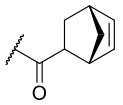

Nor1

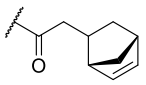

Nor2

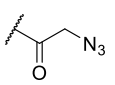

N_3

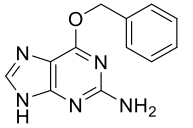

BG

Block

The quest for cell-permeable, far-red synthetic fluorophores

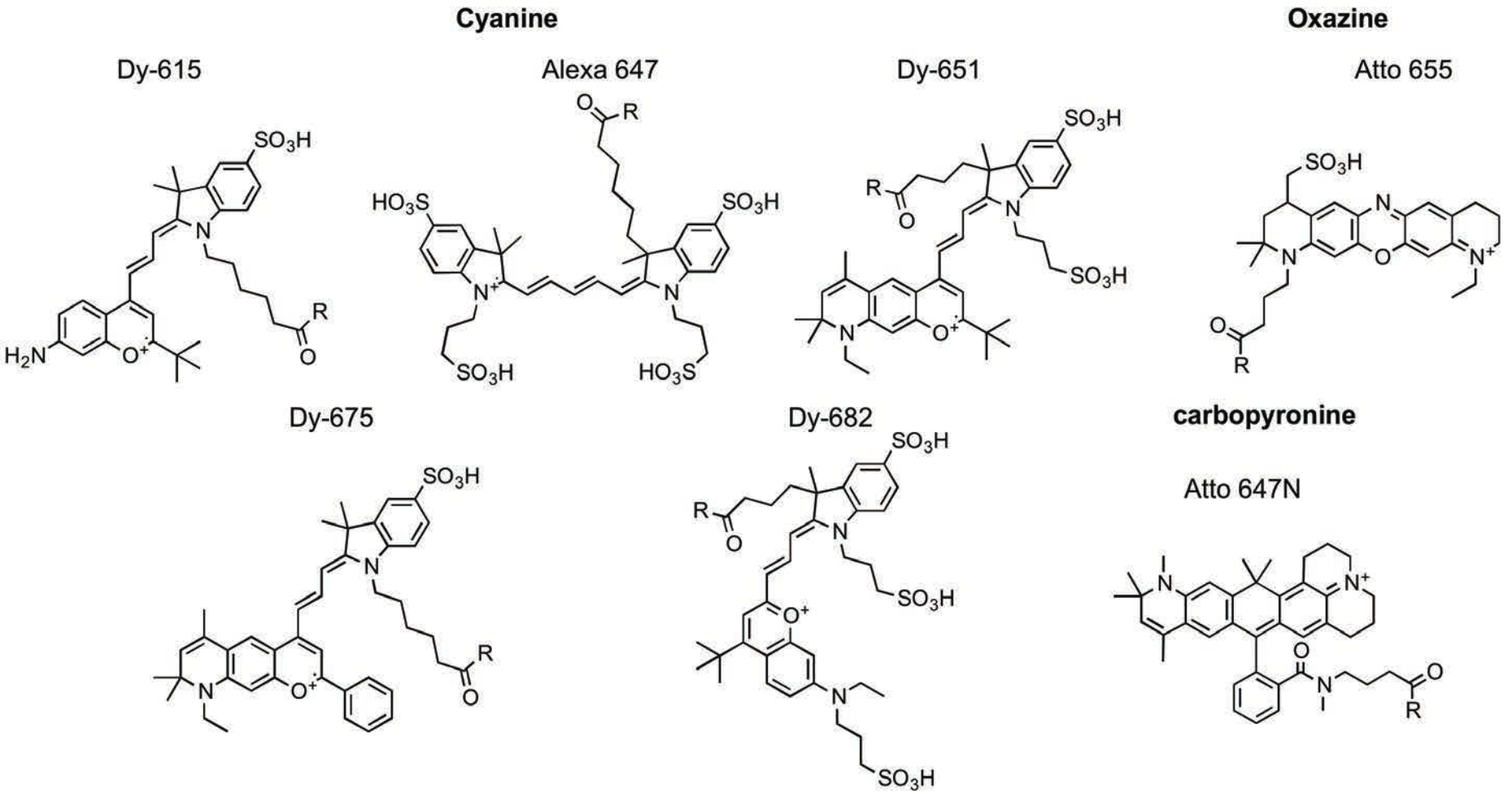

Si-rhodamine (SiR) derivatives as far-red fluorophores

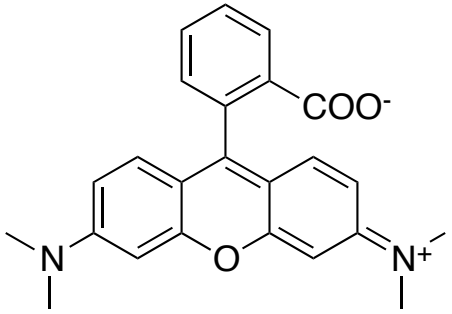

Tetramethyl-Rhodamine

Abs/Em ~ 550/570 nm

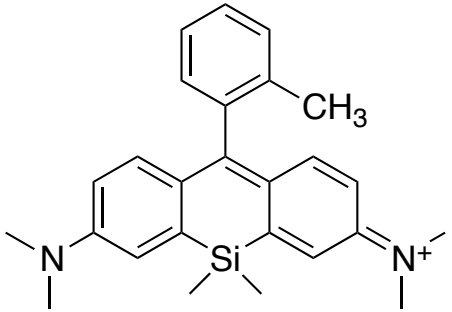

Tetramethyl-Siliconrhodamine

Abs/Em ~ 650/670 nm

For an overview see: Koide, Y., Urano, Y., Hanaoka, K., Terai, T. & Nagano, T. Evolution of group 14 rhodamines as platforms for near-infrared fluorescence probes utilizing photoinduced electron transfer. *ACS Chem Biol* **6**, 600-608 (2011)

SiR-carboxyl is an environmentally sensitive fluorophore

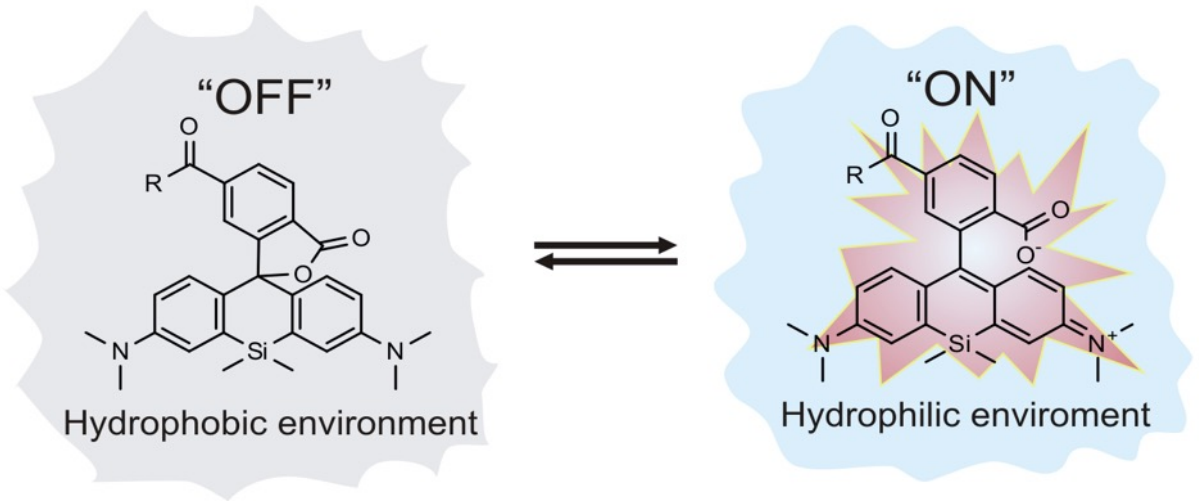

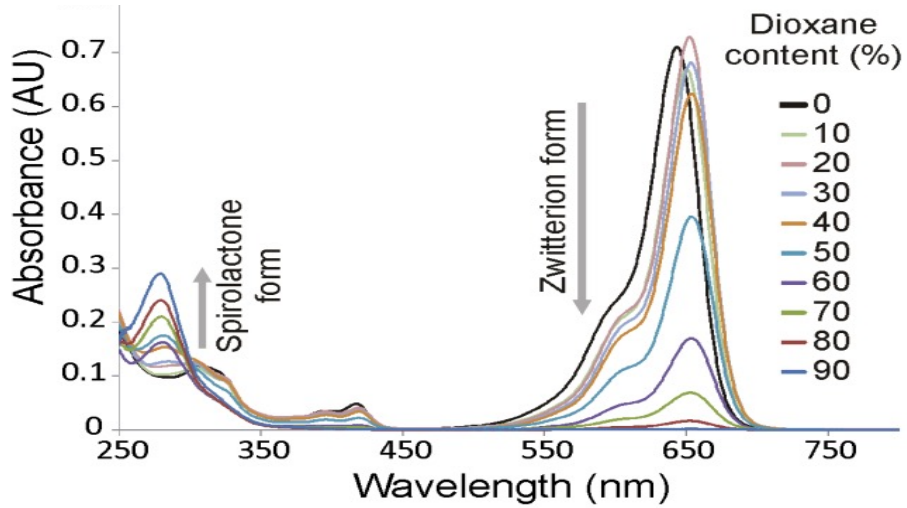

Nature Chemistry 2013

SiR dyes are fluorogenic far-red fluorophores

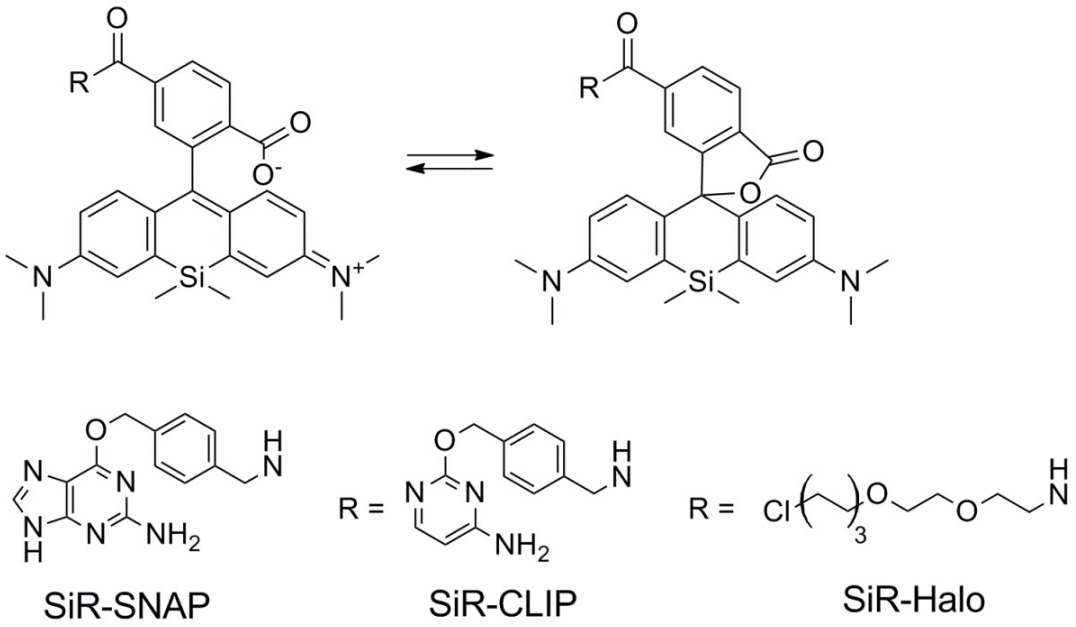

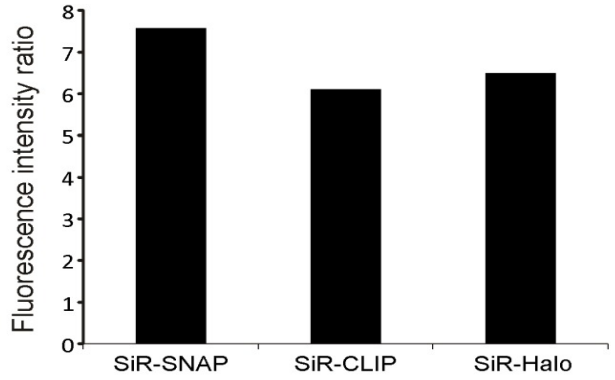

Fluorescence intensity increase upon conjugation with corresponding tag in DMEM with 10% FBS

Live-cell labeling with SiR dyes

wash

no wash

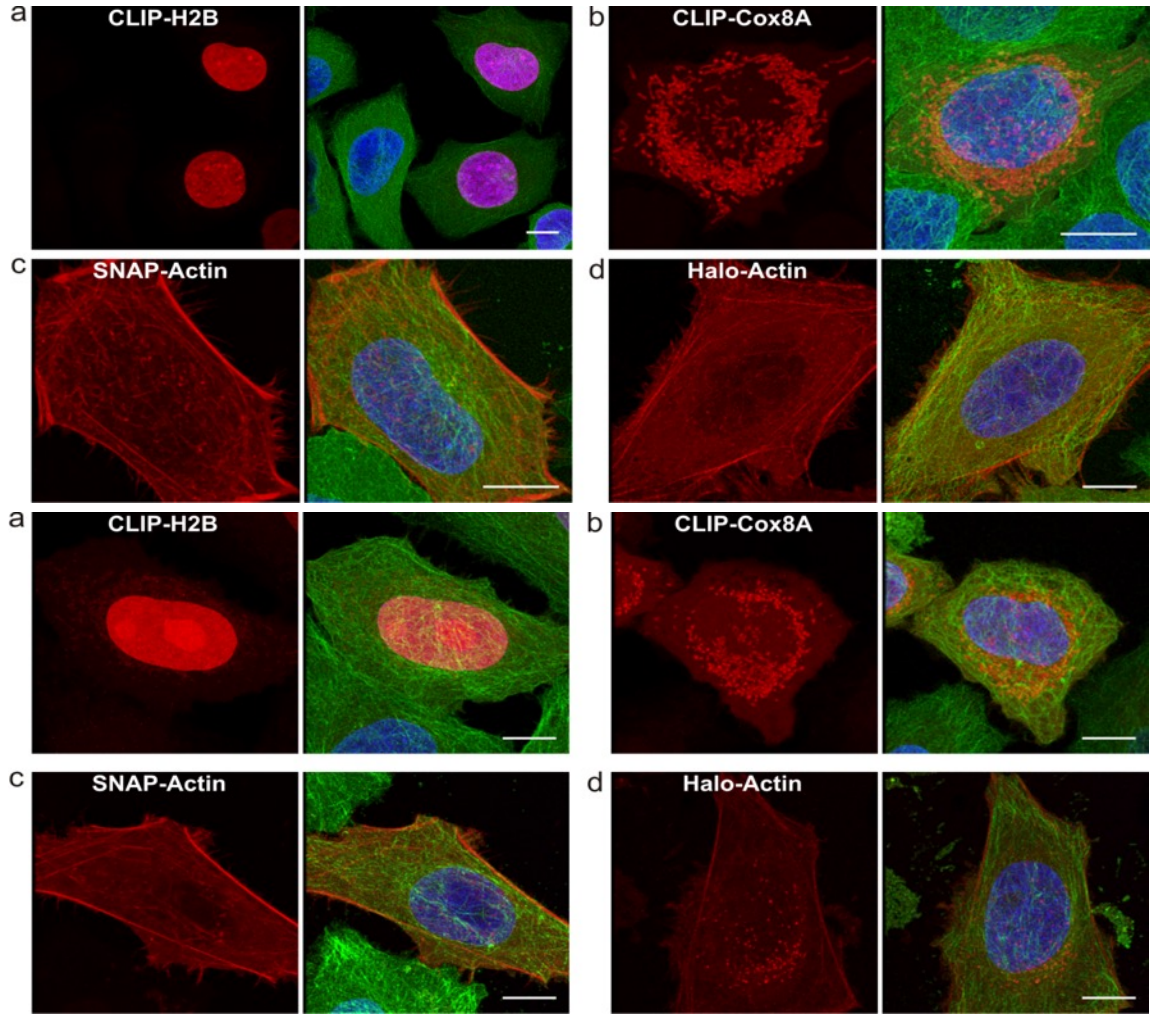

SiR dyes are fluorogenic far-red fluorophores

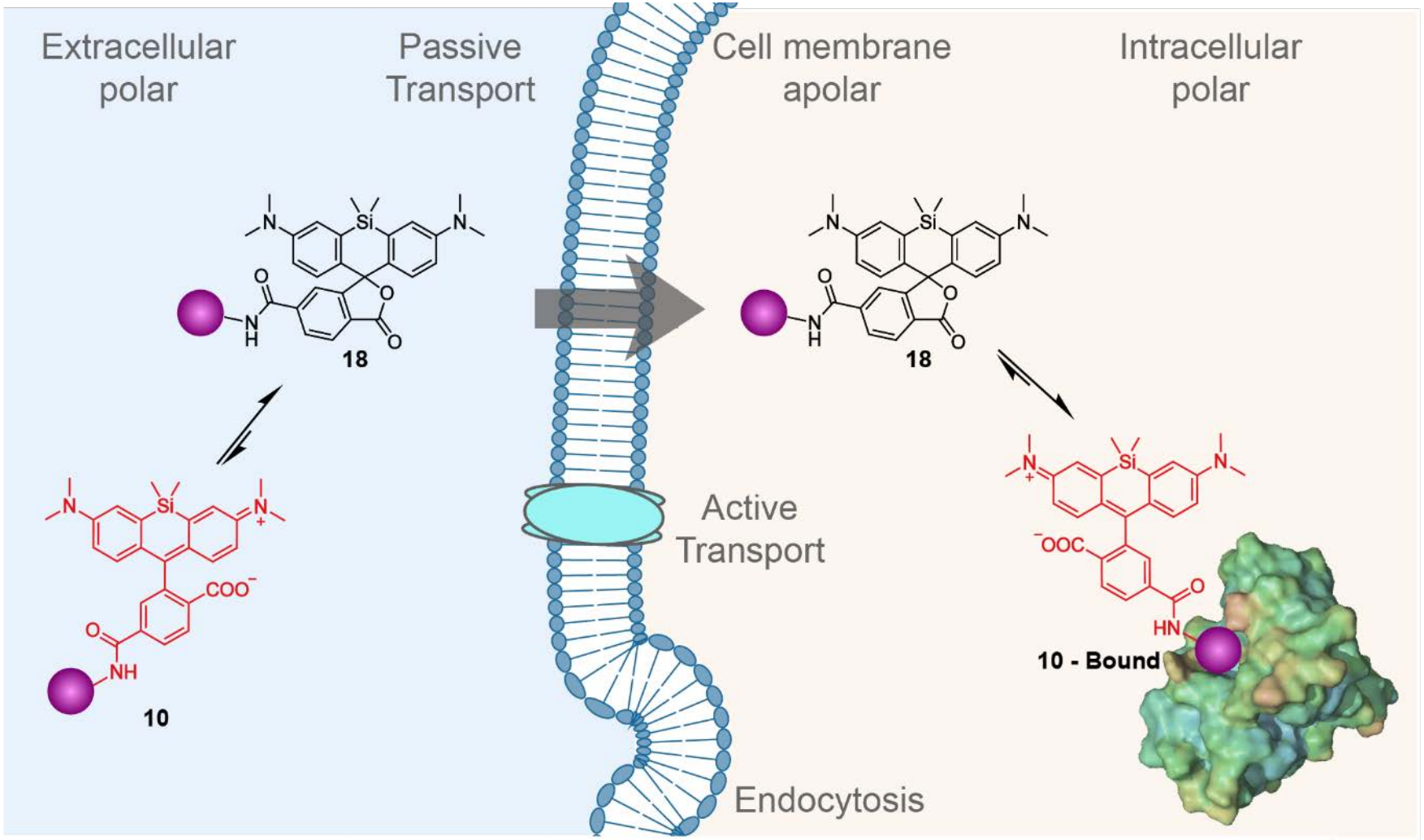

SiR dyes display high photostability

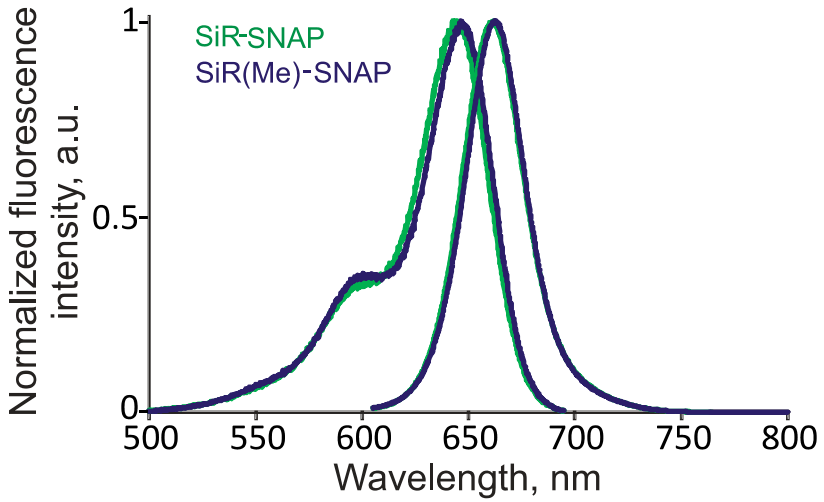

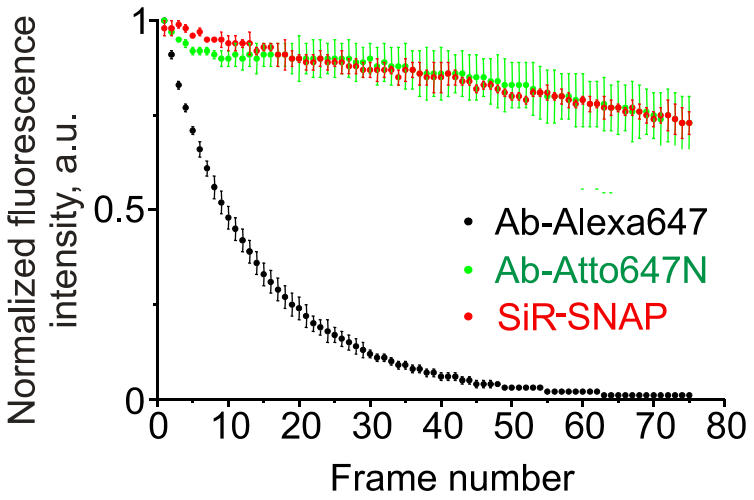

Excitation ~650 nm, emission ~670nm, QY ~40%, e_{max} ~100,000 $l*mol^{-1}*cm^{-1}$

Live-cell STED microscopy of SiR-SNAP labelled Cep41

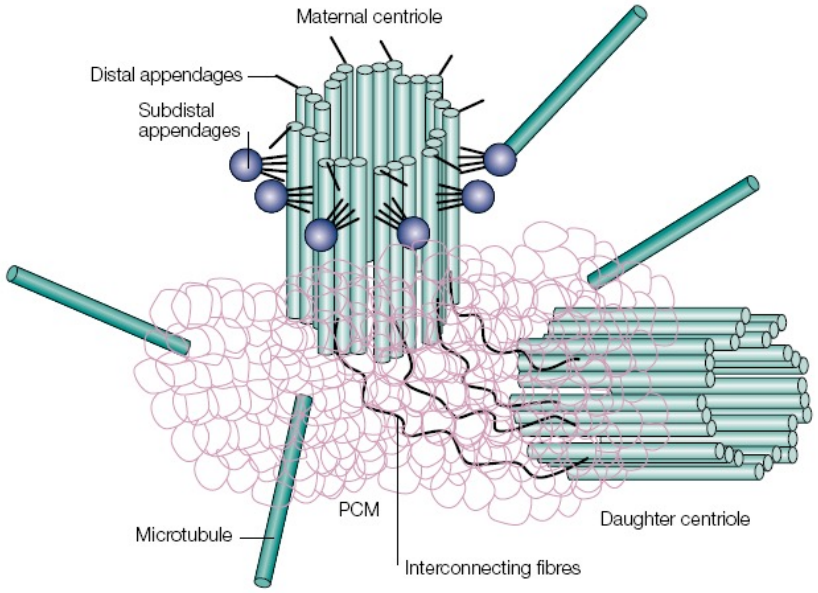

Image taken from S. Doxsey, *NATURE REVIEWS MOLECULAR CELL BIOLOGY* **2**, 688-698 (2004)

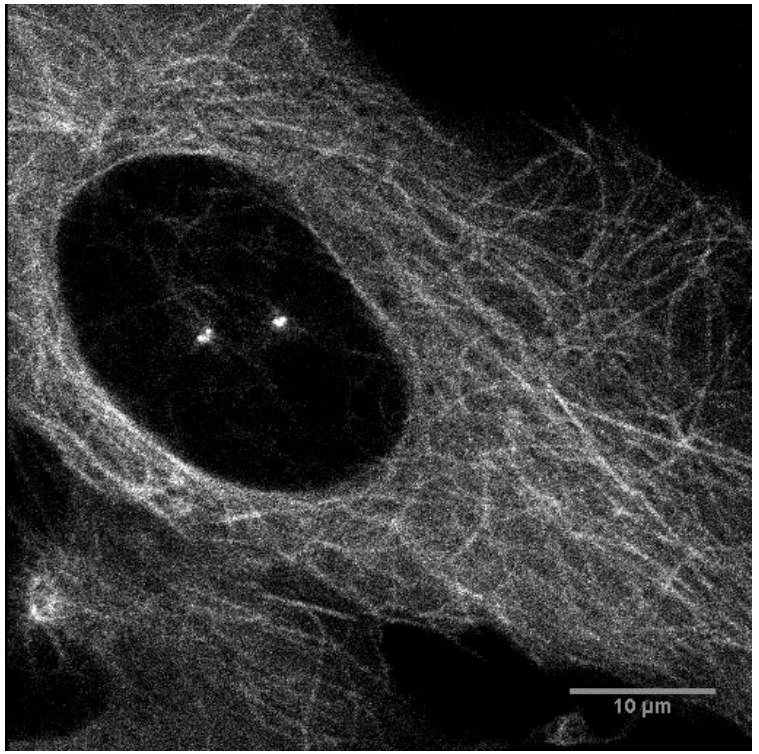

Christian Eggeling, Alf Honigmann

Nature Chemistry 2013

Staining cellular structures with dyes

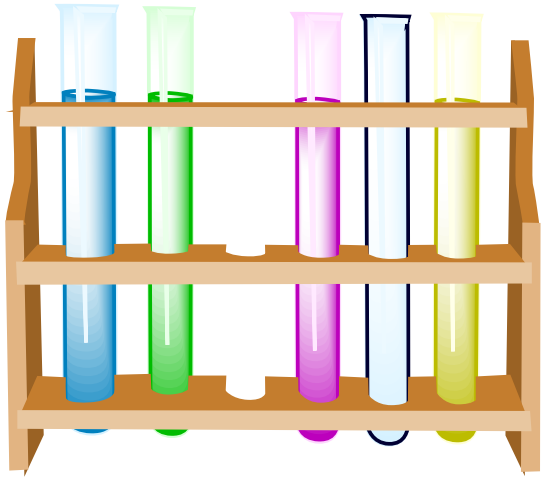

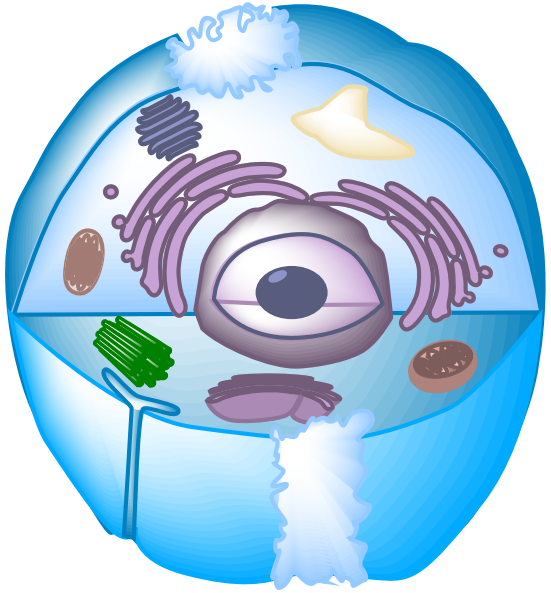

Staining cellular structures with dyes

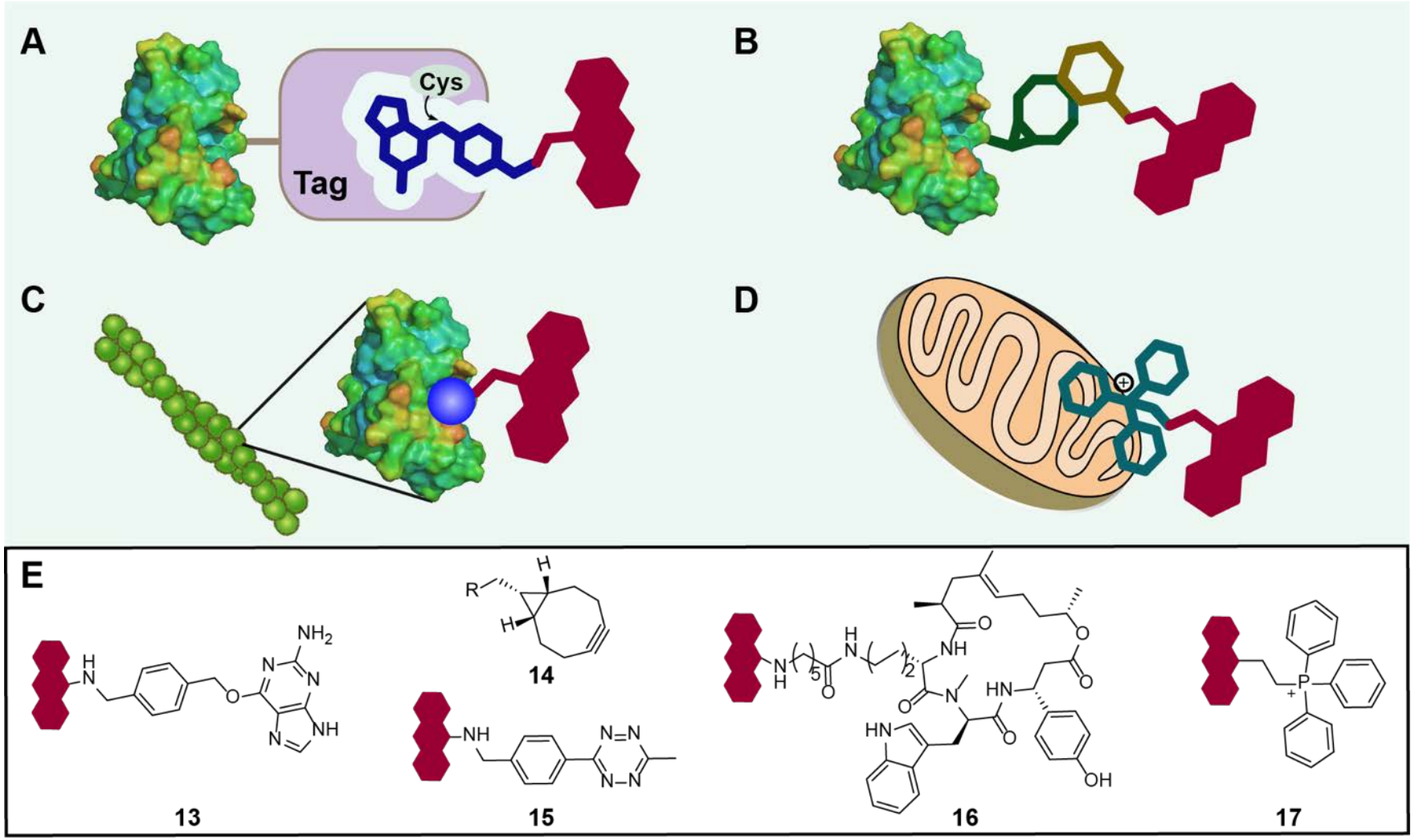

Fluorescent probes for live-cell imaging of endogenous proteins

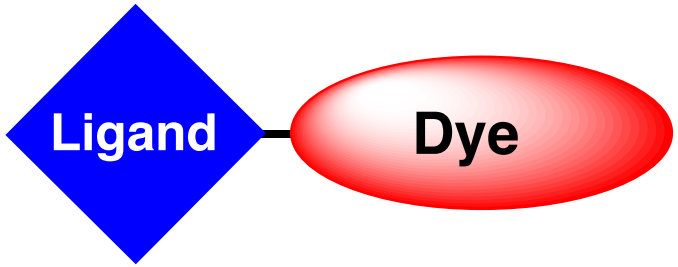

- Ligand should be highly specific and non-toxic
- Fluorophore should be far-red and fluorogenic
- Compatible with superresolution microscopy
- Applicable to different organisms

SiR-based probes for imaging of F-actin and microtubules

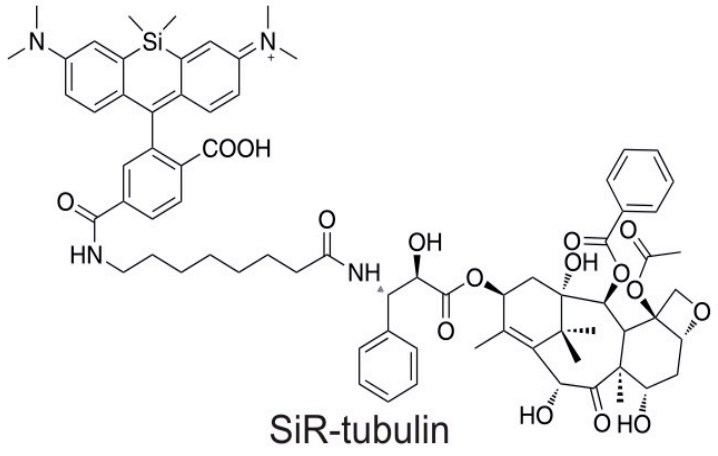

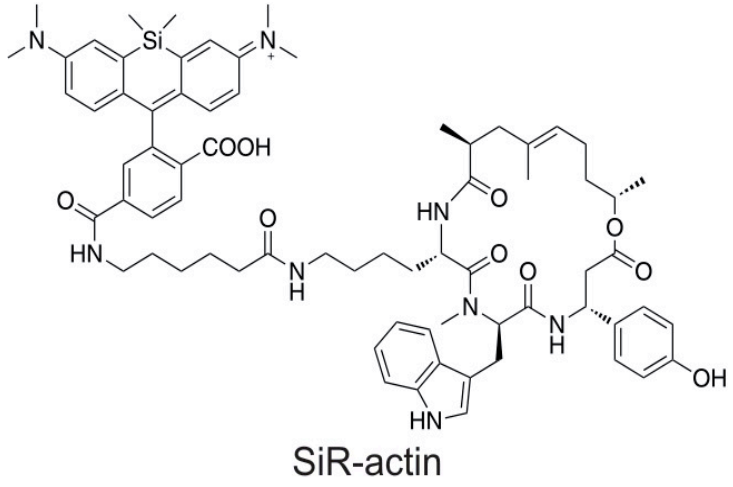

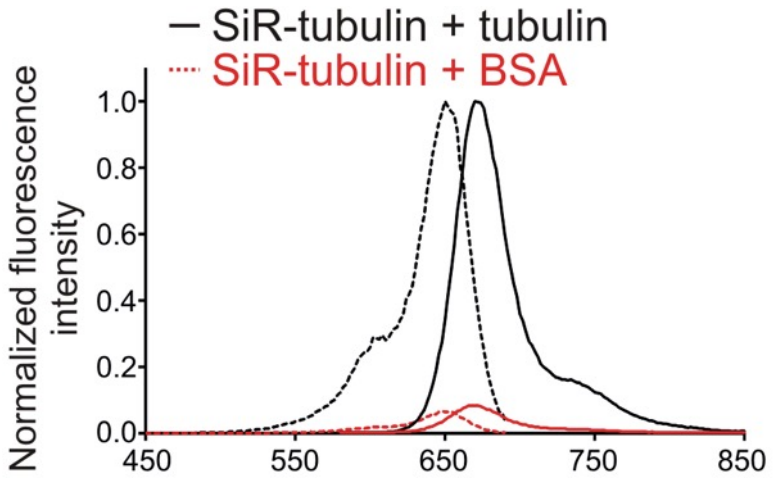

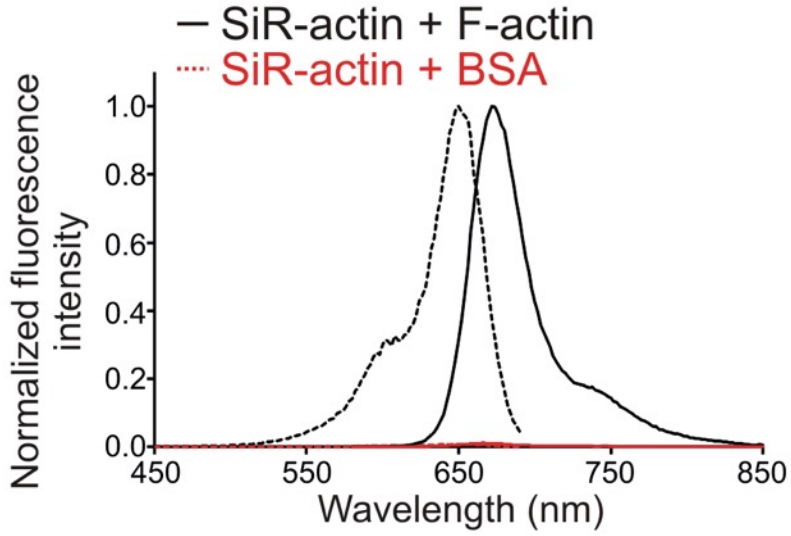

SiR-actin is based on a jasplakinolide derivative
SiR-tubulin is a docetaxel derivative

Nature Methods 2014

Fluorogenicity of SiR-based probes depends on hydrophobicity of ligand

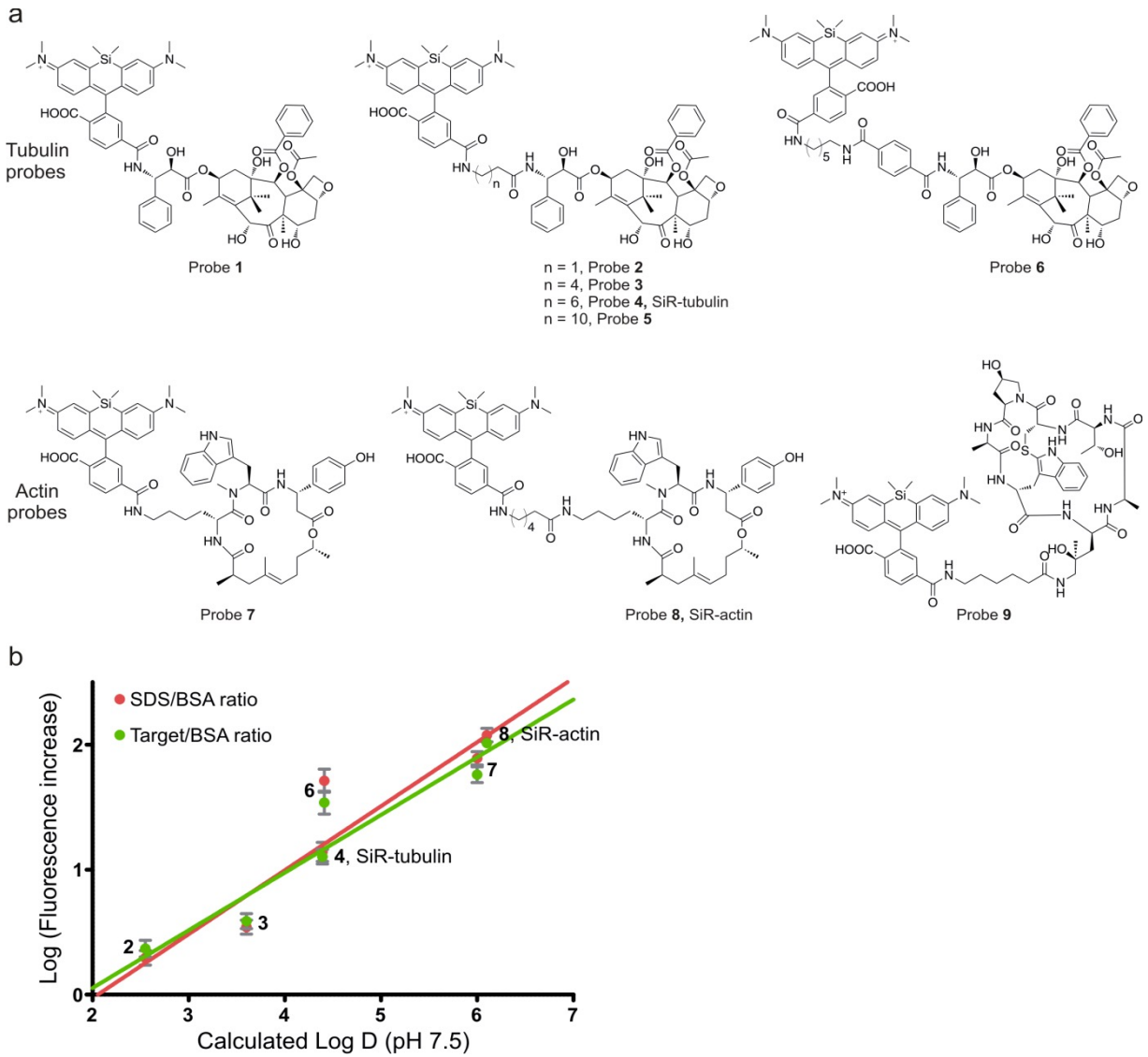

Live-cell 3D Structured Illumination Microscopy (SIM) of F-actin and microtubules

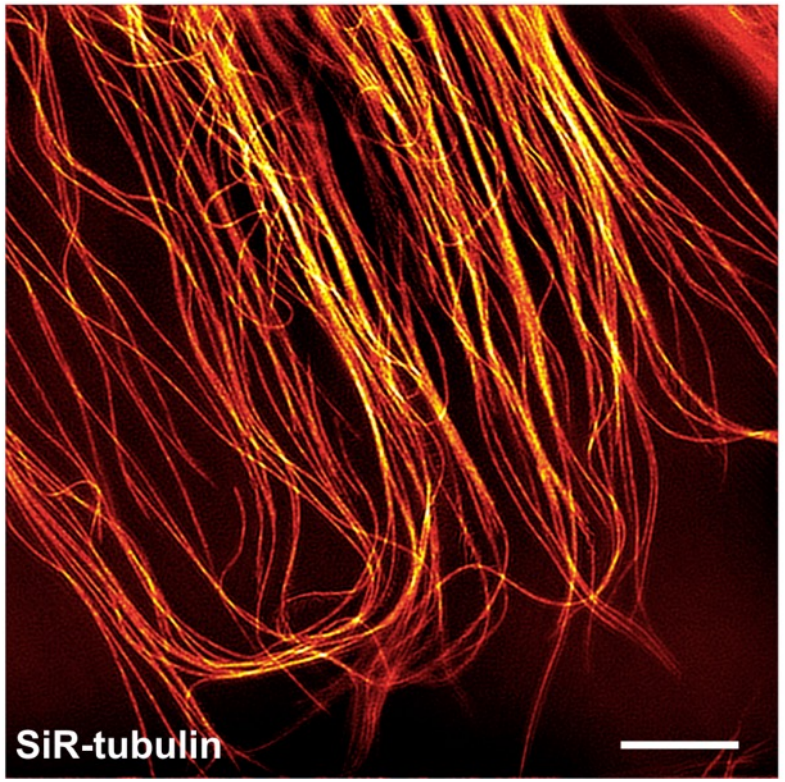

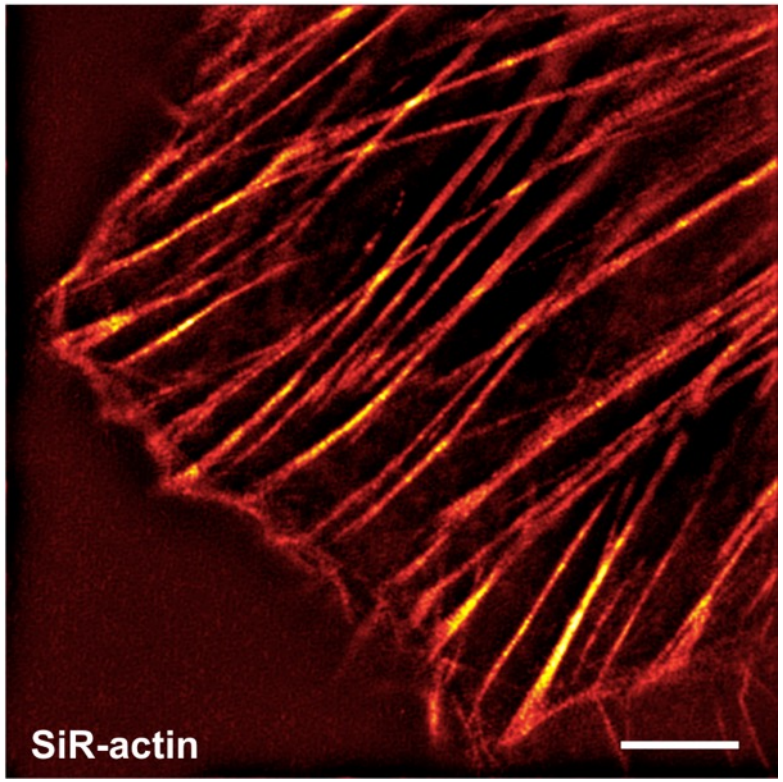

Staining with 1-3 μM of probe in DMEM + 10% FBS for about one hour with or without washing step

3D Structured Illumination Microscopy (SIM) of microtubules in living human fibroblasts

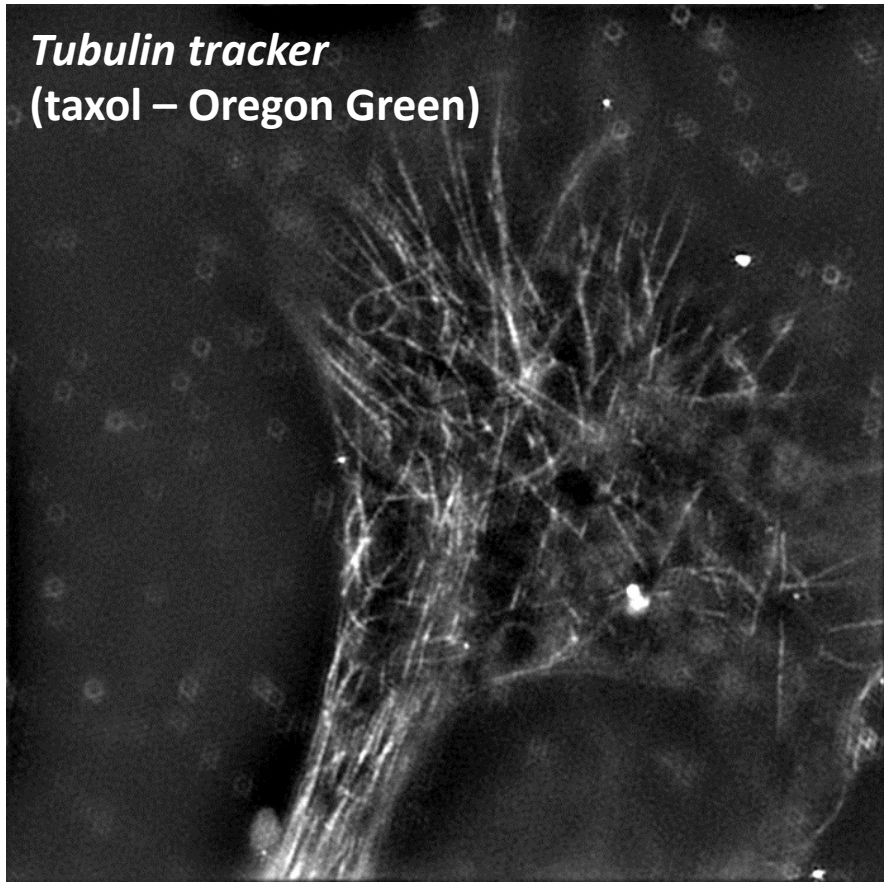

Average FWHM ~110 nm
High background

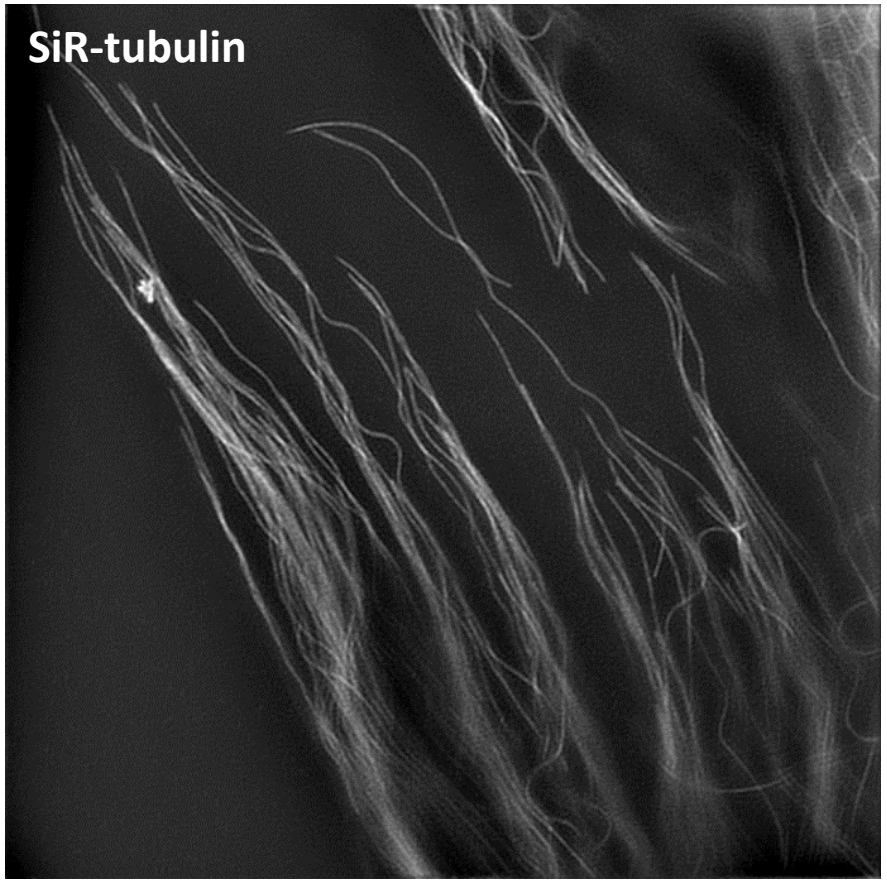

Average FWHM ~100 nm
Low background

Visualization of microtubule by SiR-tubulin in live cells at different cell cycle stages

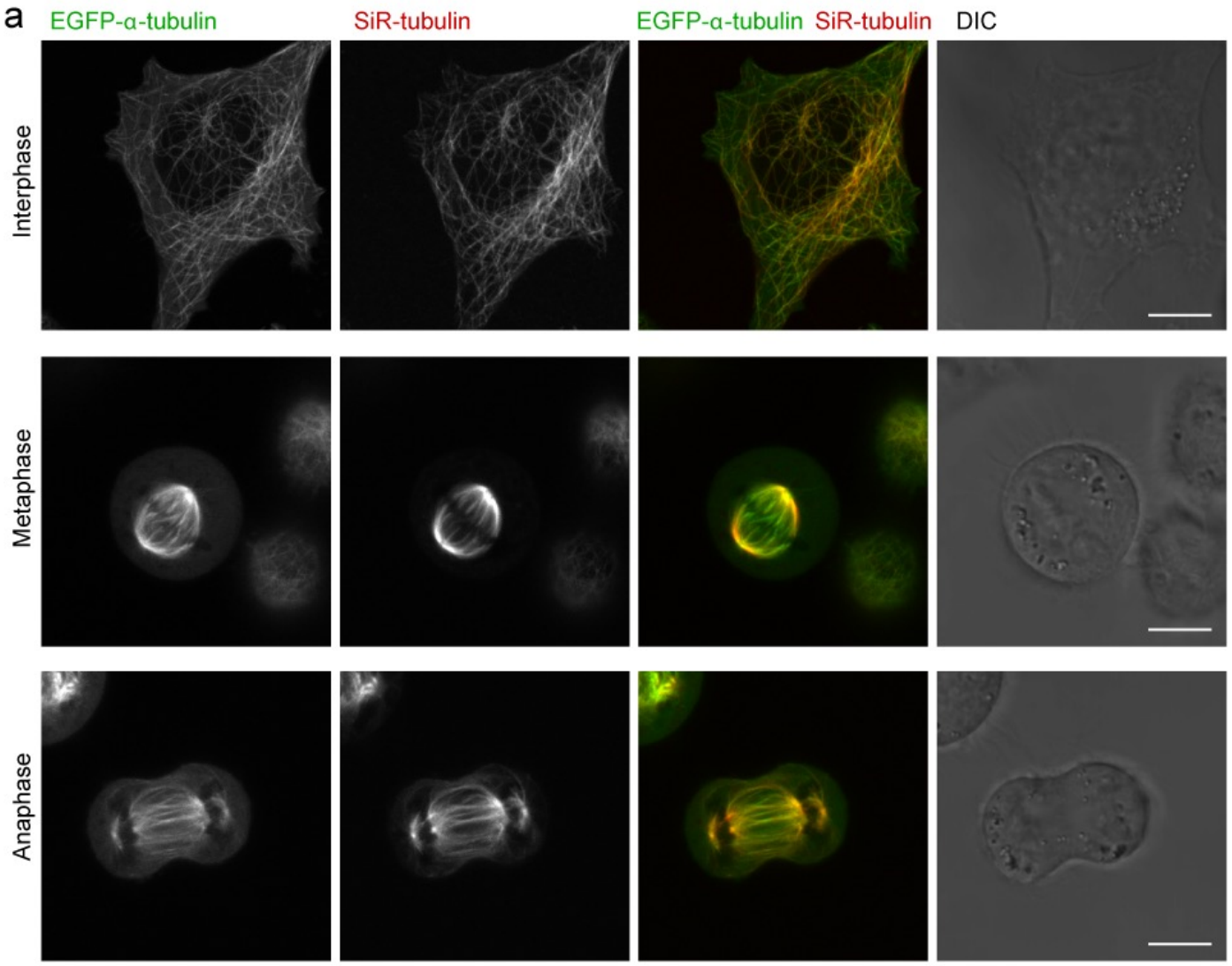

Claudia Blaukopf
Christoph Sommer
Daniel Gerlich

Visualization of actin cytoskeleton by SiR-actin in live cells at different cell cycle stages

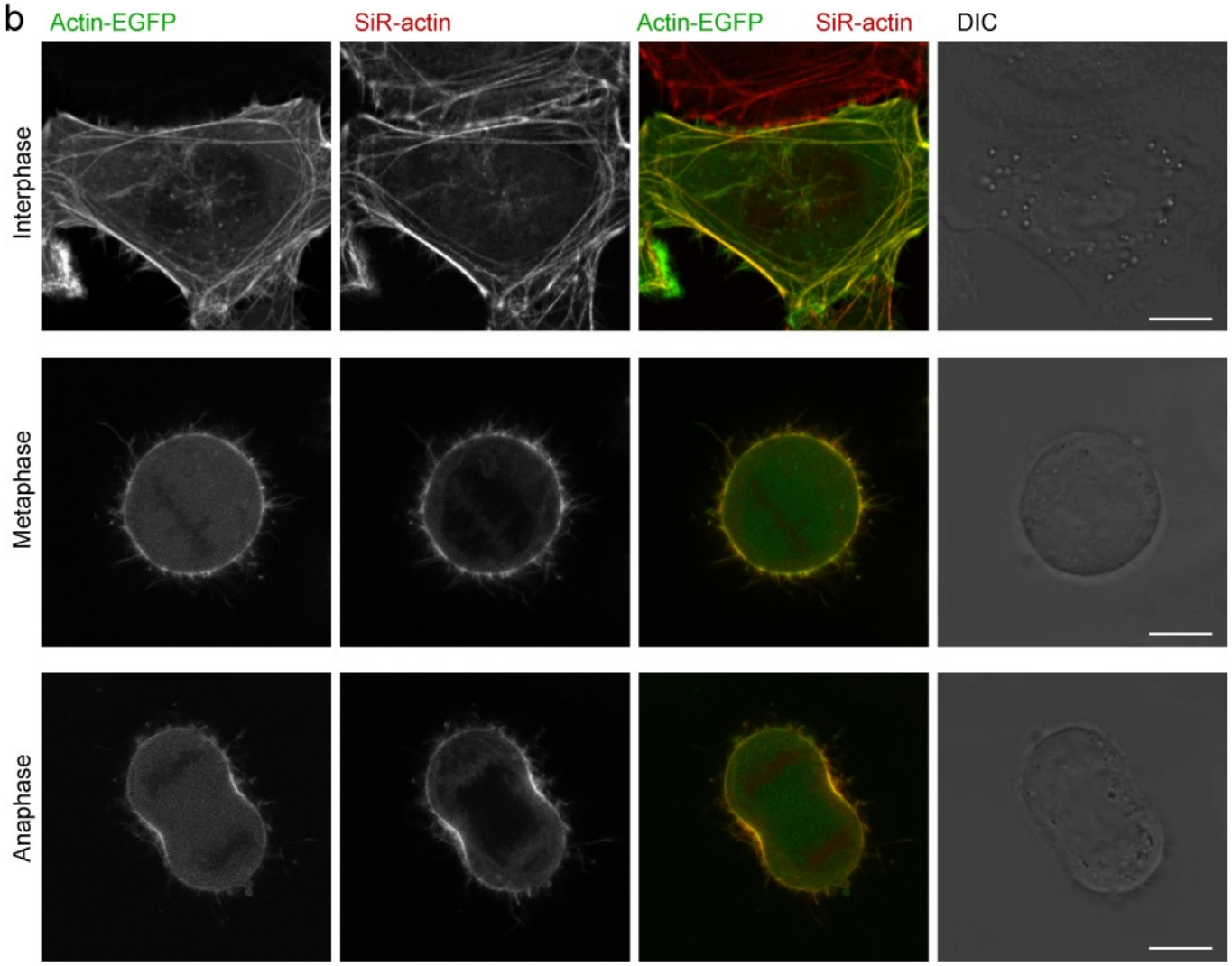

Claudia Blaukopf
Christoph Sommer
Daniel Gerlich

SiR probes display minimal toxicity

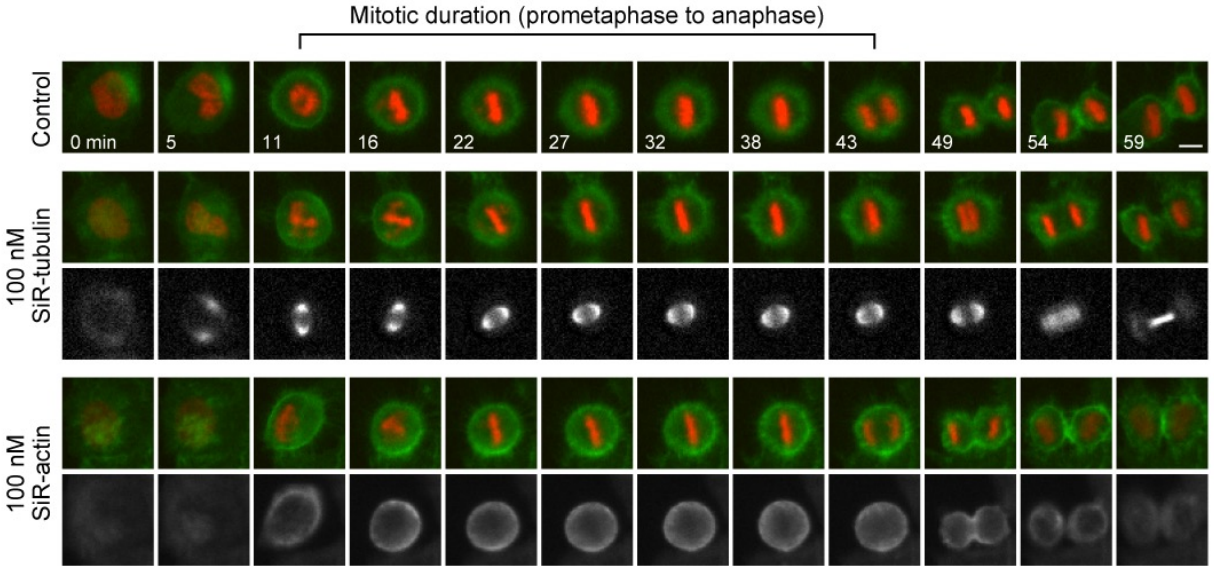

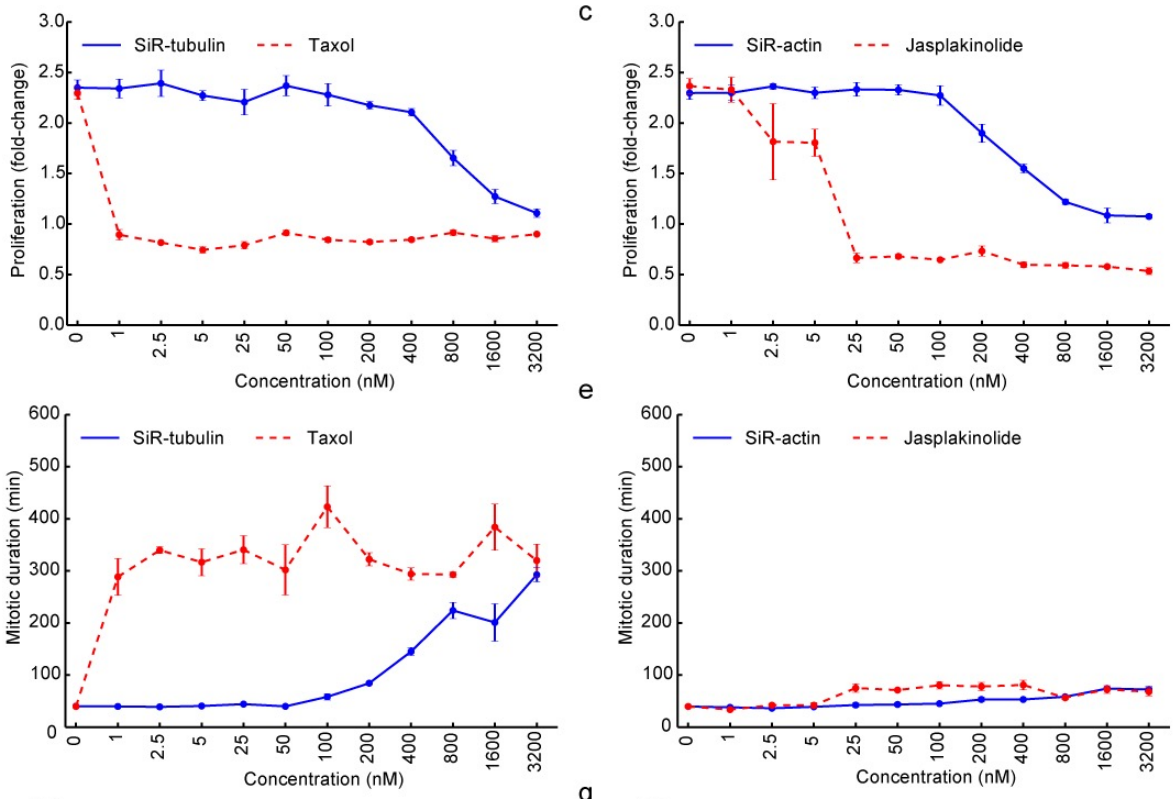

Claudia Blaukopf
Christoph Sommer
Daniel Gerlich

STED Microscopy of microtubules in living human fibroblasts

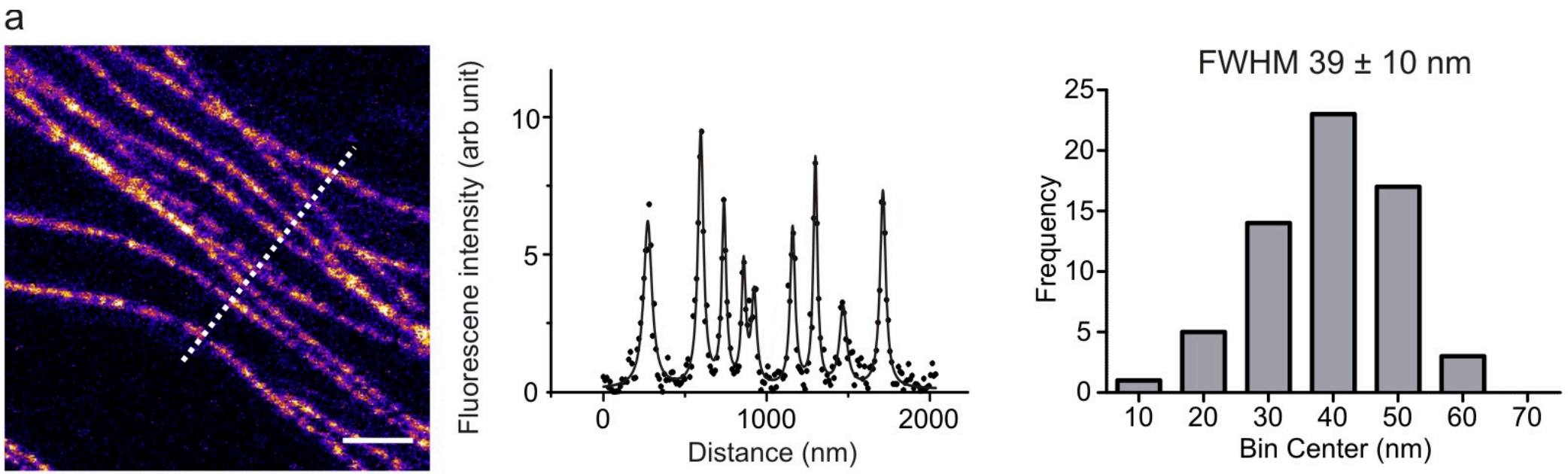

Elisa D'Este, Fabian Göttfert, Haisen Ta, Stefan Hell

Nature Methods 2014

STED Microscopy of centrosomes in living human fibroblasts

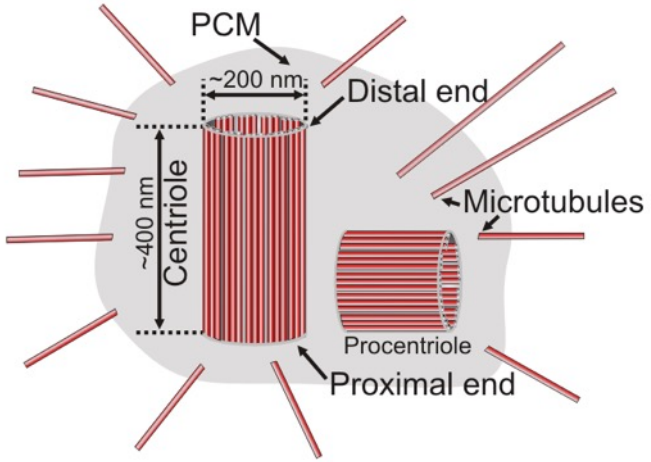

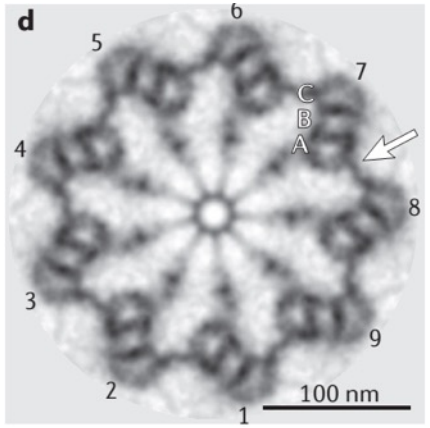

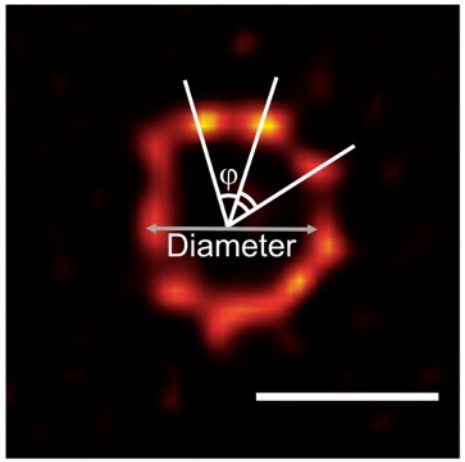

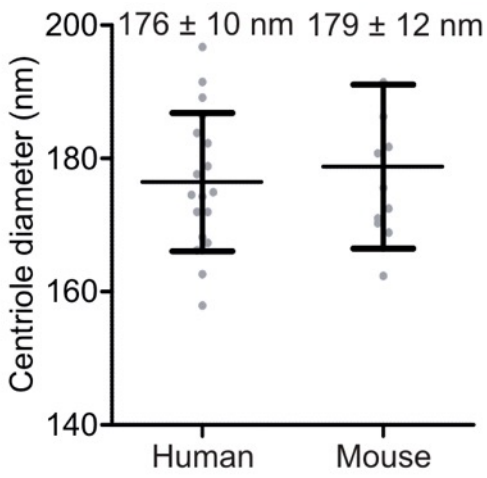

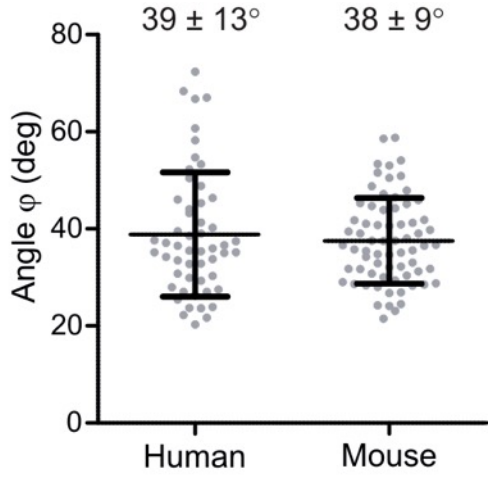

Nature Methods 2014

STED Microscopy of F-actin in living primary rat hippocampal neurons

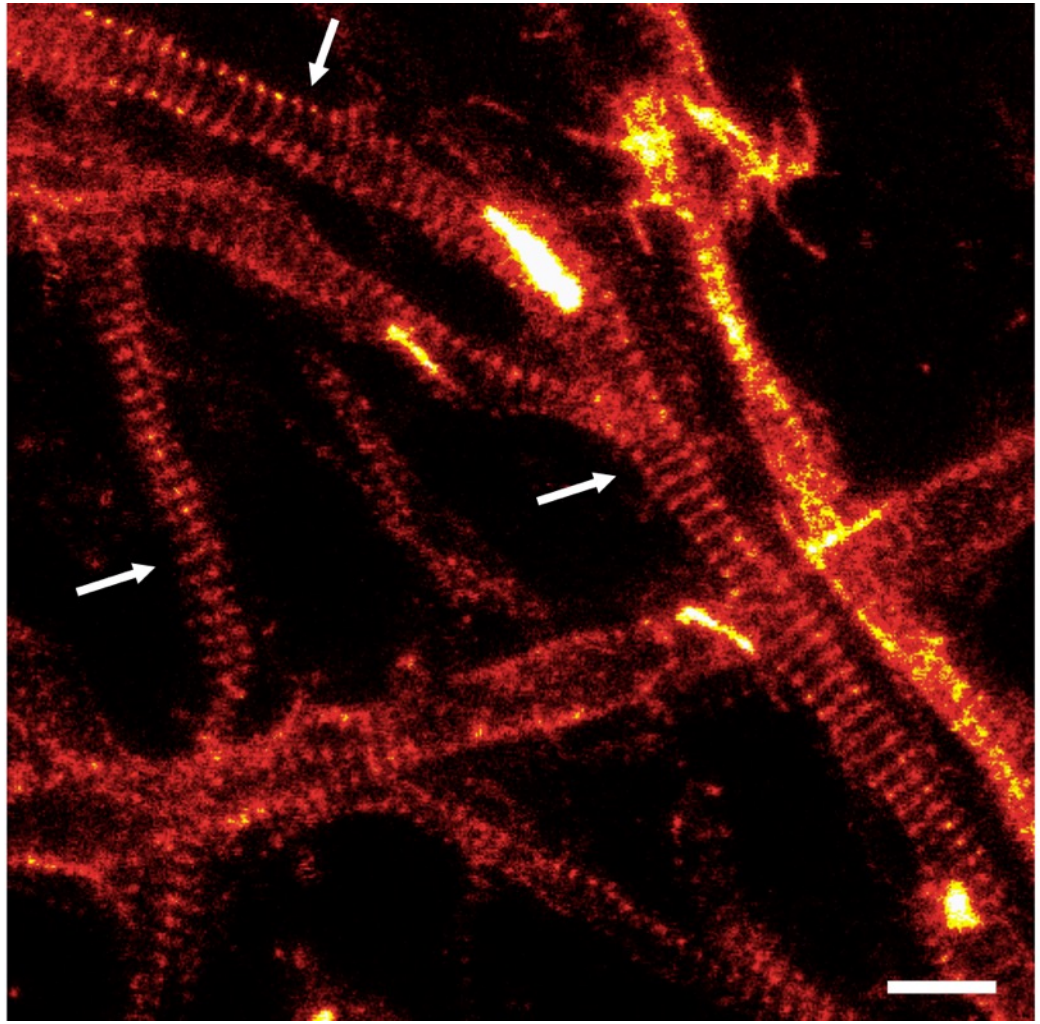

Elisa D'Este, Fabian Göttfert,
Haisen Ta, Stefan Hell

Actin forms ring-like structures in axons that are evenly spaced along axonal shafts

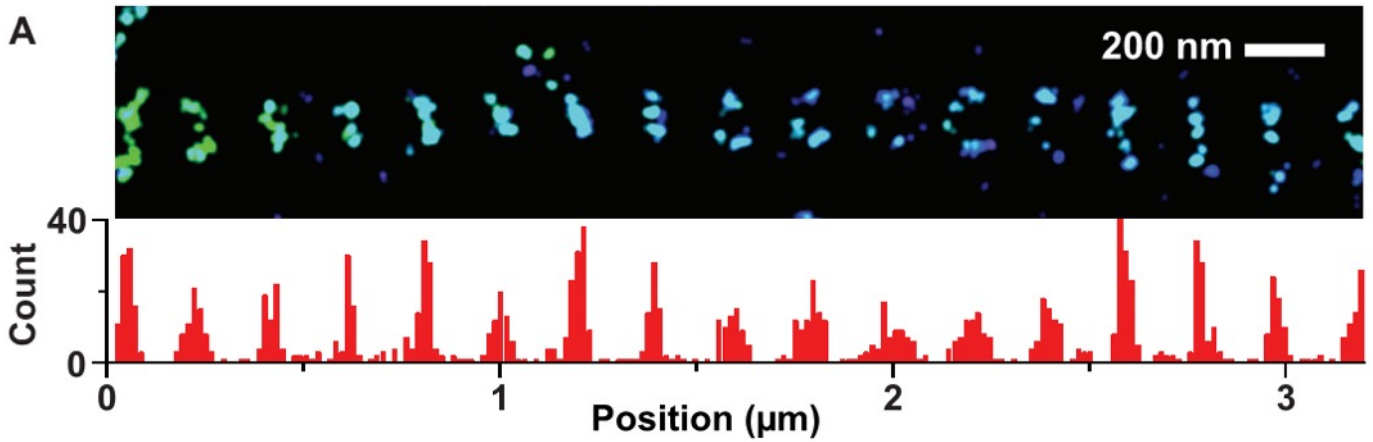

Xu, K., Zhong, G., and Zhuang, X. (2013) Actin, spectrin, and associated proteins form a periodic cytoskeletal structure in axons. *Science* ***339, 452-6.***

Observed periodical actin distribution in axons of living neurons using STED and SiR-actin

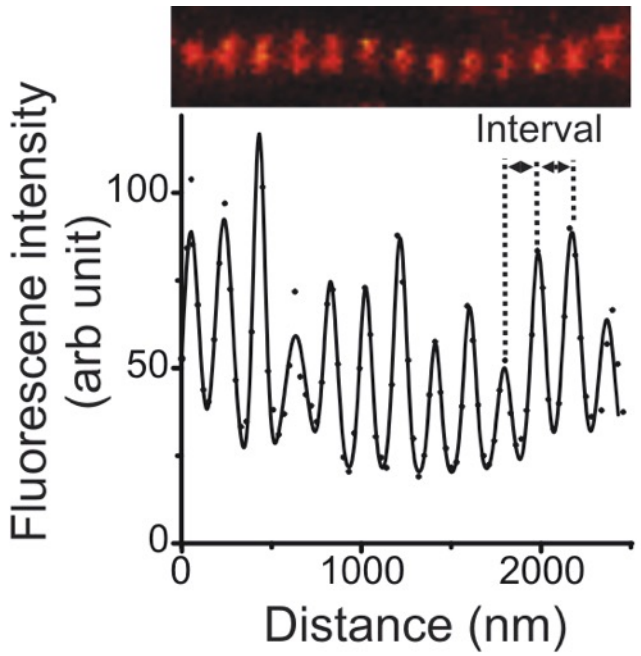

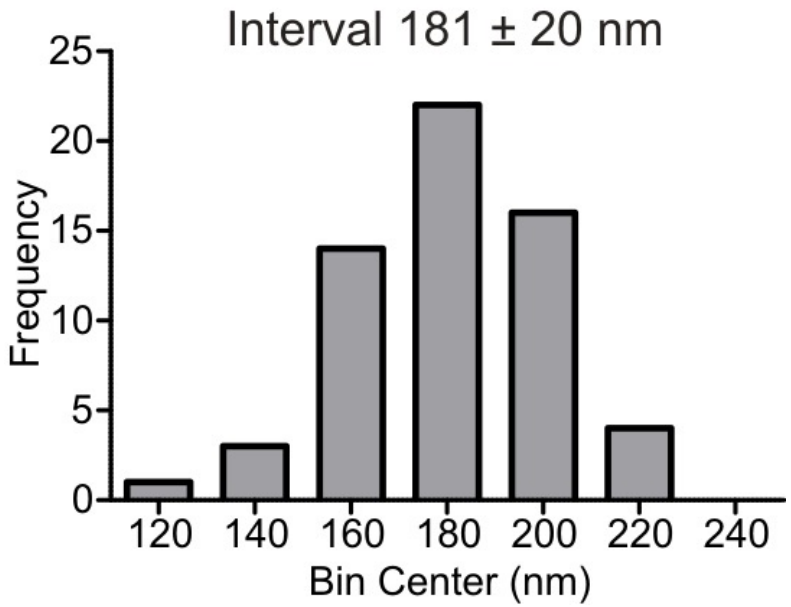

Elisa D'Este, Fabian Göttfert, Haisen Ta, Stefan Hell

Super-Resolution Imaging of the Golgi in Live Cells with a Bioorthogonal Ceramide Probe (Toomre&Schepartz)

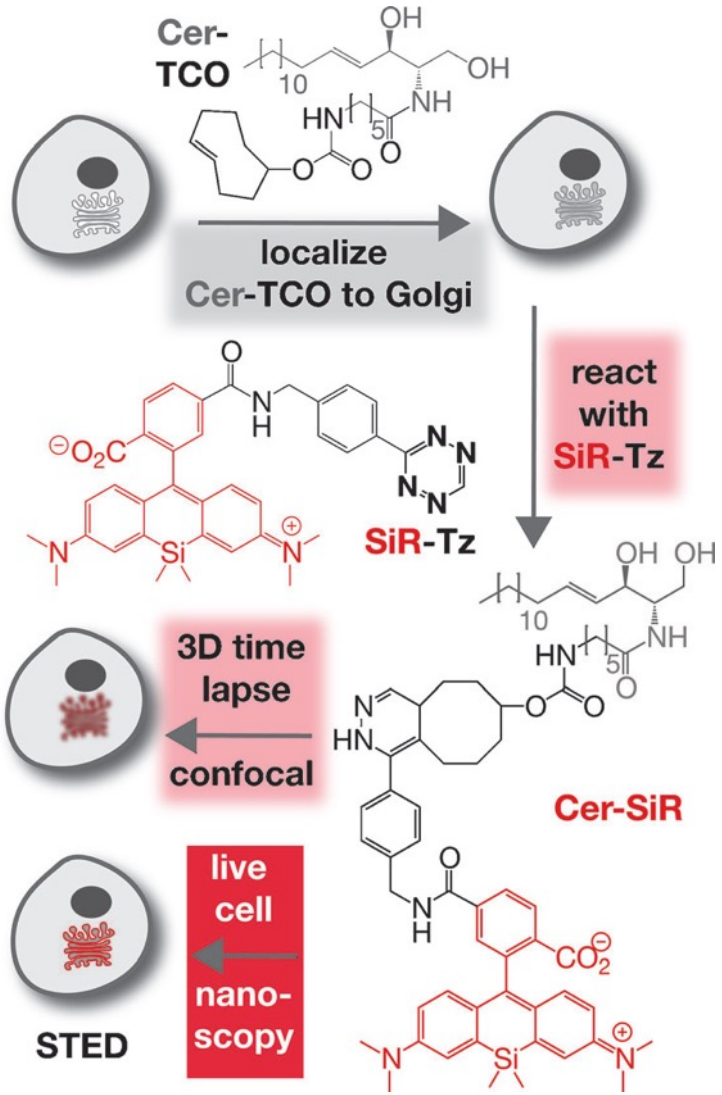

ACIE **52**, 10242 (2014)

Additional colours

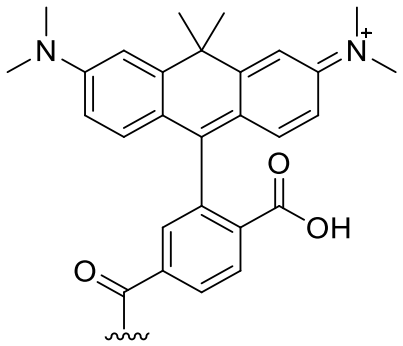

Carbopyronine (CPY)

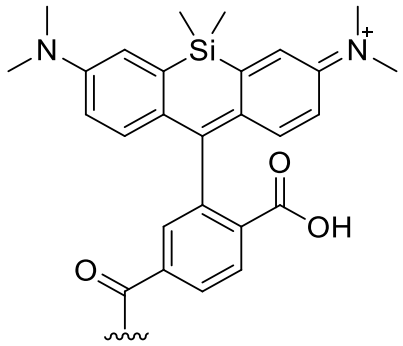

SiR

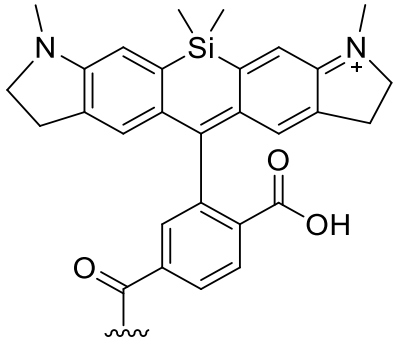

SiR700

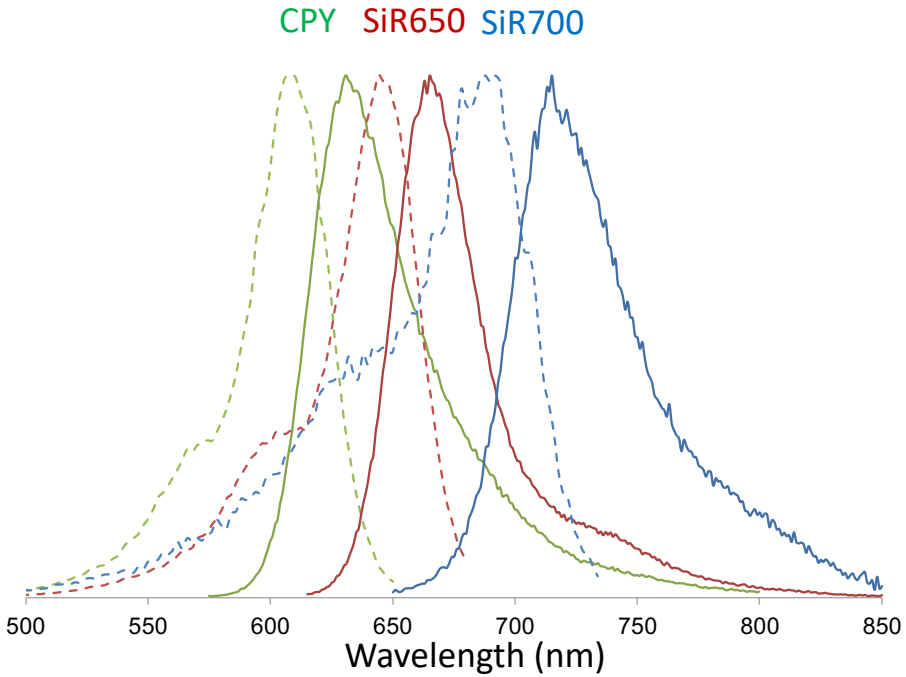

SiR and SiR700 can be excited with a single laser

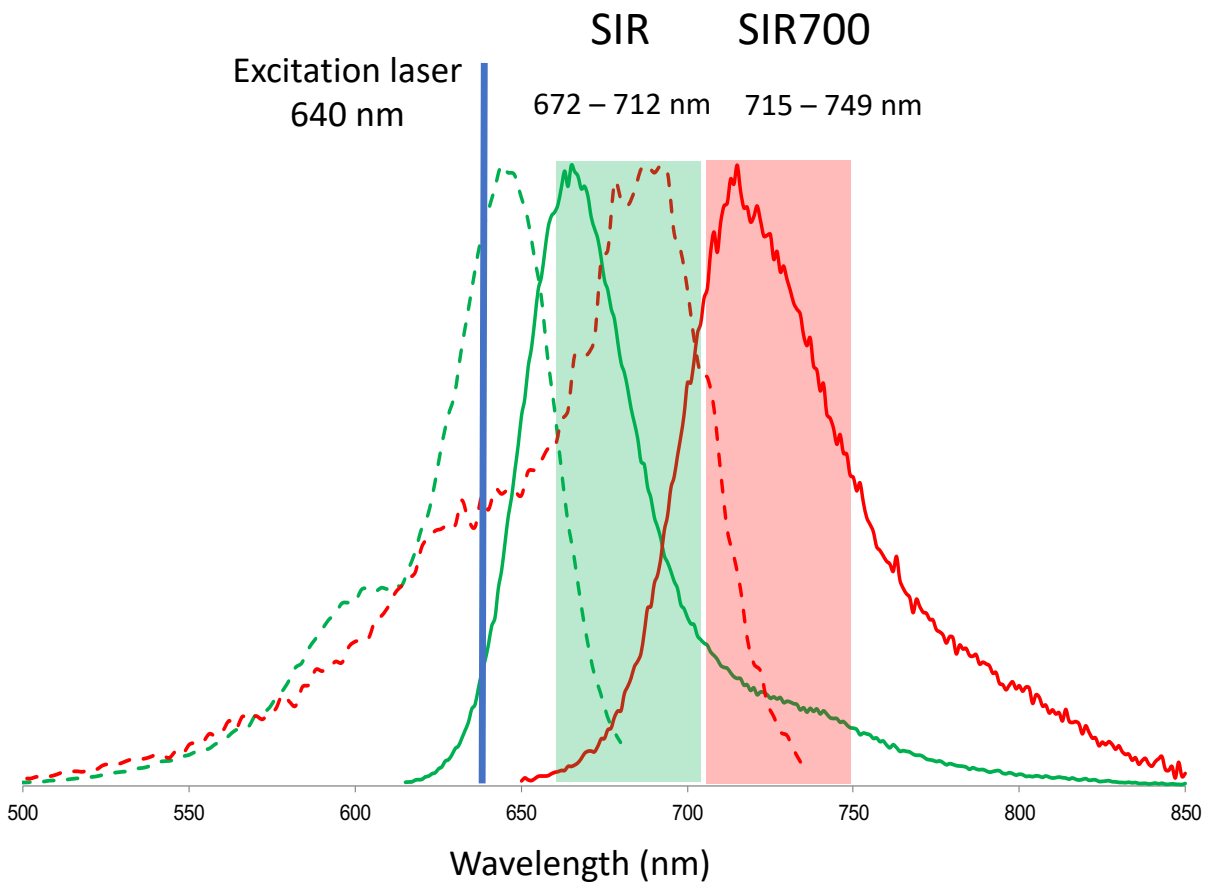

Two colour structured illumination imaging of fibroblasts with SiR-tubulin and SiR700-actin

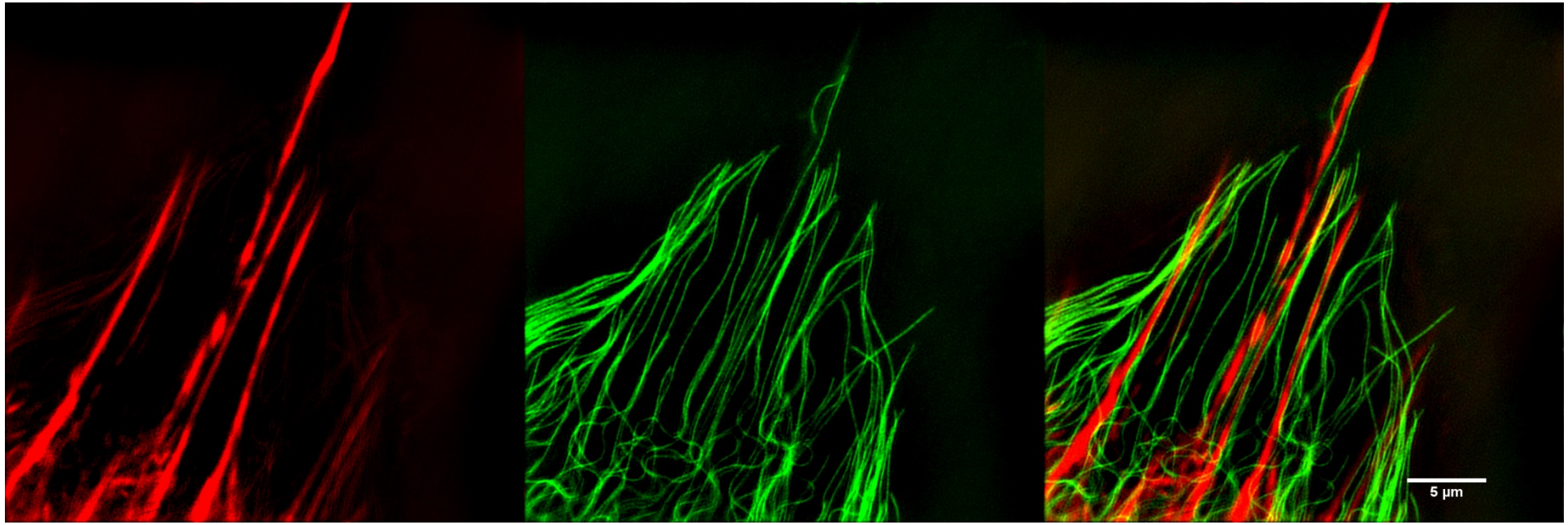

A general strategy for generating cell-permeable and fluorogenic dyes for multicolor nanoscopy

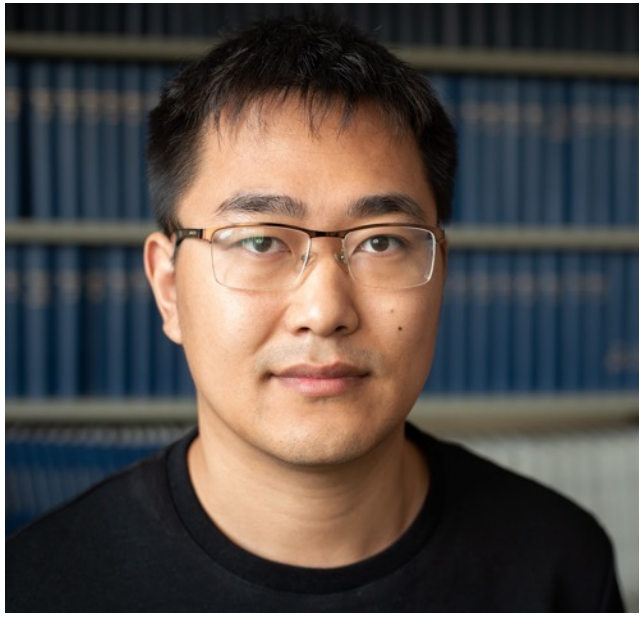

Lu Wang, Mai Tran, Birgit Koch, Lin Xue
Elisa D'Este, Julia Roberti
Nature Chemistry 2020

Favoring spirolactone formation by making the xanthene core more electrophilic

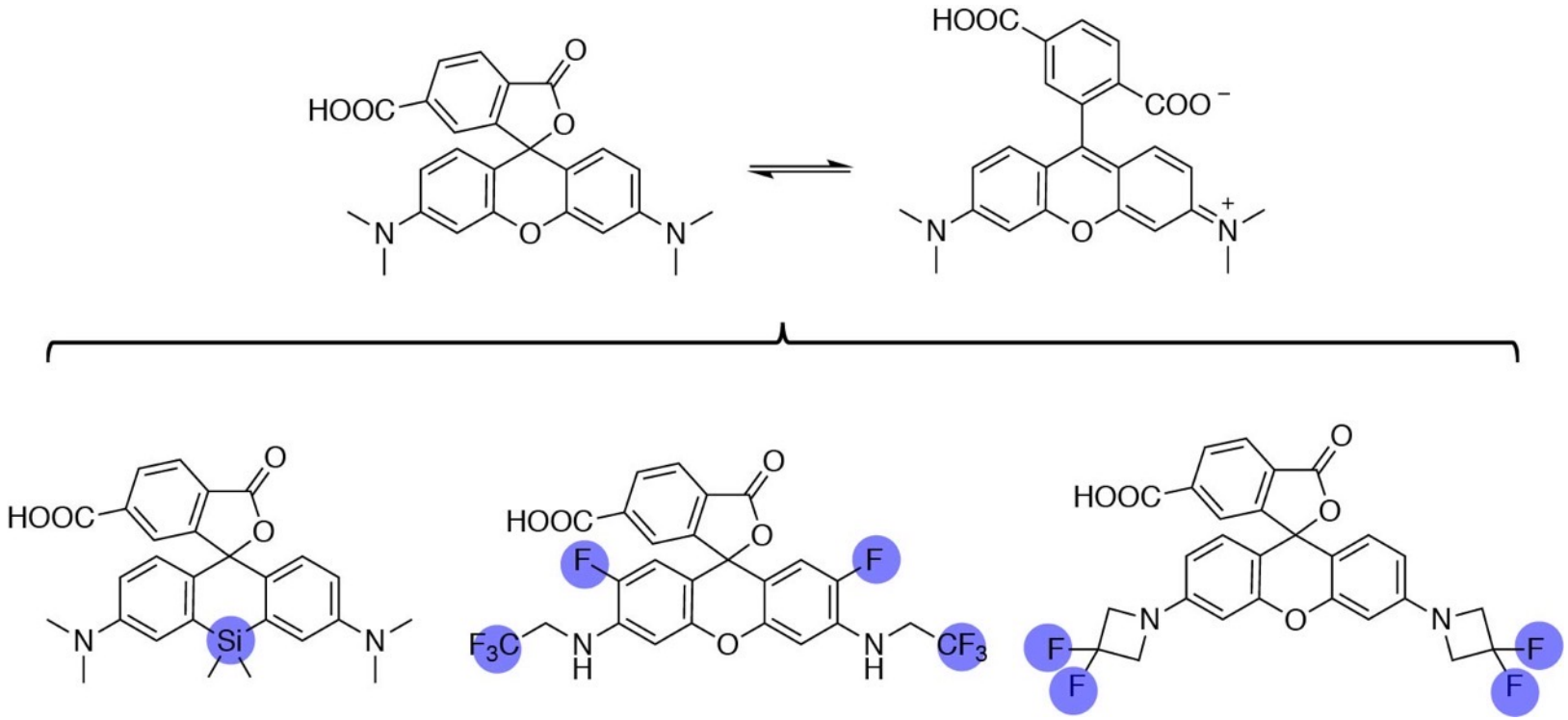

For a systematic study on how to fine-tune fluorophores for live-cell imaging see Grimm *et al. Nature Methods*,**14**, 987–994 (2017)

An alternative approach to develop fluorogenic probes for live-cell imaging

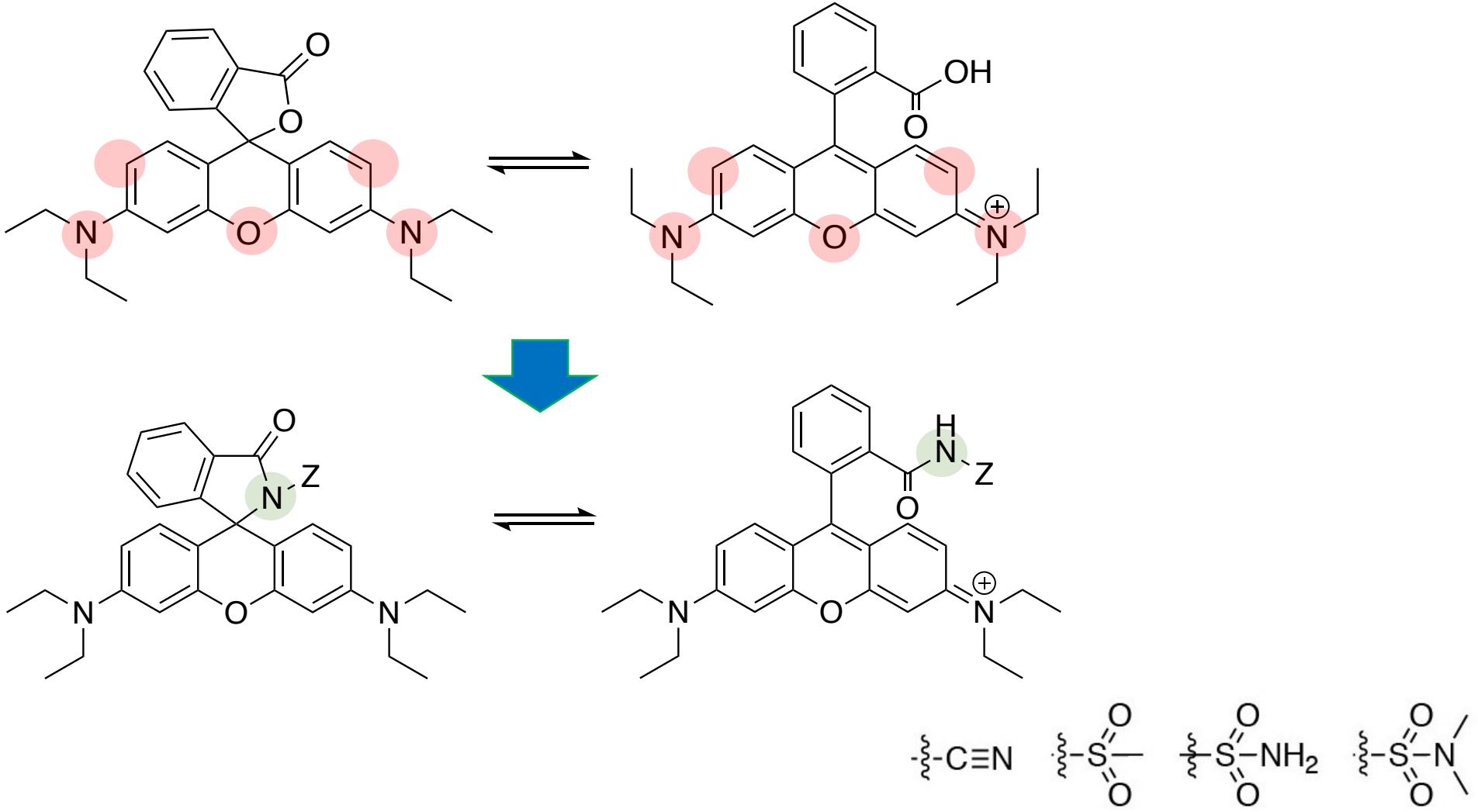

Tuning spirolactam formation of Rhodamine B derivatives

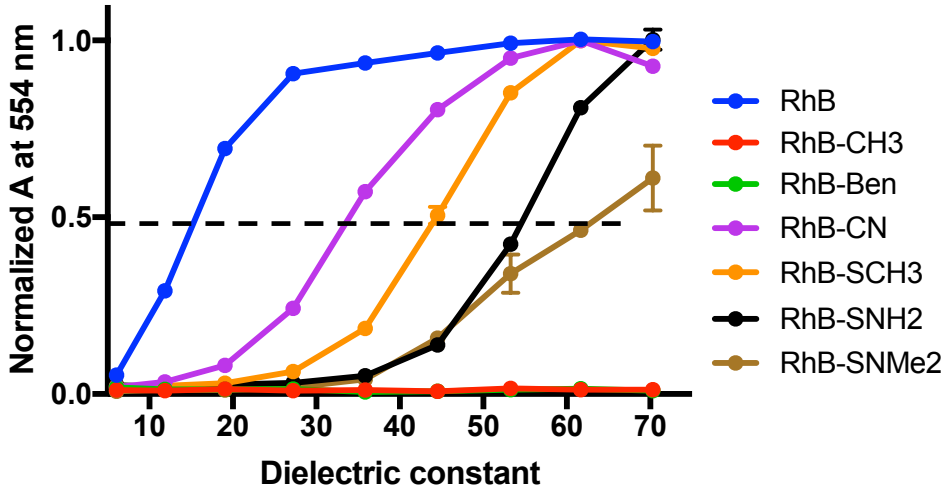

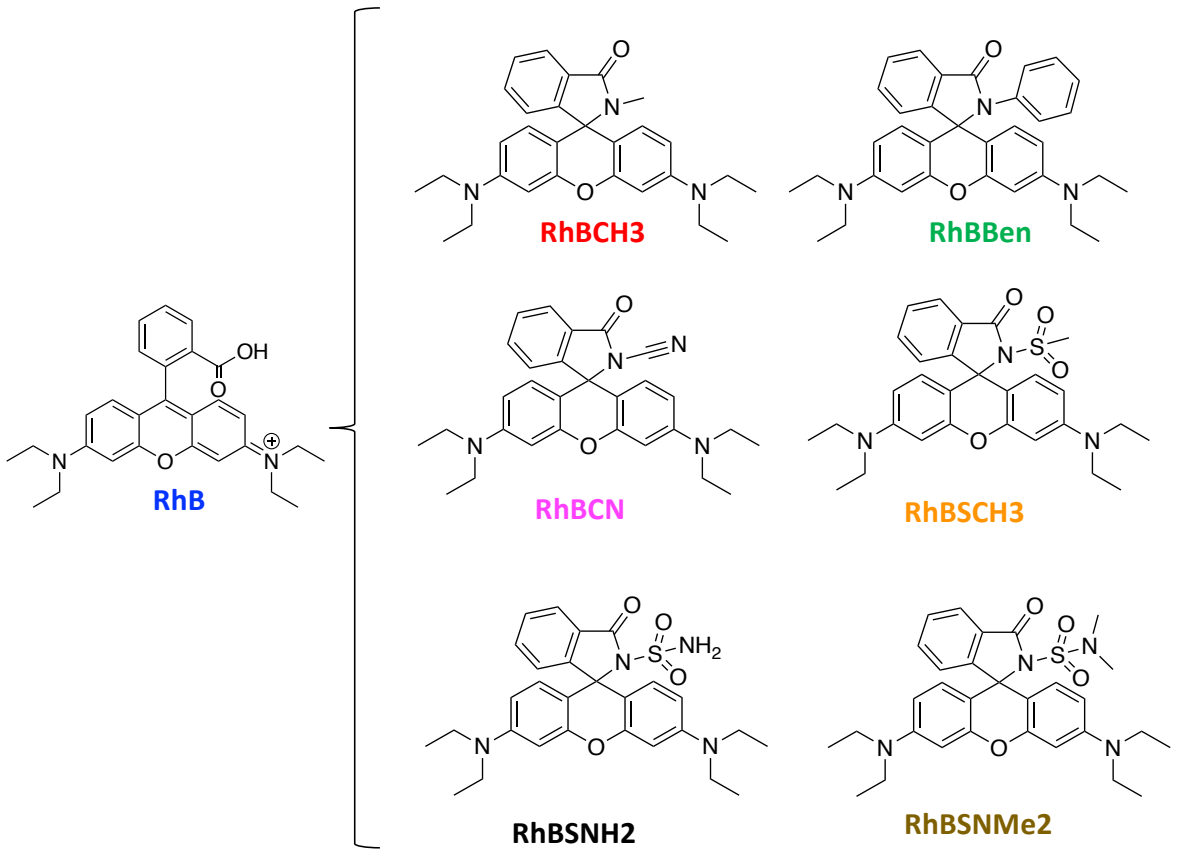

Making tetramethylrhodamine (TAMRA)-based probes fluorogenic and permeable

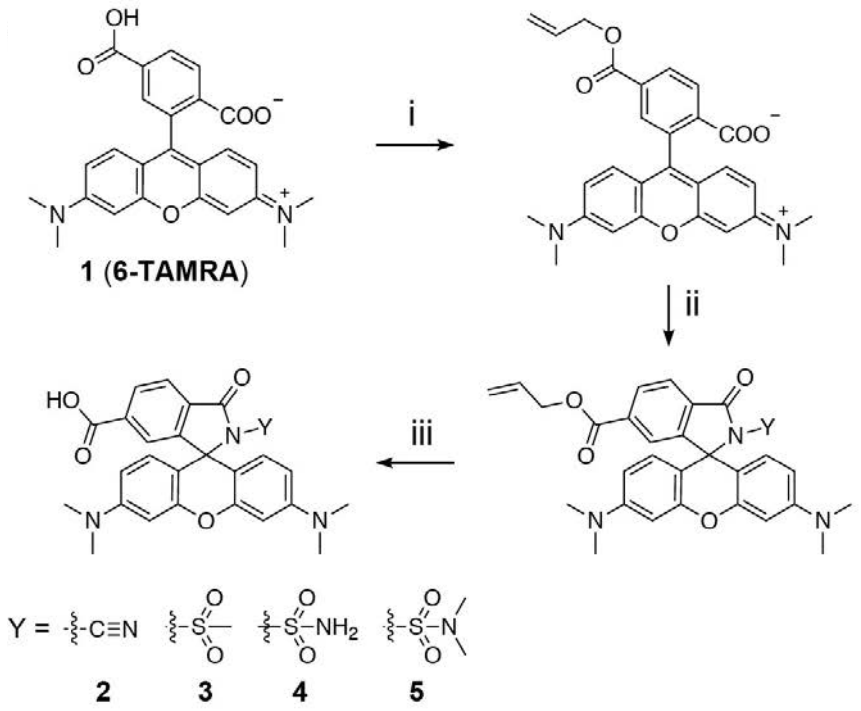

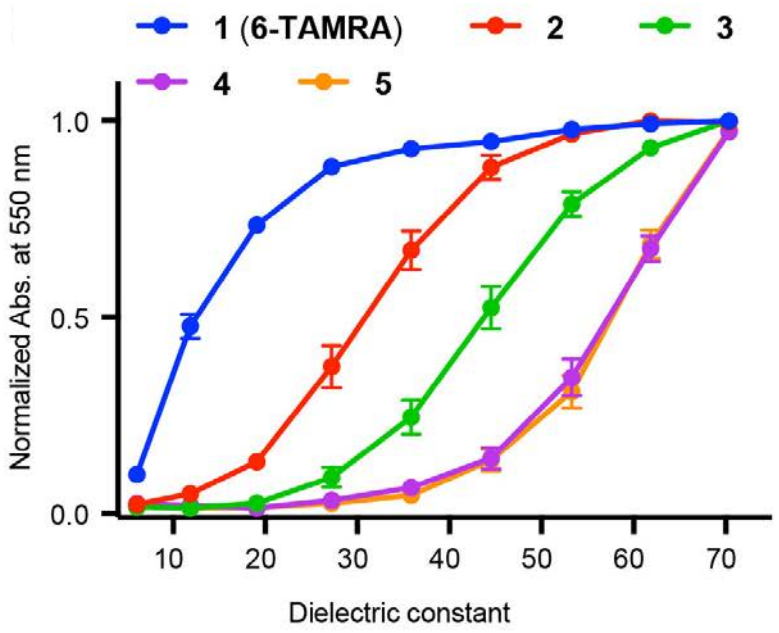

(i) allyl bromide, K_2CO_3, Et_3N, DMF, r.t. 2 h; (ii) $POCl_3$, DCM, reflux, 3 h; amines, ACN, DIPEA, r.t. 1 h; (iii) 1,3-Dimethylbarbituric acid/$Pd(PPh_3)_4$, MeOH/DCM, r.t. 1 h.

Improving the performance of TMR-based probes; MaP_{555}

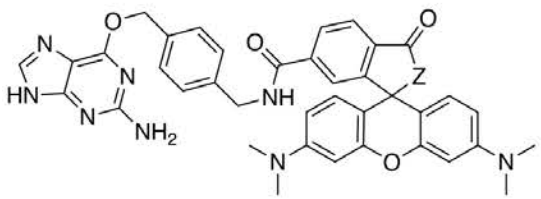

6 Z = O; **7** Z = NCN;
8 Z = NSO_2CH_3; **9** Z = NSO_2NH_2;
10 Z = $NSO_2N(CH_3)_2$

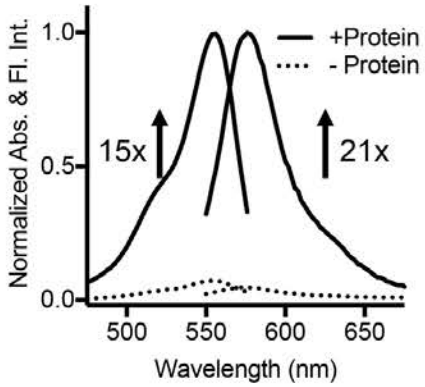

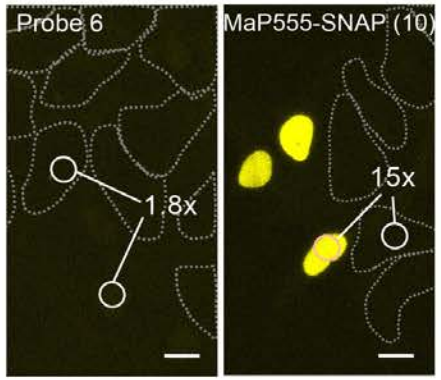

Z = $NSO_2N(CH_3)_2$

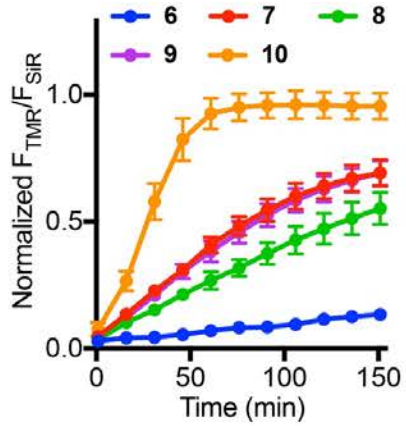

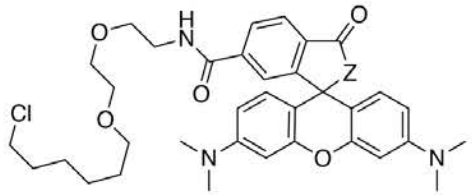

11 Z = O; **12** Z = NCN;
13 Z = NSO_2CH_3; **14** Z = NSO_2NH_2;
15 Z = $NSO_2N(CH_3)_2$

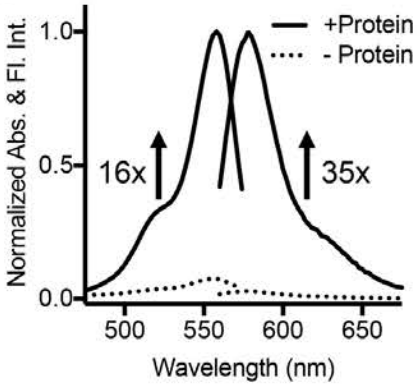

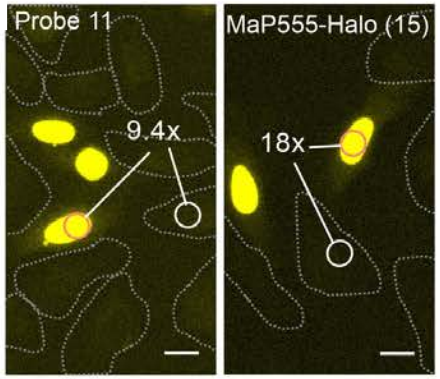

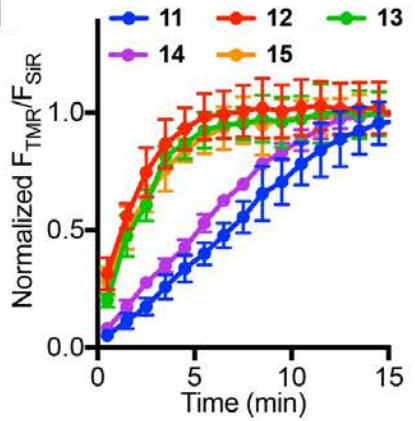

MaP_{555}-tubulin and MaP_{555}-actin

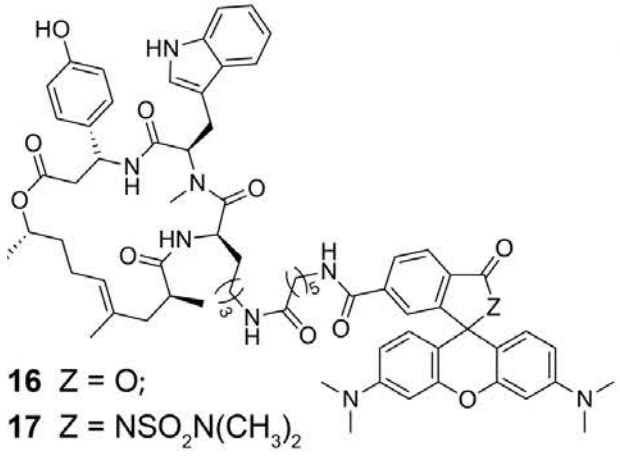

16 Z = O;
17 Z = $NSO_2N(CH_3)_2$

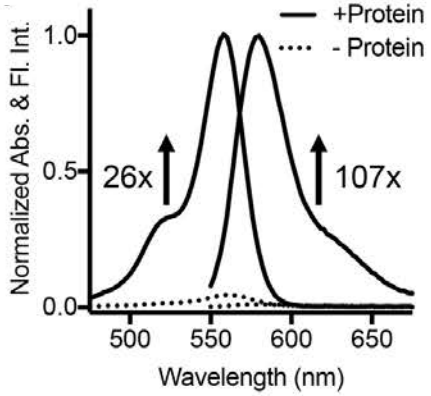

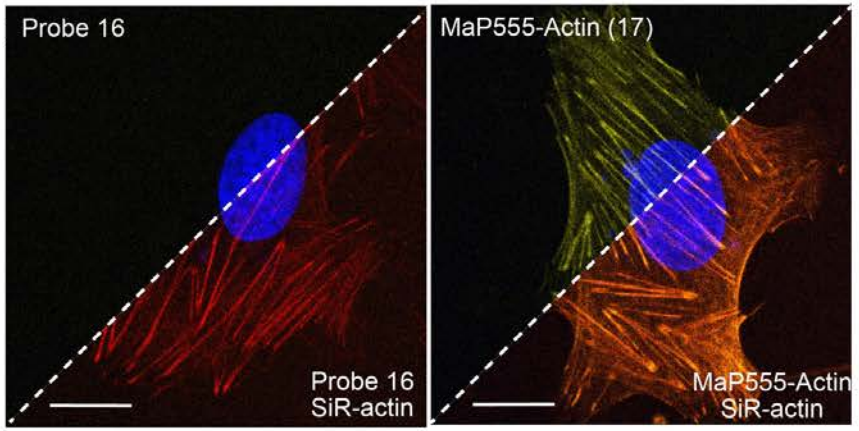

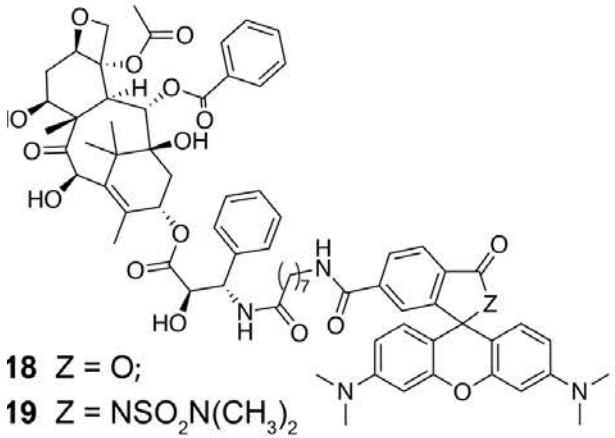

18 Z = O;
19 Z = $NSO_2N(CH_3)_2$

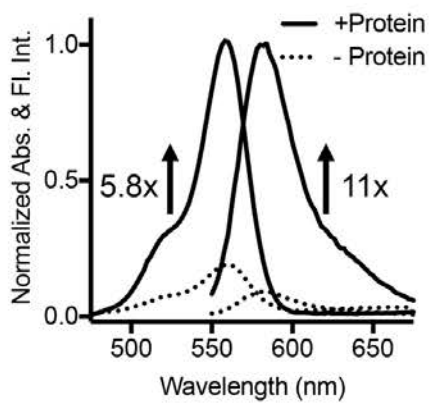

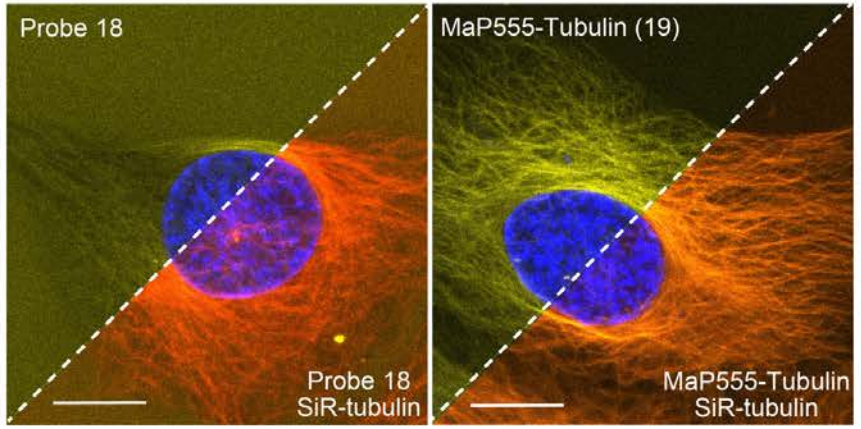

MaP probes for multi-color imaging

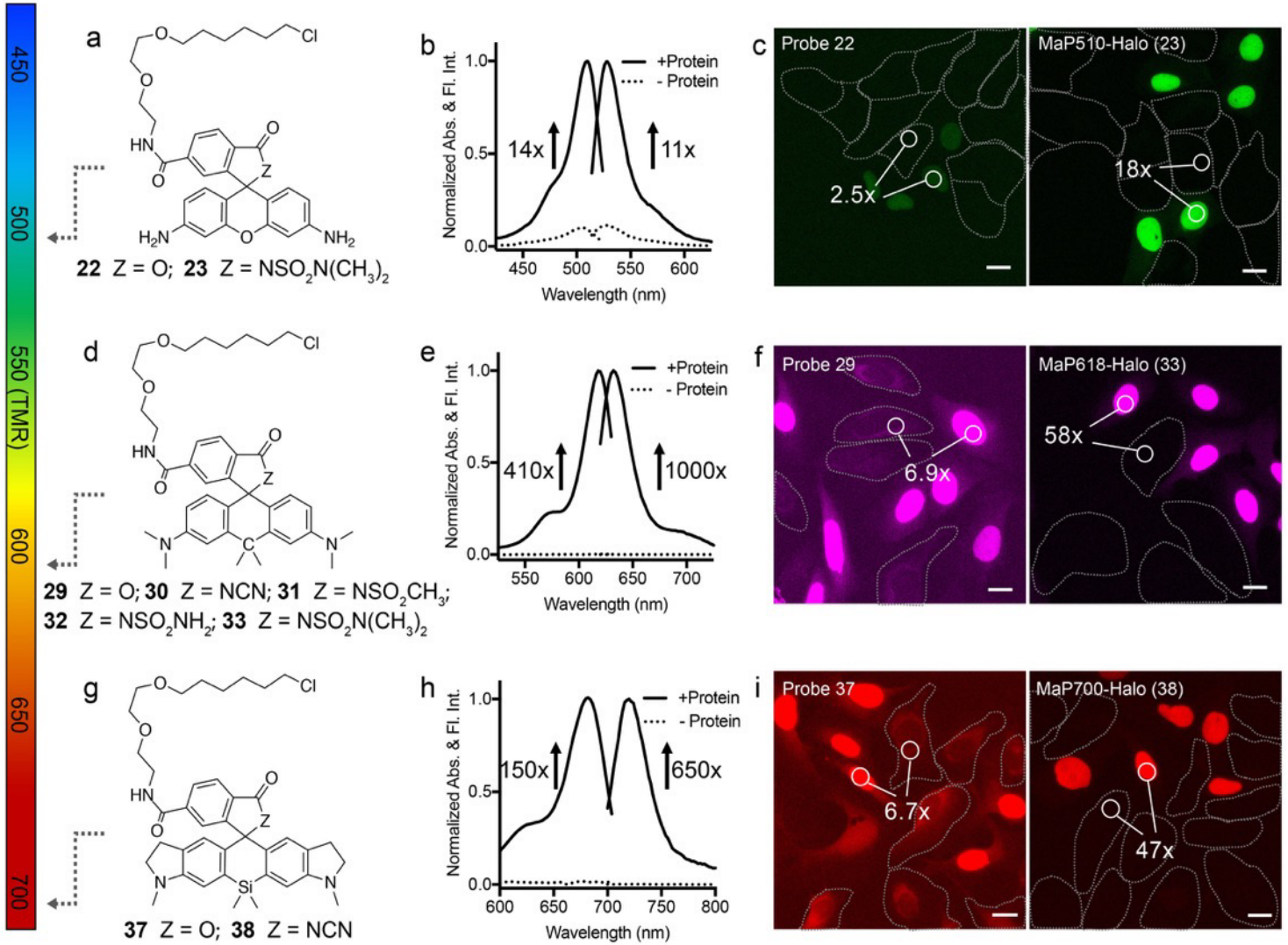

No-wash multicolor live-cell imaging with fluorogenic probes

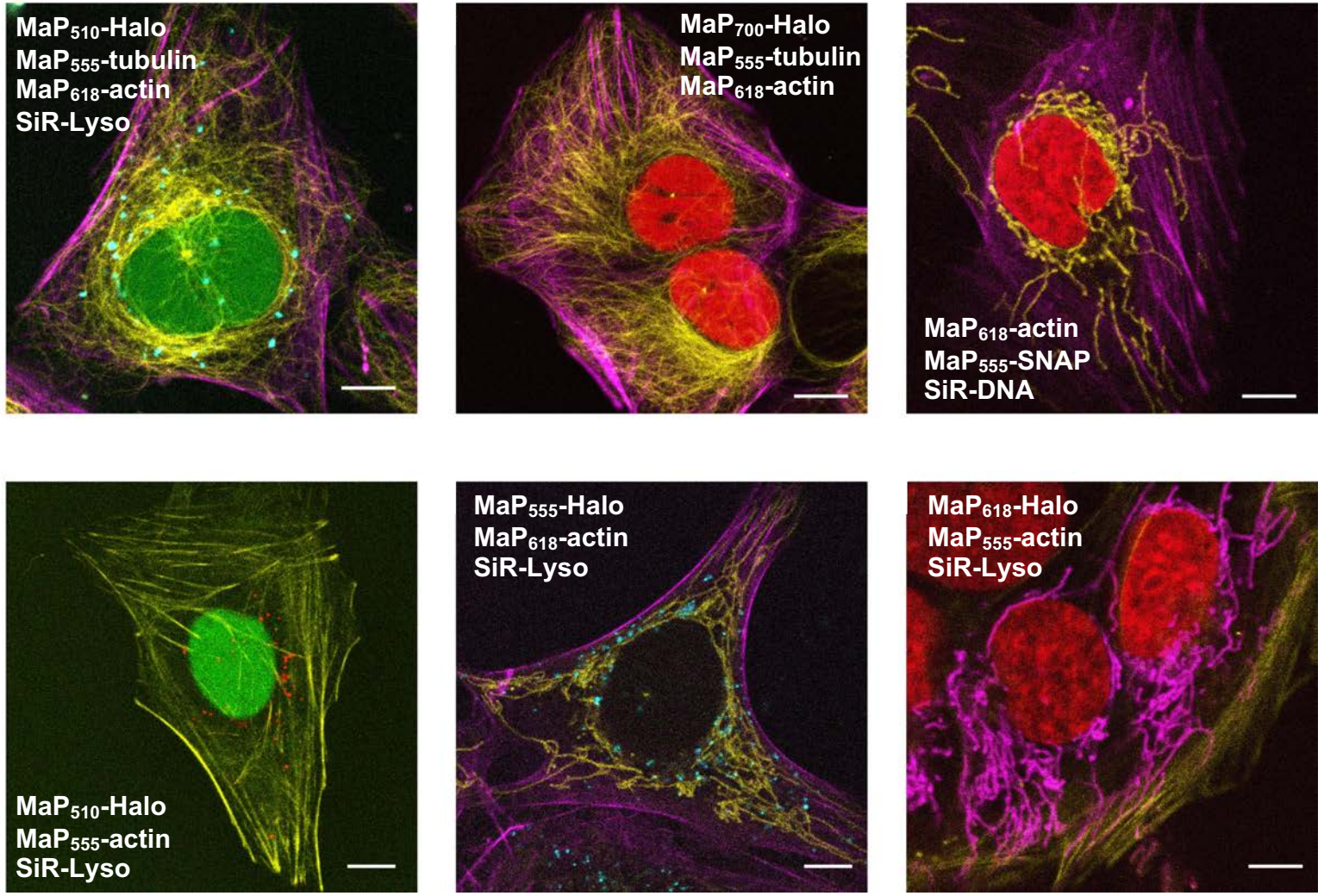

No-wash, live-cell, multicolor STED microscopy

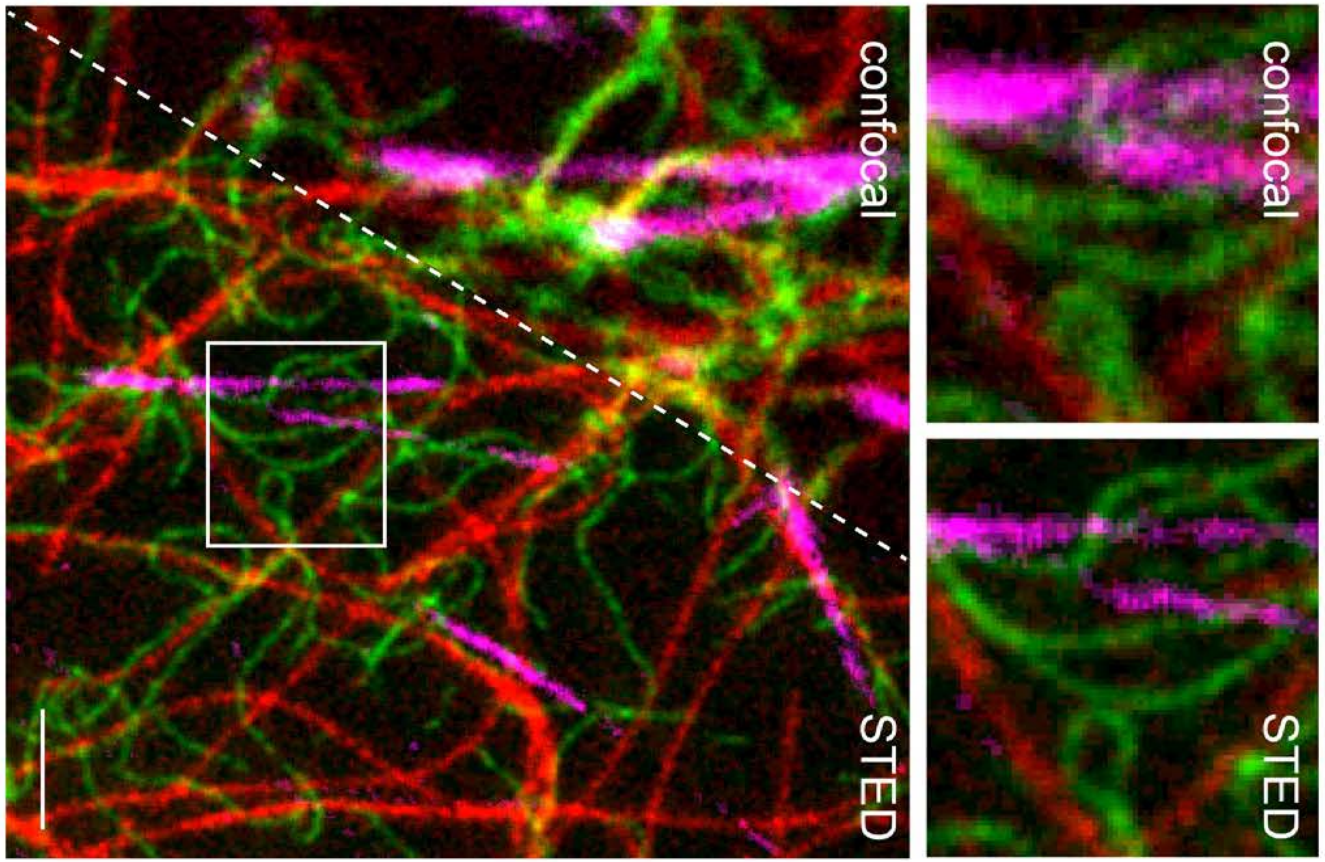

STED images of live U2OS Vimentin-Halo expressing cells stained **MaP510-Halo** (green), **MaP555-tubulin** (red), **MaP618-actin** (magenta) .
Scale bar, 2 µm.